UNIVERSITÀ DEGLI STUDI DI PADOVA

DIPARTIMENTO DI INGEGNERIA INDUSTRIALE

TESI DI LAUREA MAGISTRALE IN INGEGNERIA CHIMICA E DEI PROCESSI INDUSTRIALI

EXPERIMENTAL INVESTIGATION OF ETHANOL SEPARATION BY REVERSE OSMOSIS

Relatore: Prof. Alberto Bertucco

Correlatore: Prof. Adel Sharif, University of Surrey (UK)

Laureando: DAMIANO GATTO

ANNO ACCADEMICO 2011 – 2012

Riassunto

Dall'indagine della US Geological Survey è emerso che il 96,5% dell'acqua nel mondo è situata in oceani e mari, l'1,7% è sotto forma di ghiaccio e solo lo 0,8% è considerata *fresh water*. Inoltre, solo lo 0,327% è disponibile in laghi e fiumi. La restante percentuale si riferisce alla *brackish water*. A questi dati si aggiunge che circa il 20% della popolazione non ha accesso ad acqua pulita, che al 50% della popolazione mancano adeguati sistemi di purificazione dell'acqua e che un incremento nella potabilizzazione, fornitura e igienizzazione dell'acqua ridurrebbe dell'80% le malattie nel mondo. Infine, entro il 2025, la popolazione mondiale che vive in *water-stressed countries* passerà da un terzo a due terzi. Tutti questi dati fanno comprendere come l'approvvigionamento di acqua potabile è un grave problema per l'umanità oggigiorno e probabilmente ancor di più in un futuro molto prossimo.

L'approvvigionamento d'acqua potabile dall'acqua di mare è una delle sfide più importanti del pianeta: attualmente più di 17.000 impianti di desalinizzazione sono operativi in tutto il mondo. Gli impianti di desalinizzazione esistenti si basano principalmente su due tecnologie: impianti di desalinizzazione termici o a membrana. Gli impianti di desalinizzazione a processo termico producono *fresh water* essenzialmente per condensazione, usando quindi un passaggio di stato per separare l'acqua di mare dai sali e dalle impurità. I processi di desalinizzazione a membrana invece non coinvolgono passaggi di stato ma utilizzano una membrana semipermeabile che permette la formazione di due diverse fasi liquide. I principali processi di desalinizzazione termici sono il *Multi-Stage Flash Distillation* (MSF), *Multi Effect Distillation* (MED) e *Vapour Compression Distillation* (VCD). Essi differiscono tra loro per produttività e schema di processo e sono largamente utilizzati nel medio oriente, dove l'elevata quantità di energia necessaria per vaporizzare l'acqua è disponibile a costo relativamente basso. I principali processi a membrana usati per la dissalazione dell'acqua di mare sono l'elettrodialisi e l'osmosi inversa. L'elettrodialisi si basa sulla migrazione degli ioni soggetti ad un campo elettrico, e viene utilizzata solo per acque poco salate. Il processo di desalinizzazione a osmosi inversa invece può essere utilizzato con un vasto intervallo di salinità e, in genere, è più efficiente di qualsiasi altro processo termico di desalinizzazione perché richiede molta meno energia. Purtroppo, nonostante il forte sviluppo tecnologico degli ultimi decenni, lo stato dell'arte delle attuali tecniche di desalinizzazione sembra non essere sufficiente per soddisfare la richiesta di acqua potabile in costante aumento.

Una recente ricerca dell'US National Research Council (NRC, 2004) suggerisce fortemente di sviluppare nuove tecnologie di desalinizzazione a membrana per ridurre costi di investimento, costi di esercizio e per lo smaltimento delle soluzioni ad alta concentrazione salina. La ricerca afferma che gli obiettivi più ottimistici sono: una riduzione dal 50 all'80% dei costi di esercizio e un contemporaneo miglioramento dell'efficienza energetica del processo. Tutto ciò è possibile solo sviluppando le nuove tecnologie *break-through* a membrana nei prossimi venti anni.
Purtroppo, all'attuale stato dell'arte, il processo di desalinizzazione a osmosi inversa può arrivare a ridurre solo del 20% i costi operativi, raggiungendo il limite teorico termodinamico dell'osmosi di 1,77kWh/m^3 (per un impianto con 50% *recovery* e 100% efficienza energetica). Quindi, la ricerca afferma che devono essere considerati altri approcci di desalinizzazione per abbattere ulteriormente il consumo energetico.

Una possibile tecnologia di desalinizzazione alternativa è sicuramente rappresentata dal processo *Manipulated Osmosis Desalination* (MOD). Il processo MOD è stato sviluppato presso *University of Surrey Centre for Osmosis Research and Applications* (CORA) ed è coperto da brevetto (Sharif & Sl-Mayahi, 2005). MOD è un processo che può essere concepito come una modificazione delle tecniche esistenti di desalinizzazione: è caratterizzato dall'uso di un'unità a membrana *pressure-driven*, a osmosi inversa o nano-filtrazione, nella fase di recupero di un processo di desalinizzazione a osmosi diretta. Il processo di desalinizzazione a osmosi diretta è una tecnologia sviluppata negli ultimi anni ed è ancora in fase di sperimentazione. Esso consiste in due fasi principali: nella prima fase una membrana semipermeabile separa l'acqua di mare da una soluzione a più alta pressione osmotica (*draw solution*), l'acqua quindi tende a passare naturalmente attraverso la membrana andando a diluire la *draw solution*; nella seconda fase la *draw solution* viene concentrata in un'unità di rigenerazione specifica e successivamente riciclata al primo step, ricavando così *fresh water*. Il processo MOD permette un risparmio energetico di circa il 30% e il 90% se paragonato rispettivamente al processo di desalinizzazione a osmosi inversa e in generale ai processi termici. La riduzione dell'energia necessaria a desalinizzare l'acqua è dovuta sostanzialmente alla minor pressione con cui opera l'impianto. Infatti, nel primo step, la pressione è di soli 2bar per vincere le perdite di carico e assicurare un flusso costante attraverso la membrana, in quanto il processo è naturale. Inoltre, nel secondo step, la bassa pressione osmotica della *draw solution* diluita consente di ricavare *fresh water* con una pressione di circa 25bar, molto inferiore ai 55-60bar normalmente necessari per un processo di desalinizzazione a osmosi inversa. Oltre al risparmio energetico, ci sono altri vantaggi: minor tendenza di *fouling* e *scaling* (deposito di uno strato di impurità o sali sopra la membrana), maggior durata delle

membrane, post-trattamenti meno intensivi, alti valori di *recovery*, flusso elevato d'acqua attraverso la membrana, minor produzione di brina, assenza di *membrane compaction* e pre-trattamenti non necessari. Nonostante i numerosi vantaggi, il processo MOD, e in generale i processi di desalinizzazione a osmosi diretta, presentano alcune limitazioni. La prima è dovuta all'*Internal Concentration Polarization* (ICP) che diminuisce fortemente la *driving force* nel primo step a osmosi diretta. Questa limitazione è superabile sviluppando un'apposita membrana per l'osmosi diretta che riduca il fenomeno della polarizzazione internamente alla membrana. Il secondo limite è rappresentato dalla scelta della *draw solution* più idonea. La *draw solution*, nella maggior parte dei casi, è la soluzione di un sale in acqua; essa deve avere precise caratteristiche: economicità, alta pressione osmotica rispetto all'acqua di mare, facilità di separazione dall'acqua, non tossicità e stabilità a pH neutro. Due impianti MOD sono operativi a tutt'oggi con risultati brillanti ed uno è in costruzione, ma la scoperta di una *draw solution* più adatta potrebbe rendere il processo ancora più conveniente.

L'obiettivo di questa tesi è stato di testare la fase di rigenerazione del processo MOD utilizzando una *draw solution* di acqua ed etanolo, determinando sperimentalmente l'efficienza della rigenerazione tramite osmosi inversa.
I contenuti della tesi sono organizzati come segue.
Il Capitolo 1 descrive in generale i processi di desalinizzazione termici e a membrana. Inoltre, esso introduce il concetto di pressione osmotica e le sue proprietà.
Il processo di desalinizzazione a osmosi inversa è ampiamente discusso nel Capitolo 2: principi fondamentali, membrane, modelli di trasporto di massa, impiantistica, costi, fattori limitanti, impatti ambientali e future soluzioni tecnologiche.
Il Capitolo 3 descrive il nuovo processo MOD, partendo dai principi della dissalazione a osmosi diretta.
Il metodo sperimentale, la strumentazione usata e le caratteristiche della *draw solution* sono spiegati nel Capitolo 4.
Il Capitolo 5 mostra i risultati sperimentali ottenuti, i commenti e le considerazioni.

L'obiettivo è stato sviluppato e raggiunto attraverso alcuni esperimenti usando un impianto a osmosi inversa (prodotto da SpinTke Filtration Inc.) e testando due tipi diversi di membrane *flat-sheet* (TFC®-ULP prodotta da Koch Membrane System e RO989pHt® fornita da Alfa Laval) a differenti pressioni (2-20 bar) e concentrazioni di etanolo in alimentazione (0.29-3.66% v/v). La concentrazione di etanolo dei campioni di permeato e retentato è stata misurata utilizzando un gas cromatografo (detector a ionizzazione di fiamma) e i dati sono stati elaborati usando il modello *Solution-Diffusion*.

I risultati sperimentali hanno evidenziato che la membrana TFC®-ULP è più adatta a separare acqua ed etanolo tramite osmosi inversa, in confronto con la membrana RO989pHt®, perché raggiunge lo stesso valore di ritenzione di etanolo permettendo un flusso di acqua maggiore. Purtroppo, la ritenzione di etanolo è solo di circa il 40%, un valore non sufficiente a recuperare completamente l'etanolo, ovvero rigenerare la *draw solution*, nell'unità ad osmosi inversa. Inoltre, il permeato così ottenuto non è potabile secondo gli standard della World Health Organization (WHO); potrebbe però essere conforme solo per alcune applicazioni industriali.
Ci sono diversi fattori che concorrono all'ottenimento di un valore di ritenzione di etanolo così basso: il basso peso molecolare dell'etanolo, il basso valore della sua *cross-sectional area*, l'affinità chimica dell'etanolo per il polimero della membrana (poliammide acrilica) e la forte tendenza dell'etanolo a stabilire forti legami idrogeno.

Il lavoro sperimentale ha portato al raggiungimento di buoni risultati, ma presenta alcune limitazioni. Sarebbero necessari altri dati sperimentali investigando un intervallo più vasto di concentrazioni e pressioni, per capire con precisione il comportamento delle membrane. Inoltre, andrebbero testati altri tipi di membrane. In aggiunta, l'effetto della temperatura sui parametri operativi è stato solo parzialmente oggetto di esame e potrebbe essere affrontato in lavori futuri.

Si suggerisce di considerare altri tipi di unità di separazione, per sviluppare un sistema di separazione acqua-etanolo ibrido che possa recuperare efficientemente l'etanolo e produrre *fresh water* conforme con gli standard della WHO. Per esempio, un'unità ad osmosi inversa potrebbe operare a valle di una colonna di distillazione, o di un processo di assorbimento o di un'unità a pervaporazione. In aggiunta, lo studio delle interazioni tra etanolo e il polimero della membrana, potrebbe portare allo sviluppo di membrane *grafted* o *cross-linked* specifiche per la separazione di acqua ed etanolo, le quali possono arrivare ad alti valori di ritenzione, come dimostrato da alcuni studi passati.
Si è fiduciosi che questo studio possa essere d'aiuto per lo sviluppo e la progettazione dell'unità di recupero del processo MOD, con una soluzione di etanolo come *draw solution*.

.

Abstract

The purpose of the research was to investigate the recovery efficiency of an ethanol draw solution in the reverse osmosis regeneration step of the Manipulated Osmosis Desalination (MOD) process. The research was conducted through several experiments at different ethanol feed concentrations and feed pressures at room temperature by using a Reverse Osmosis (RO) laboratory cell and two different kinds of flat sheet commercially available thin film composite membranes (TFC®-ULP and RO98pHt®).

The research found that TFC®-ULP membrane is the most suitable option for RO water-ethanol separation in comparison to RO98pHt® membrane because it reaches the same ethanol rejection allowing a higher water flux across the membrane. However, the ethanol rejection of both membranes is not enough to ensure the completely recover of the draw solution.

The possible shortcoming of the research could be the limited ethanol feed concentration and feed pressure range, the restricted types of RO membranes used and the lack of the temperature variation. Nevertheless, these results are helpful to investigate the key factors of the low ethanol rejection such as the chemical affinity for the membrane polymer and the high tendency to form hydrogen bonding, in order to develop grafted or cross-linked membranes which might arrive at higher ethanol rejection values. In addition, hybrid water-ethanol separation processes involving a RO unit and another unit type (such as a distillation column, an adsorption unit or a pervaporation unit) could be studied in order to reach a complete recover of the draw solution in the MOD process to conform the product water to the World Health Organization (WHO) standards.

Table of contents

Introduction

The US Geological Survey found that 96.5 % of the water in the world is situated in oceans and seas, and 1.7 % is located in ice caps. Circa 0.8 % is considered to be fresh water and only 0.327% is available in lakes and river. The other percentage is made up of brackish water. Furthermore, approximately 1.2 billion people (about 20% of the world's population) do not have access to safe drinking water, 50% of the world's population lacks sufficient water purification system, so that an improvement in water supplies, sanitation and water treatment will result in the reduction of 80% of the world's diseases. Moreover, over one-third of the world's population lives in water-stressed countries, and this figure is expected to rise nearly two-thirds by 2025, because the demand of fresh water is increasing (Greenlee *et al.,* 2009 and Menachem *et al.,* 2011). All these data help to understand how the availability of fresh water will drastically decrease in the near future.

The supply of drinkable water from sea water and ground water is one of the most important challenges of the world: nowadays more than 17,000 both thermal and membrane desalination processes are operated worldwide. However, this seems not to be sufficient, and any developments to the current state-of-the-art of the desalination processes are expected to take place soon.

A recent review by the US National Research Council (NRC, 2004) strongly suggested the support of further developments in application of novel membrane technologies in order to "reduce energy and capital cost and brine disposal". The review affirms the most "optimistic" limit of outcome is a 50 to 80 percent capital and operating cost reduction, together with a parallel increase in energy efficiency, by using the application of new "break-through" technologies over the next twenty years. For current state-of-the-art of Sea Water Reverse Osmosis (SWRO) systems, the maximum optimistic reduction is 20%, which represent the Reverse Osmosis process thermodynamics limit of 1.77kWh/m^3 for a 50% recovery rate and a 100% energy recovery in seawater applications. Hence, the review asserts that, to obtain further reductions in energy, a different desalination approach is recommended (NRC, 2004).

One possible alternative desalination technology could be the novel Manipulated Osmosis Desalination (MOD) process. MOD is a pioneering modification of the existing desalination techniques: it is characterized by the use of a pressure-driven membrane step (Reverse Osmosis or Nanofiltration) in the recovering stage of a Forward Osmosis (FO) desalination process. MOD process has been developed at the

University of Surrey's Centre for Osmosis Research and Applications, CORA (Sharif & Al-Mayahi, 2005).

The aim of this thesis is to investigate and test a draw solution of water and ethanol in the regeneration step of the MOD process, examining the efficiency of a Reverse Osmosis (RO) unit.

The object has been developed by carrying out several experiments using a laboratory cell and by testing two different types of flat-sheet membranes at different feed pressures and concentrations.

The contents of this Thesis are outlined in the following.

Chapter 1 provides a general overview of both thermal and membrane based industrial desalination process. In addition, the osmotic pressure and its properties are introduced.

Reverse osmosis desalination principles and process are widely described in Chapter 2. A brief introduction of reverse osmosis principles is given, while a special attention is placed in membranes, mass transfer models, RO plants, costs, limiting factors and current trends of RO.

Chapter 3 describes the novel Manipulated Osmosis Desalination process, focusing on forward osmosis principles.

The experimental methods for the bench-scale cell and the characteristic of the draw solution are explained in Chapter 4; while Chapter 5 shows and discusses the experimental results. Finally, some considerations of the experimental work are given at the end of the Thesis.

The author would like to thank the Faculty of Engineering and Physical Sciences at the University of Surrey and, in particular Prof. Alberto Bertucco and Prof. Adel Sharif for giving me the opportunity to do my master thesis work in such a blooming-science-thoughts place. Deepest gratitude goes to Dr. Al-aibi and Eng. Aryafar, for their constant presence and help throughout the work.

Chapter 1

Desalination: General overview

Water desalting, or desalination, has long been used by water-short nations world-wide to produce or increase their drinking water supplies. The variety of weather, industry and agriculture further development, higher living standard conditions, population growth and subsequent increase in demand for water in arid and coastal areas are contributing to a heightened interest in water desalination. The ratio of the average amount of withdrawal to the amount of long term available freshwater resources is called “water stress index”. A value of 40% indicates acute water scarcity, and one of 10% is considered as the lower limit of water scarcity. Many nations, like Israel, Cyprus and Malta, have a “water stress index” higher than 40% and many other have the “water stress index” between 40% and 10% (Fritzmann *et al*., 2007).

This is only an example to understand the reason why the world tends to intensify the use of desalination processes as a mean to reduce current or future water scarcity. Tapping into the seas seem to be the only suitable option available to solve fresh water scarcity issue.

In this chapter a general overview of the main desalination processes is given in Section 1.1, and the osmotic pressure is described in Section 1.2.

1.1 Desalination processes

The industrial desalination processes deal with the separation of nearly salt-free fresh water from seawater or brackish water, where salt is concentrated in the rejected brine stream (Figure 1.1) and fresh water is the wanted product. Fresh water can be defined as containing less than 1000 mg/L of Total Dissolved Solid (TDS) (Schenkeveld *et al*., 2004).

Above 1000 mg/L, properties such as colour, taste, corrosion propensity and odour can be adversely affected.

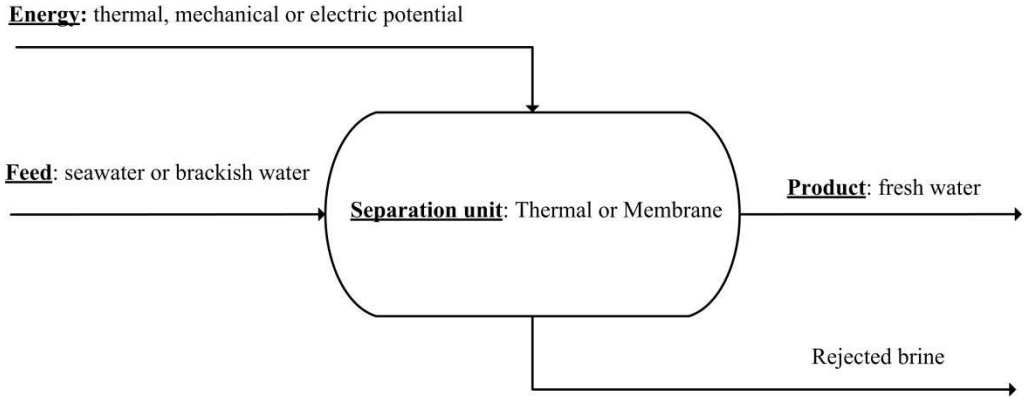

Figure 1.1. *Block Flow diagram of desalination process.*

In the 17th century, desalination first began to be developed for commercial use aboard ships to produce drinking water. Countries began to develop advanced distillation technology in the late 18th century, including investigations into chemical addition. The early use of desalination on a large scale for municipal drinking water production was in the Middle East in 1960s. Membranes then began to be studied, improved and used in desalination processes. The first successful RO plants used brackish water as the feed was built in the late 1960s. Over the past 40 years, impressive improvements in RO membrane technology elevated RO to be the primary choice for new distillation facilities. The worldwide desalination capacity is shown in Figure 1.2 as a function of the time over the past 60 years (Greenlee *et al.*, 2009).

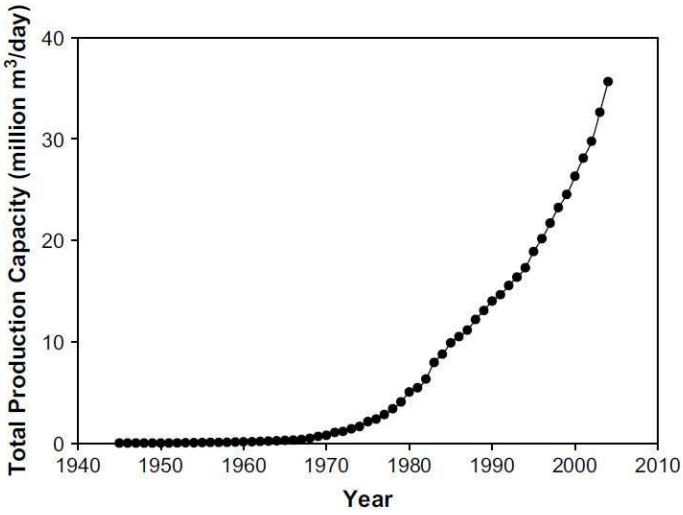

Figure 1.2. *Total desalination production capacity as a function of the time over the past 60 years (Greenlee et al., 2009).*

Nowadays, more than 17,000 desalination plants are operated all over the world (Raluy *et al.*, 2006). The Middle East holds approximately 50% of the world's production

capacity with Saudi Arabia being the world leader (26%). The United States ranks second (17%), while in Europe the majority of the plants are in Spain and Italy (Greenlee *et al.*, 2009).

Desalination processes are generally divided by their separation mechanism into two primary categories:

- thermal desalination (*phase change processes*): Multi-Stage Flash Distillation (MSF), Multi-Effect Distillation (MED), Vapour Compression Distillation (VC or VCD);
- membrane processes (*single-phase processes*): Reverse Osmosis (RO), Electrodialysis (ED).

Thermal desalination splits salt from water by evaporation and condensation, whereas in a membrane desalination water diffuses across a membrane, while salts are almost completely retained. Reverse Osmosis (RO) and Multi-Stage Flash (MSF) are the techniques that are most extensively used. MSF is the most frequently applied in the Middle East, RO is the most common option in seawater and brackish water desalination in the area around Mediterranean Sea. Thermal desalination is more energy intensive than membrane based desalination (in fact it is present where energy is available at low prices: Middle East), but can better deal with more saline water and delivers even higher permeate quality (Fritzmann *et al*., 2007).

The choice of the most appropriate desalination processes for a particular solution is not unique. There are a lot of parameters to consider and several factors come into play, such as (Schenkeveld *et al*., 2004):

- quality and quantity of water resources available: phase-change processes tend to be utilized for the treatment of high salinity waters (sea water); membrane processes are used over a wide range of salinity from brackish to sea water, while ED is limited to brackish water applications (see Table 1.1 and Table 1.2). In Figure 1.3 it is shown the range of applicability of desalination processes, with the reference to the World Health Organization (WHO) TDS limit for drinking water (500 ppm);
- optimisation of energy and water requirement;
- availability of energy resources: energy consumption in membrane process is directly related to the salinity of the feed water, whereas in thermal process it has only a little impact;
- plant size: it is normally dictated by the fresh water demand. Each plant has a limit size to be considered. The MSF process has been developed for very large scale applications (10-60,000 m^3/day) while for membrane processes there is a wide range of sizes available for each application.

Table 1.1. *Feed water classified by TDS (Schenkeveld et al., 2004).*

Water	TDS[mg/L]
Potable water	<1000
Low salinity brackish water	1,000-5,000
High salinity brackish water	5,000-15,000
Seawater	15,000-50,000

Table 1.2. *TDS concentration for selected water bodies around the world (Schenkeveld et al., 2004, and Greenlee et al., 2009).*

Water body	TDS[mg/L]
Baltic sea	7,000
Pacific Ocean	34,000
Mediterranean Sea	38,000-40,500
Atlantic Ocean	38,500-40,000
Red Sea	41,000-42,000
Gulf of Oman	40,000-48,000
Persian Gulf	42,000-45,000
Dead Sea	275,000

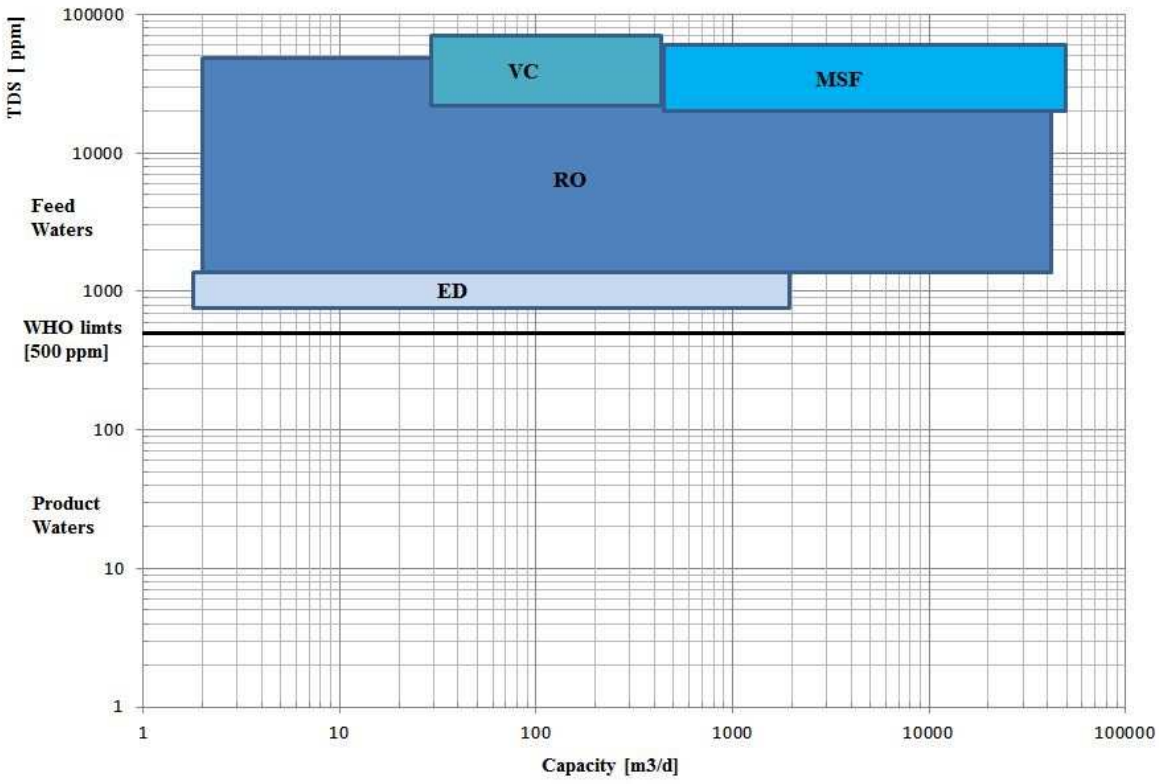

Figure 1.3. *Ranges of applicability for desalination processes (modified from Schenkeveld et al., 2004).*

1.1.1 Thermal processes

In thermal processes, salt-water is boiled and then the vapours are condensed to produce salt-free water. Over 40% of the world's desalted water is produced in this way.

1.1.1.1 Multi-Stage Flash Distillation

In this process (Figure 1.4) seawater raises its temperature flowing through a series of heat exchangers. Then it passes through a series of stages, each one at a successively lower temperature and pressure. In each stage, a process of decompression and flashing generates steam that is successively condensed in heat exchangers forming fresh-water. Heat Exchangers Net provides an efficient energy recovery, re-utilizing the initial heat.
MSF is the most largely used desalination processes, in terms of capacity. This is due to the simplicity of the process, the developed and well-knows scaling control and the flexibility of performance control varying stages number. The maximum performance ratio obtained is around 13 units of water per unit of steam, and the process is developed for continuous operation and high plants (Schenkeveld *et al.*, 2004). Recent estimations indicate a unit cost of fresh water produced of 1.40US$/m^3 (Van der Bruggen *et al.*, 2003).

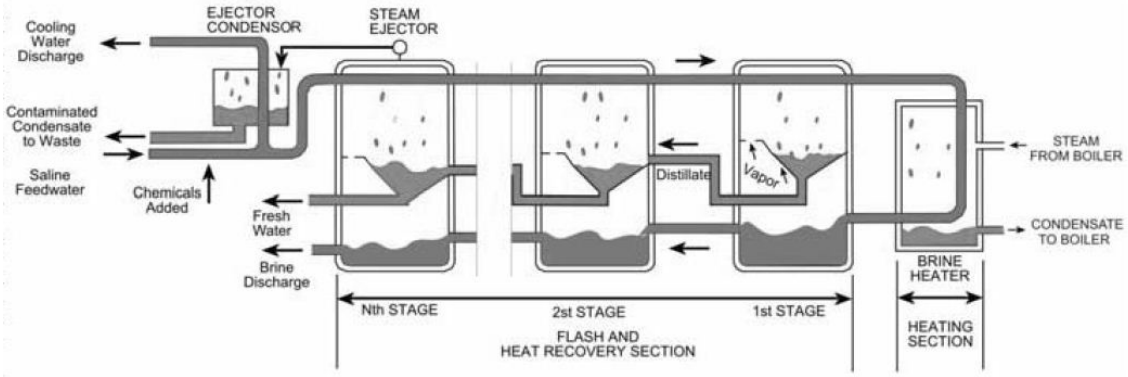

Figure 1.4. *Multi-Stage Flash Distillation process scheme (Fritzmann* et al.*, 2007).*

1.1.1.2 Multi-Effect Distillation

MED is a desalination process based on thin-film evaporation approach, where steam is produced by two means: by flashing and by evaporation. A thin-film of salt-water evaporates in a chamber, and the vapour generated flashes in a successive step (or "effect"), at lower temperature and pressure, giving additional heat for vaporization to the salt-water, and condensing in fresh water (Figure 1.5).
MED process is used when thermal evaporation is preferred or required. There is no large mass of brine recirculating round the plant, so that the pumping requirement, scaling effect and the necessary power are reduced. Moreover MED processes are

usually operated in small plants with high performance ratios. Recent estimations indicate a unit cost of 1US$/m^3 (Van der Bruggen *et al.*, 2003).

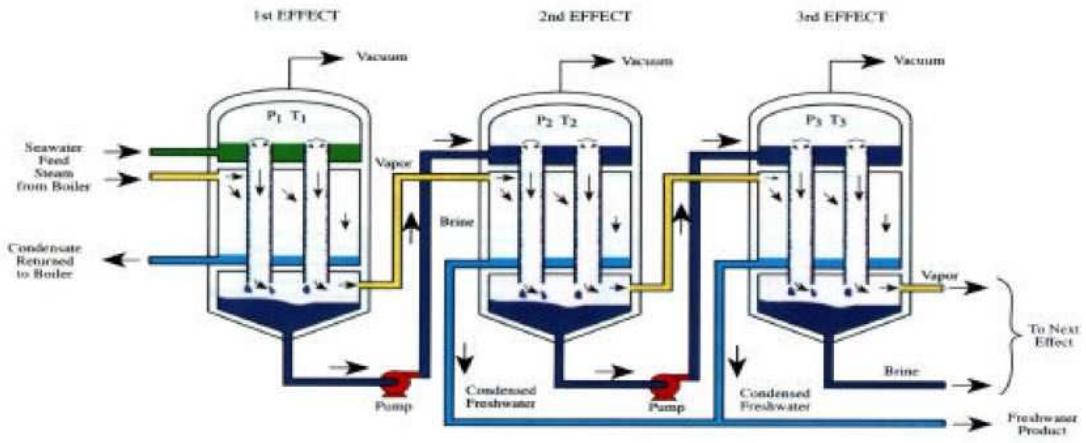

Figure 1.5. *Multi-Effect Distillation process scheme (Schenkeveld et al., 2004).*

1.1.1.3 Vapour Compression Distillation

As in MED process, the steam produced in one effect is then used as heat input in the successive effect, which is at lower temperature and pressure. But it is not simply heating one end of the plant and cooling the other. The main difference between MED, MFD and VCD is that in this last process, the steam produced in the last effect is compressed, raising its temperature, and sent to the first effect as heat input (Figure 1.6). So VCD does not require a thermal input as MED and MFD.

The compression step represents the major energy requirement. There are two types of compressor: mechanical compressor (expensive but relatively efficient) and thermo-compressor (cheaper but less efficient). VCD process is particularly suited for relatively small output plants.

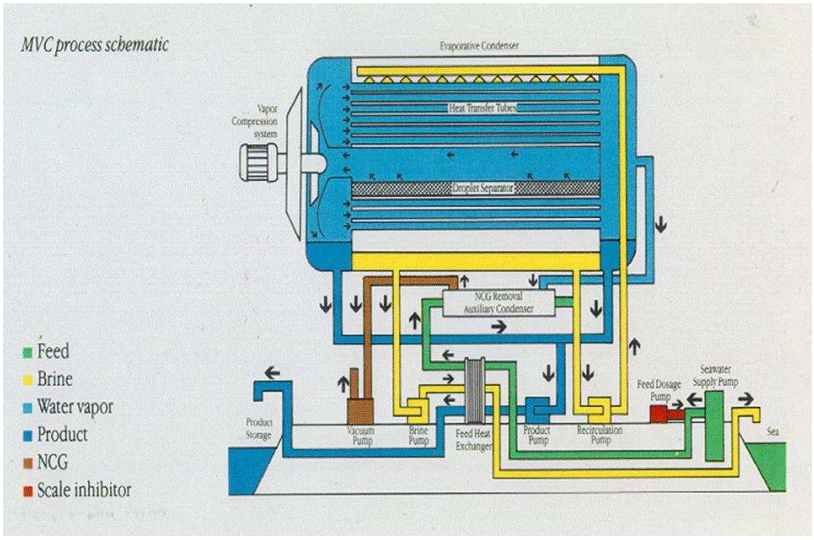

Figure 1.6. *Vapour Compression Distillation process scheme (Schenkeveld et al., 2004).*

1.1.2 Membrane processes

In membrane processes, dissolved salt is separated from water using a semi-permeable membrane. It is a single-phase process because water is not vaporized during desalination.

The membranes used in desalination processes are a thin selective separator between two salinity different phases. There are various types of membranes, the most used in industrial processes mainly involve: Microfiltration (MF), Ultrafiltration (UF), Nanofiltration (NF) and Reverse Osmosis (RO).

All these membrane are pressure-driven but they have different ranges of filtration. MF, UF and NF membranes have been developed to provide different levels of filtration for particles smaller than those caught by conventional filtration system. These are relatively new and are still being experimented, mainly for pre-treatment (Schenkeveld *et al*., 2004).

In Table 1.3 a summary of the different membranes processes is shown.

Table 1.3. *Summary of the characteristic of the different membrane processes (Al-Zuhairi, A., 2008).*

Process	Driving force [bar]	Separation principle	Main applications
Microfiltration	0.1 -1	Filtration	Bacteria filter water and wastewater treatment
Ultrafiltration	0.5 - 10	Filtration	Concentrating macromolecular solutions and water and wastewater treatment
Nanofiltration	5 - 20	Filtration – electrostatic interaction	Partial water softening
Reverse osmosis	8 – 100	Solution diffusion mechanism	Brackish and seawater desalination

The only process which can remove sodium chloride is Reverse Osmosis. A short introduction to RO technology is given in the following, while it is completely described in Chapter 2. In addition, also Electrodialysis, another membrane process, is used in desalination technologies.

1.1.2.1 Reverse Osmosis

Reverse osmosis is a process where pressure is used to push salt-water through a semi-permeable membrane that allows the passage of water and rejects salts. Advance in

Reverse Osmosis has been directly connected to the development of membrane technology. A good membrane should be able to allow the passing of high flux of water and limit the amount of salt flow. The energy required is directly linked to the salinity of the water being treated. The estimated cost of reverse osmosis is 0.8US$/$m^3$ (Van der Bruggen *et al.,* 2003).

1.1.2.2 Electrodialysis

Electrodialysis is the only desalination process which uses electricity as the fundamental process energy. An electric charge through the solution draw metal ions to the positive plate on one side, and anions migrate to the anode. Between anode and cathode there is a pair of membranes, one of which allows the passage of cations and the other one of anions. In this way between the two membranes a low salinity region is created (see Figure 1.7).

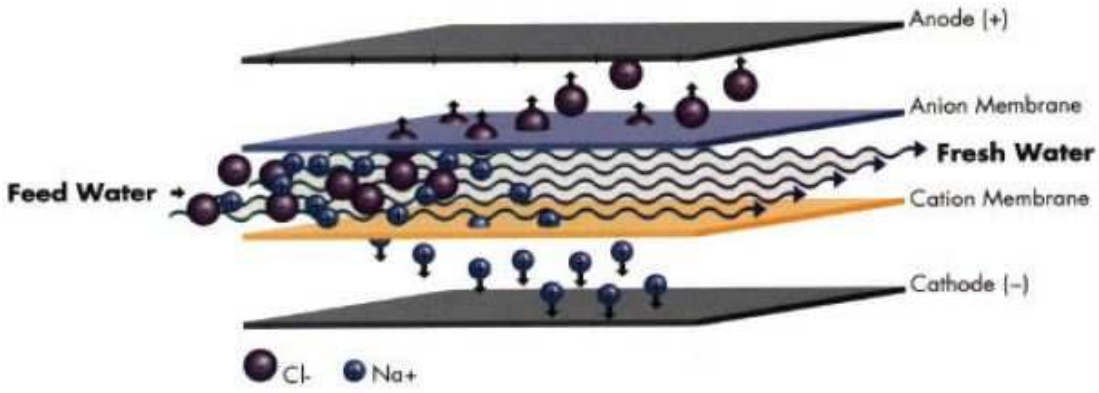

Figure 1.7. *Electrodialysis cell (Schenkeveld et al., 2004).*

An electrodialysis plant is built putting together a lot of electrodyalisis-cell, about 300. The membranes are about 1m^2 and are very tiny to reduce the electrical resistance. As in each membrane processes the feed-water has to be pre-treated before entering into the cells. Recent developments regard the periodically reversing of the charges. After a given time period the polarity of the electrodes is changed: this is called Electrodialysis Reversal (EDR). This technique reverses the flow through the membrane: there is a slight loss in productivity immediately following the change, but fouling (thin layer deposits over the membrane) is significantly prevented. The energy costs are directly proportional to the amount of salt removed. It means that ED and EDR processes are usually used only for brackish water application.

1.1.3 Comparison between thermal and membrane desalination processes

Thermal desalination is more energy intensive than membrane based desalination; however it better deals with more saline water and it can deliver even higher permeate quality (Fritzmann *et al*., 2007). Thermal processes are largely use in the Middle East, because of the wide availability of energy sources necessary to run the process. MFD requires more salt-water input than RO and maintenance costs are considerably high. MED is used only for smaller-scale desalination because the costs for large facilities are very high. MED and MFD require thermal input and electric power, while VCD require only electric power, because the thermal input is given by mechanical compression. RO necessitate salt-water pre-treatment to avoid fouling, scaling (formation of a thin layer of precipitated salts) and the degradation of the membrane. RO membranes are not favoured by: high salinity, high temperatures, high silt density, high bacteria activity and pollution. Otherwise it can be used with a large salinity range. ED is used only with low salinity waters because the electric energy required is directly proportional to salt concentration. On the other hand EDR membranes are less sensitive to fouling and there are no scale phenomena, so no anti-scaled chemical are required (Schenkeveld *et al*., 2004).

All in all, the advantages in using thermal desalination processes are the following (Mehdizadeh, 2006):

- suitability in dual process (power/water) plant;
- suitable for high-salinity waters;
- availability especially at low cost of energy;
- reliability and maturity;
- long operation experience;
- large-scale size units.

Advantages of membrane processes are (Mehdizadeh, 2006):

- low energy consumption;
- moderate costs (lower capital and operation costs);
- easier operation and maintenance;
- compact and modular units;
- faster delivery time of plant;
- advances in RO membranes and technology;
- decoupling of power and desalination plants (due to water demand growth factor of 11% over 4% of power);
- hybrid of three or more processes;
- ambient temperature processes.

The desalination processes are energetically expensive because of the second law of thermodynamic. Salt-water is a higher entropy system than salt-free water:

$$[H_2O] + [NaCl] \leftrightarrow [H_2O + NaCl] + E \ , \quad (1.1)$$

where E is the energy required: dissolution enthalpy, osmotic pressure, or ebullioscopy gradient. In real industrial processes the energy requirement is a little higher than the theoretical value due to the technology inefficient factor. It has been calculated that the power needed to desalinate salt water (25 °C and 35g/L of TDS) by reverse osmosis is 0.75kWh/m^3 (2.7kJ/m^3) (Rognoni, 2010).
It is interesting to compare this value with the necessary energy to evaporate water in thermal processes: the latent heat of vaporization of water at 100 °C and 1atm is about 2258kJ/kg (627kWh/m^3). Most of this energy is then recovered during condensation but the different energy efficiency is evident.
Energy requirement for thermal desalination processes is generally represented by the Performance Ratio (PR: units of water produced per unit of steam consumed), while for membrane processes, the Specific Energy Consumption (SEC: kilowatt hour per unit flow rate of product water) is used.
A comparison of the most important characteristics involved in the predominant desalination processes is shown in Table 1.4.

The recent world-wide trend is to improve and develop membrane processes technology because membrane desalination is less costly than thermal one and growth-possibility is promising. The current policy is to use RO plants for brackish water and hybrid MSF-RO plants for sea-water application (Mehdizadeh, 2006).
One emerging desalination process is Forward Osmosis (or direct osmosis). This technique involves the natural passage of the water through the membrane, due to the difference of the osmotic pressure from the salt water and a draw solution. Forward osmosis process and the novel Manipulated Osmosis Desalination (MOD) process are widely described in Chapter 3.

Table 1.4. *Comparison of predominant desalination processes (modified from Committee on Advancing Desalination Technology, 2008 and Schenkeveld et al., 2004)*

	SWRO[(1)]	MSF	MED	MVC[(2)]	BWRO[(3)]	ED
Operating temperature [°C]	<45	<120	<70	<70	<45	<43
Pre-treatment requirement	High	Low	Low	Very Low	High	Medium
Main energy form	Mechanical (electrical)	Steam (heat)	Steam (heat)	Mechanical (electrical)	Mechanical (electrical)	Mechanical (electrical)
Heat consumption [kJ/kg]	NA	250-330	145-390	NA	NA	NA
Performance ratio (PR)	-	8-10	12-14	-	-	-
Electrical energy use [kWh/m^3]	2.5-7	3-5	1.5-2.5	8-15	0.5-3	~0.5 per 1,000 mg/L of ionic species removed
Typical single train capacity [m^3/d][(4)]	<20,000	<76,000	<36,000	<3,000	<20,000	<12,000
Product water quality, TDS [mg/L]	200-500	<10	<10	<10	-	-
Per cent ion removal	-	-	-	-	99-99.5%	50-95%
Typical water recovery[(5)]	35-50%	35-45%	35-45%	23-41%	50-90%	50-90%
Reliability	Moderate	Very high	Very high	High	-	-

(1) Sea water Reverse Osmosis. (2) Mechanical Vapour Compression. (3) Brackish Water Reverse Osmosis. (4) For the purpose of this table, a train is considered a process subsystem which includes the high-pressure pump, the membrane array(s), energy recovery devices and associated instrumentation/control. (5) Water recovery = (produce water flow / raw water flow) x 100.

1.2 Osmotic pressure

Osmotic pressure has to be clearly defined in order to understand membrane processes. In nature, osmosis is a frequent phenomenon and it depends on the presence of a selective membrane: certain component of a solution (ordinarily the solvent) can pass through the membrane, while one or more of the other components are rejected. This type of membrane is called *semi-permeable membrane*.

Consider a system divided in two parts by a semi-permeable membrane, as shown in Figure 1.8. Compartment 1 contains pure solvent A (phase α), and compartment 2 contains a solution of solute B in the same solvent A (phase β). The membrane allows the passage of A but it is impermeable to B. When such a system is set up (Figure 1.8a), with equal liquid level in both sides, it is found that solvent A flows from compartment 1 to compartment 2 (Figure 1.8b). This flow is called osmosis and it is caused form the natural tendency to equalize the concentrations of each compartment.

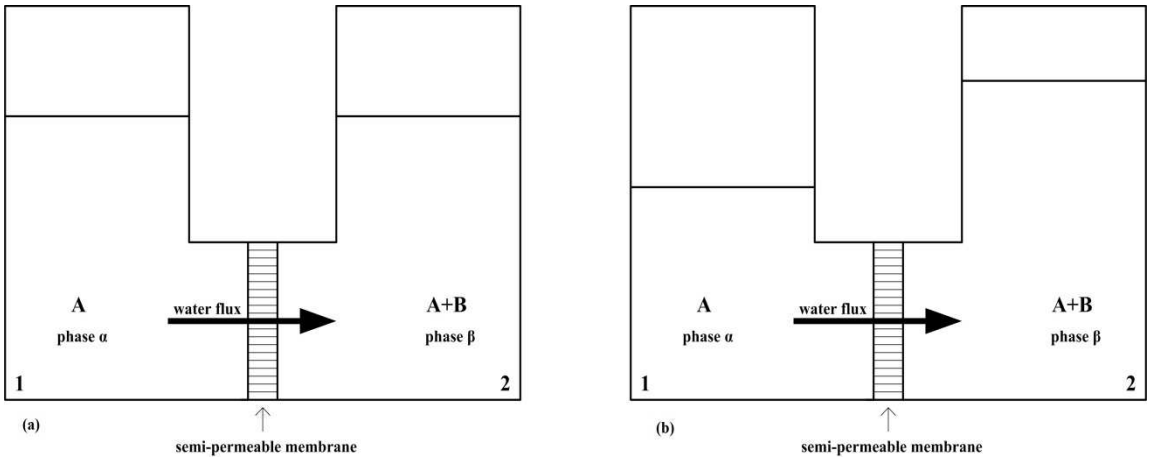

Figure 1.8. *Schematic diagram of osmosis phenomena.*

The flow of solvent A causes the rising of the level in side 2. The hydrostatic pressure of side 2 becomes higher than that on the pure solvent and it tends to generate an opposite flow form side 2 to side 1. Eventually, an equilibrium point is reached when the net flow through the membrane is null: the osmotic force is exactly balanced by the pressure difference. The pressure difference between the two sides required to produce zero flow of solvent is called *osmotic pressure*. It is a property of the solution and it does not depend on the membrane, if the membrane is truly semipermeable.

Solutions which have the same osmotic pressure are *isosmotic*. A solution is *hyperosmotic* than another one if its osmotic pressure is greater; meanwhile it is *hypoosmotic* in the opposite case. The flow goes always from the *hypoosmotic* solution to the *hyperosmotic* one. Two solution separated by a selective membrane are *isotonic* if the net flow is null. *Isotonic* and *isosmotic* are not synonymous: whether two *isosmotic*

solutions are also *isotonic* depends on the properties of the membrane, because it can allow the passage or rejection also of other species (Thain, 1967).

1.2.1 The thermodynamics of osmosis

A better definition of osmotic pressure is based on a thermodynamic function, the chemical potential of the solvent: '*the osmotic pressure of a solution is that pressure which must be applied to the solution to make the chemical potential of the solvent in the solution equal to that of the pure solvent at the same temperature.*' (Thain, 1967).
The chemical potential is defined by Gibb's equation,

$$dU = TdS - pdV + \sum_i \mu_i dN_i \ , \tag{1.2}$$

where U is the internal energy, T the temperature, S the entropy, p the pressure, V the volume, and μ_i and N_i respectively the chemical potential and number of moles of component i. By definition, the chemical potential is expressed in terms of the Gibbs free energy G:

$$\mu_i = \left(\frac{\partial G}{\partial N_i}\right)_{T,p,N} \ , \tag{1.3}$$

and also

$$v_i = \left(\frac{\partial \mu_i}{\partial \mathrm{p}}\right)_{T,p,N} \ , \tag{1.4}$$

where v_i is the partial molar volume of component i.
Considering Figure 1.8, there are two phases at the same temperature and with different concentration of solute B in the solvent A: phase α and phase β. The pressure in phase α is P, while the pressure in phase β is $P + \pi$. The equilibrium is reached when:

$$\mu_A^{\alpha} = \mu_A^{\beta} \ . \tag{1.5}$$

The chemical potential in a solution is given by:

$$\mu_A^{\alpha} = \mu_{pureA}^{\alpha}(T, P) \ , \tag{1.6}$$

$$\mu_A^{\beta} = \mu_{pureA}^{\beta}(T, P + \pi) + \mathrm{RT} \ln a_A \ , \tag{1.7}$$

where a is the activity, related to composition through $a_A = \gamma_A x_A$; γ is the activity coefficient of A and x_A its mole fraction. Assuming that the molar volume does not vary with pressure (incompressible fluid) and according with equation (1.4):

$$\mu_{pureA}(T, P + \pi) = \mu_{pureA}(P) + \pi v_{pureA} \ . \tag{1.8}$$

Equation (1.5) can be written as

$$\pi = -\frac{RT}{v_{pureA}} \ln a_A \ . \tag{1.9}$$

If the solution in compartment 2 is very diluted (there is little solute B), equation (1.9) can be further simplified: x_A is close to unity, so that also γ_A is close to unity, and $\ln(1 - x_B) = -x_B$. Equation (1.9) becomes:

$$\pi = -\frac{RT}{v_{pureA}} \ln x_A = -\frac{RT}{v_{pureA}} \ln(1 - x_B) = \frac{RT}{v_{pureA}} x_B \ . \tag{1.10}$$

If the solution is very diluted then $x_B \ll 1$, $n_B \ll n_A$ and $x_B \approx n_B/n_A$, where n is the number of moles. The total volume is $\approx n_A v_{pureA}$, and equation (1.10) becomes:

$$\pi = \frac{\mathrm{RT}\, x_B}{V} = \frac{RT\rho_B}{MW} \ , \tag{1.11}$$

where ρ_B is the mass concentration of solute B and MW is its molecular weight.
Equation (1.11) is called the Van't Hoff equation for osmotic pressure. Van't Hoff formulated a kinetic theory of dilute solutions. This theory is based on the analogy between dilute solutions and ideal gases: the osmotic pressure of a dilute solution is the same as the pressure which the solute would exert if it existed as a gas occupying the same volume as the solution (Thain, 1967).
Van't Hoff equation shows how osmotic pressure is directly proportional to the concentration of the solute molecules but it is independent of their type. The kinetic theory is based on two main assumptions: the solution is very dilute and it is incompressible. In this way van't Hoff equation is a limiting law, for finite concentration it is useful to write a series expansion in mass concentration ρ_B. (Praunsnitz, 1999):

$$\pi = RT\rho_B\left(\frac{1}{MW} + B\rho_B + C\rho_B^2 + \cdots\right) \ , \tag{1.12}$$

where B, C etc. are the osmotic viral coefficients. B represents intermolecular forces between two solute molecules.

The *osmolarity* of a solution regards the depression of the activity of the solvent. The osmotic pressure of a solution is not a 'real pressure' in the solution, but measures the depression of the solvent activity in the solution. In non-ideal solutions, the activity of the solvent depends on which solute is present and its concentration.

For non-ideal solutions Van't Hoff equation can be improved introducing the osmotic coefficient Φ, which considers the deviation from the ideal behavior. Furthermore if the solute associates or dissociates, the number of moles decrease or increase and also the osmotic pressure decreases or increases. Equation (1.11) becomes:

$$\pi = i_v \Phi \frac{RT\rho_B}{MW}, \tag{1.13}$$

where

$$\Phi = -\frac{x_A}{x_B} \ln a_A \ , \tag{1.14}$$

$$a_A = x_A \gamma_A \ . \tag{1.15}$$

and i_v is the Van't Hoff factor, which is the number of moles truly dissociated when one mole of solid solute is dissolved (e.g. for NaCl i_v=2).

1.2.2 Osmotic pressure properties

The osmotic pressure, that measures the activity of the solvent, can be related thermodynamically to other properties likewise dependent of the activity of the solvent: freezing-point depression, the depression of vapour solvent pressure, the elevation of boiling point. Furthermore the osmotic pressure can be used in many applications to calculate the molecular weight of the solute.

The aim of this paragraph is to show how osmotic pressure (π) change compared to: solute concentration (c_B), temperature (T) and molecular weight (MW). Secondly, the osmotic coefficient Φ is calculated for different solution using OLI's software (OLI System Inc. 2006) and van't Hoff relationship. The OLI System software predicts the properties of solution via thermodynamic modeling based on experimental data.

Figure 1.9 shows how osmotic pressure normally increases with concentration and with temperature. A solution of NaCl at 15, 25 and 35°C is been investigated using OLI's software.

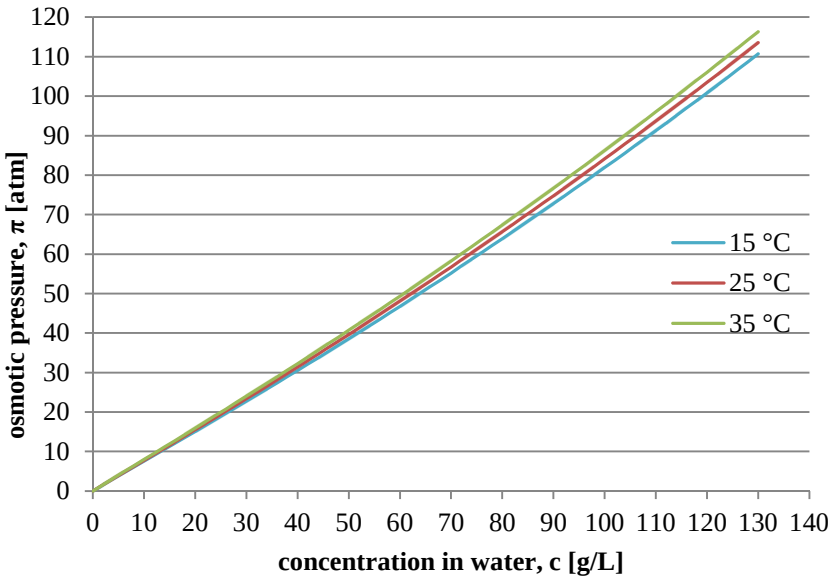

Figure 1.9. *The osmotic pressure π as a function of NaCl concentration in water at 15, 25, 35 °C. Values calculated using OLI's software (OLI System Inc., 2006).*

In Figure 1.10 a comparison is shown between the osmotic pressure of different types of salts. The osmotic pressure of NaCl (MW=58.443g/mol) is higher than those of KCl (MW=74.55g/mol) and $MgSO_4$ (MW=120.37g/mol). As the molecular weight increases, the osmotic pressure decreases.

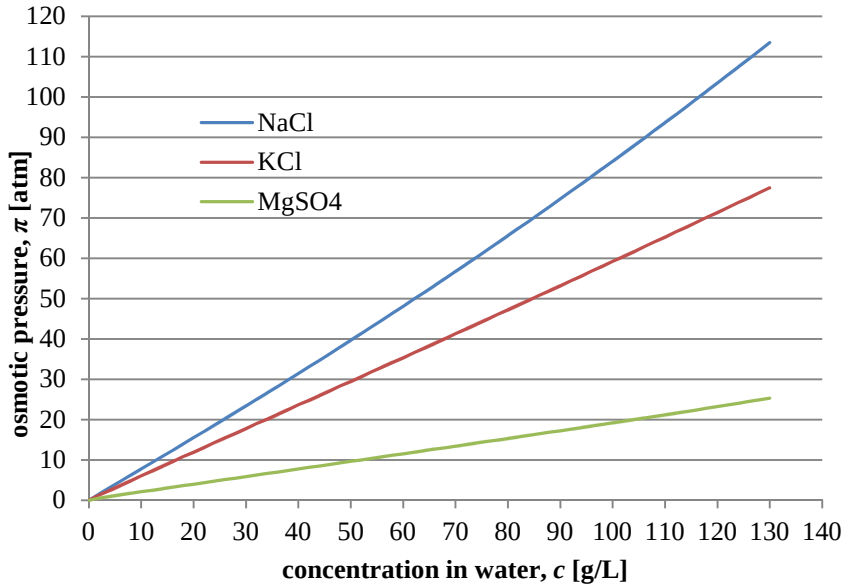

Figure 1.10. *The osmotic pressure π as a function of NaCl, KCl and $MgSO_4$ concentration in water at 25°C. Values calculated using OLI's software (OLI System Inc., 2006).*

The osmotic coefficient is also a function of temperature. While the osmotic pressure increases with increasing temperature (see Figure 1.9), the osmotic coefficient decreases with increasing temperature as shown in Figure 1.11. The osmotic coefficient has been

calculated from the ratio between the osmotic pressure values obtained with OLI's software, and the ideal π values obtained by van't Hoff relationship (eqn. (1.13) with Φ=1).

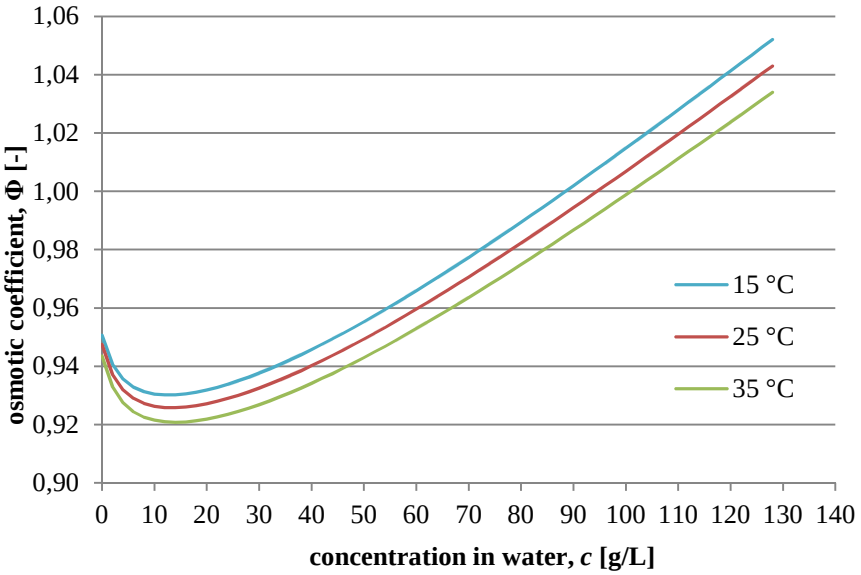

Figure 1.11. *The osmotic coefficient Φ as a function of NaCl concentration in water at 15, 25 and 35°C. Values calculated using OLI's software (OLI System Inc., 2006) and Eqn. (1.13) with Φ=1.*

In Figure 1.12 a comparison of the osmotic coefficient of two different salts (NaCl and $MgSO_4$) is shown.

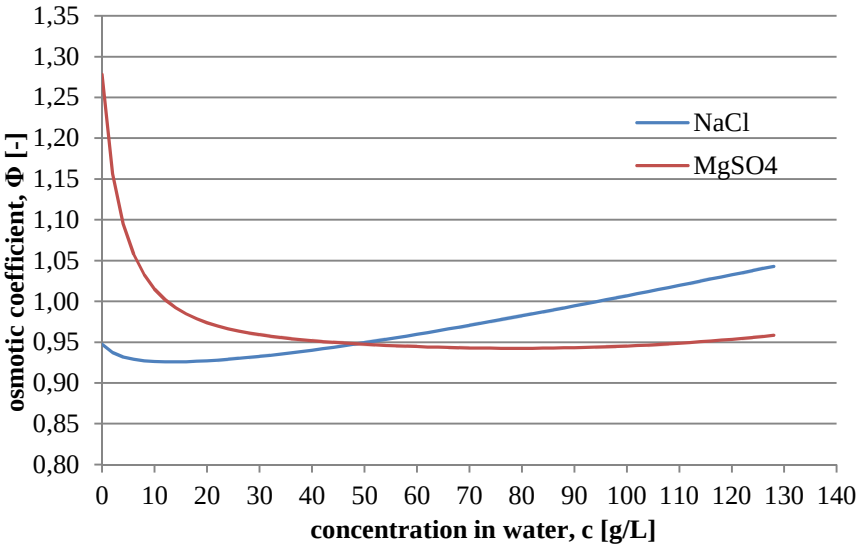

Figure 1.12. *The osmotic coefficient Φ as a function of NaCl and $MgSO_4$ concentration in water at 25°C. Values calculated using OLI's software (OLI System Inc., 2006).*

1.2.3 Osmotic pressure data verification

In this paragraph the osmotic pressure data calculated with OLI's software are compared with experimental data in order to validate OLI's calculation.

Water-sodium chloride verification

Figure 1.13 shows a comparison between π values of NaCl solutions in water at 25°C, calculated by OLI's software, van't Hoff relationship (Eqn. (1.13) with Φ=1) and Eqn. (1.13) with Φ from experimental data (Hamer & Wu, 1972). It is clear that van't Hoff relationship is valid at low salt concentration. At higher concentration the osmotic coefficient has to be considered in order to describe the non-ideal behaviour. In addition, it is evident that OLI's software calculations follow the experimental trend acceptably.

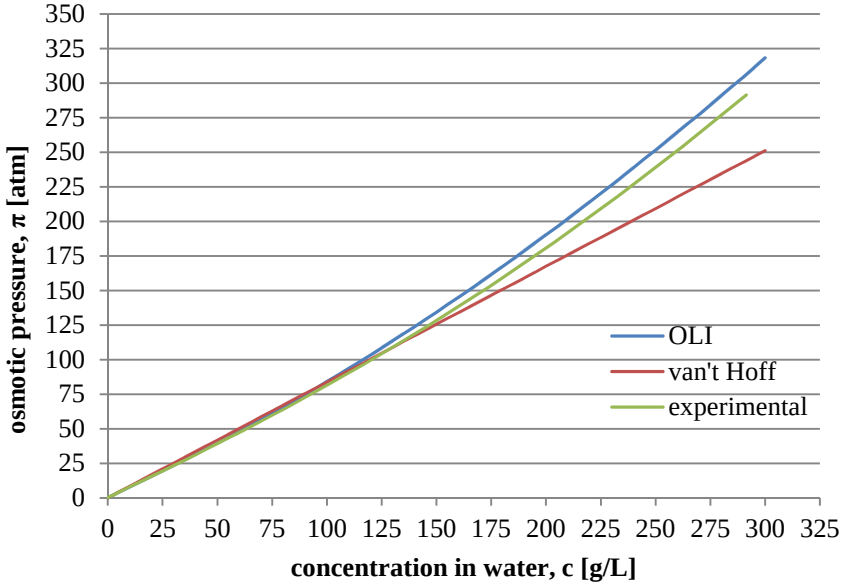

Figure 1.13. *The osmotic pressure π as a function of NaCl concentration in water at 25°C. Values calculated using OLI's software (OLI System Inc., 2006), Eqn. (1.13) with Φ=1 and Eqn. (1.13) with Φ from experimental data (Hamer & Wu, 1972)*

The errors between OLI's calculation and the experimental data are shown in Table 1.5 and calculated with the following equation:

$$e[\%] = \frac{\pi_{exp} - \pi_{calc}}{\pi_{exp}} 100 \ . \qquad (1.16)$$

The percentage error at the sea concentration (about 40 g/L) is 7.67%. So that means that OLI's software can be used to calculate the osmotic pressure of water-sodium chloride solutions for reverse osmosis processes.

Table 1.5. *Percentage errors between water-NaCl π experimental data and OLI's calculation.*

c[g/L]	π_{exp}[atm]	π_{calc}[atm]	e[%]
0.06	0.05	0.05	0.91
5.83	4.56	4.87	6.86
40.79	31.68	34.11	7.67
104.89	85.61	87.72	2.47
174.81	153.24	146.21	-4.59
262.22	253.61	219.31	-13.53

Water-ethanol verification

There are no experimental data available about the osmotic pressure of ethanol in water to make a direct comparison with OLI's simulations. However, it is possible to obtain water activity coefficients values from Aspen Plus® (Aspen Technology, Inc.). The activity coefficients are calculated by the NRTL model, which uses model parameters obtained from a regression of experimental data. Subsequently, the water activity is calculated from Eqn. (1.15), the osmotic coefficient from Eqn. (1.14) and finally the osmotic pressure from Eqn. (1.13).

Figure 1.14 and Figure 1.15 show a comparison between π values of different ethanol solutions in water at 25°C, calculated by OLI's software, van't Hoff relationship (Eqn. (1.13) with Φ=1) and Eqn. (1.13) with Φ calculated from Eqn. (1.14 and 1.15).

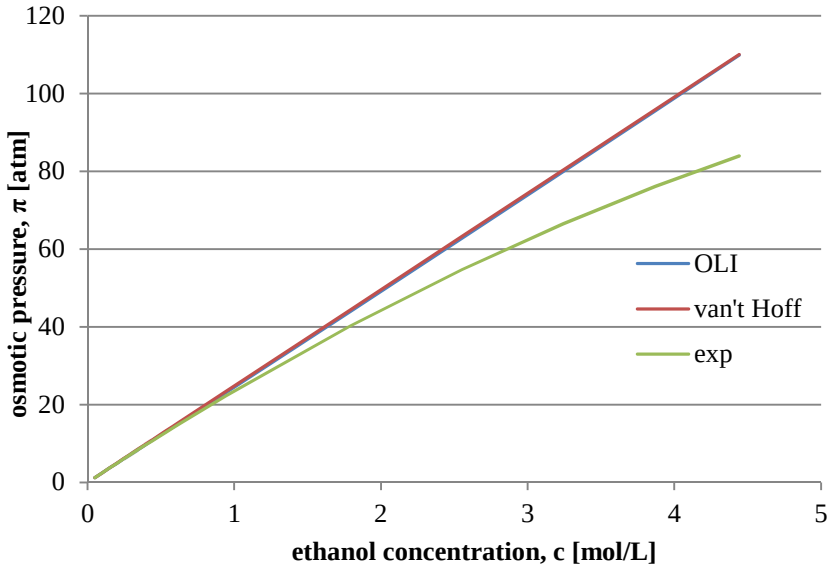

Figure 1.14. *The osmotic pressure π as a function of ethanol concentration [0-4.5mol/L] in water at 25°C. Values calculated using OLI's software (OLI System Inc., 2006), Eqn. (1.13) with Φ=1 and Eqn. (1.13) with Φ calculated from Eqn. (1.14 and 1.15)(γ from experimental data, Aspen Plus®).*

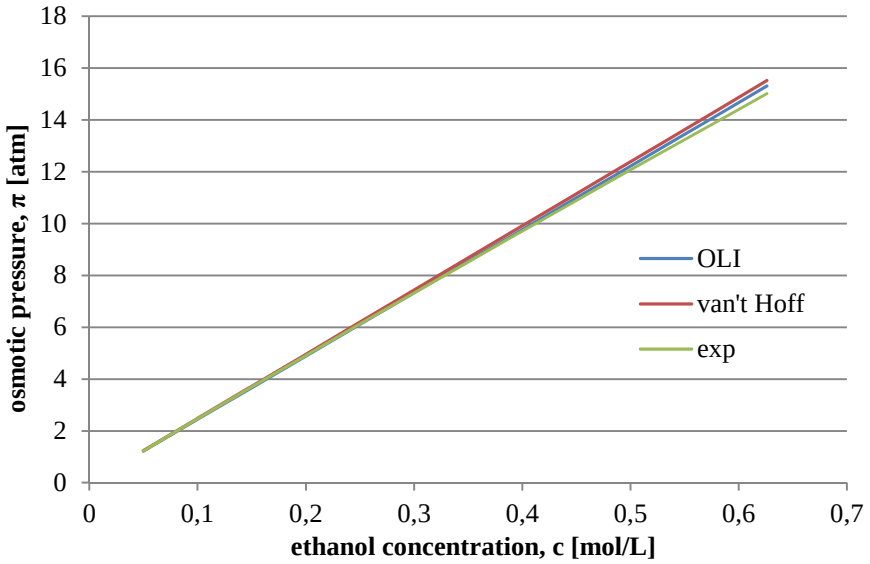

Figure 1.15. *The osmotic pressure π as a function of ethanol concentration [0-0.63mol/L] in water at 25°C. Values calculated using OLI's software (OLI System Inc., 2006), Eqn. (1.13) with Φ=1 and Eqn. (1.13) with Φ calculated from Eqn. (1.14 and 1.15)(γ from experimental data, Aspen Plus®).*

From Figure 1.14 it is evident that OLI's software simulation follows the trend of van't Hoff relationship, reaching the maximum error of about 30% from the calculation based on the experimental activity data for an ethanol solution of 4.5mol/L. It seems that the osmotic coefficient correction on the osmotic pressure is not included in OLI's calculations.

However, it is clear from Figure 1.15 that van't Hoff relationship, OLI's software calculations and the calculation based on the experimental activity data follow the same trend for the ethanol concentration range used in the experimental work, with a maximum error of 1.95% at 0.63mol/L.

Chapter 2

Reverse Osmosis process

The aim of this chapter is to describe Reverse Osmosis desalination process, from the basic principles to the trends towards the future, passing through the plant technology.

2.1 General principles

Osmosis is a natural phenomenon in which a solvent passes through a semipermeable membrane from the side with lower concentration of solute (compartment 1) to the side with higher solute concentration (compartment 2) (see Figure 2.1a). The driving force is the gap between the chemical potential of the two sides. At equilibrium this flow is null and the pressure different between the two sides is called osmotic pressure. If a hydrostatic pressure higher than the osmotic pressure is applied to compartment 2, a reverse flow of solvent, opposite to the natural osmotic flow, is generated from compartment 2 to compartment 1. This is called Reverse Osmosis (see Figure 2.1b).

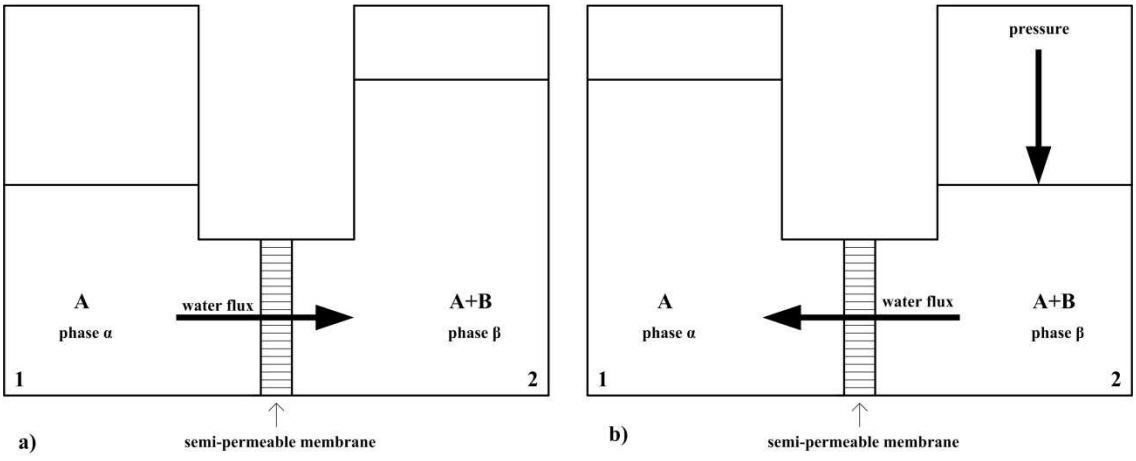

Figure 2.1.*Schematic diagram of (a) direct osmosis and (b) reverse osmosis phenomena.*

The result of reverse osmosis phenomenon is the growing of the concentration of solute in compartment 2 and the diluting of the solution in compartment 1.

Reverse Osmosis is used in a large number of applications; the most important use is desalination. The membrane ideally rejects all colloidal and dissolved matter from an

aqueous solution (e.g. brackish water or sea-water), producing a permeate stream, which consist in almost pure water, and a concentrate brine stream. In Figure 2.2 a schematic diagram of a membrane system is shown. The concentration c [kg/m^3] refers to the solute and q [m^3/s] is the volumetric flow rate.

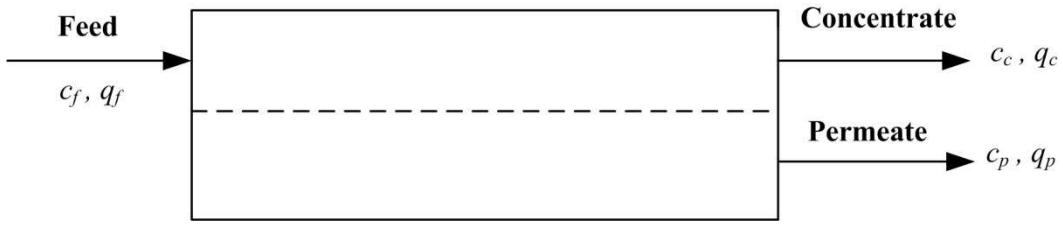

Figure 2.2.*Schematic diagram of a membrane system.*

There are some important parameters to know about membrane processes. The first one is the recovery or yield (S). It is a measure of the fraction of the feed flow which passes through the semipermeable membrane:

$$S \equiv \frac{q_p}{q_f} \ . \tag{2.1}$$

The second parameter is the volume reduction (VR) that indicates how much the brine is concentrated:

$$VR \equiv \frac{q_f}{q_c} \ . \tag{2.2}$$

The last parameter is the retention or rejection (R). It is a measure for the quantity of solute rejected by the membrane:

$$R \equiv \frac{c_f - c_p}{c_f} = 1 - \frac{c_p}{c_f} \ . \tag{2.3}$$

2.2 Reverse osmosis membranes

Reverse osmosis could appear similar to filtration, because both processes involve removing liquid from a mixture by passing it through a device that only allows the passage of the solvent. However there are important differences between RO and any kind of filtration. The most important is the osmotic pressure itself. RO processes are based on applying a hydrostatic pressure higher than the osmotic pressure. On the

contrary, the osmotic pressure is negligible in ordinary filtration. A second difference is that filtration processes are continuous processes meanwhile in RO processes the removing of the solvent cause the rising of the concentration of the brine and an according rising of the osmotic pressure. Moreover, the membrane in RO processes has to be supported in order to reach the necessary mechanical strength. Finally, the main difference is the smaller particle size which can be separated by RO in comparison with the other pressure driven membrane separation processes used in water treatment, as it is indicated in Figure 2.3.

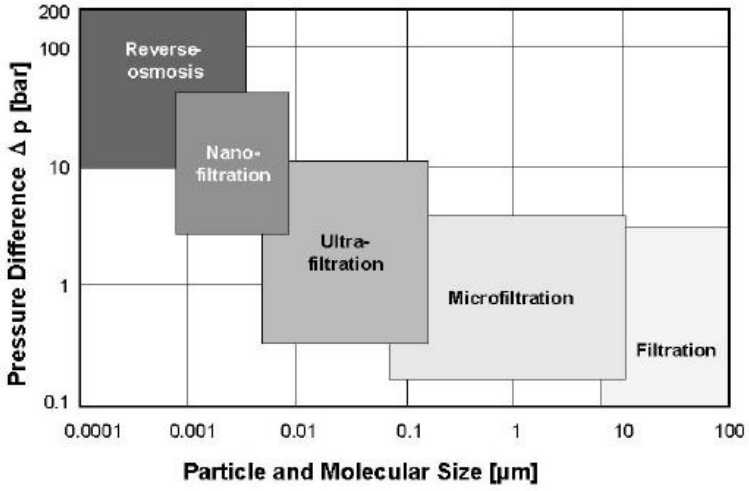

Figure 2.3.*Separation capabilities of pressure driven membrane separation processes (Fritzmann et al., 2007).*

2.2.1 Types of membrane

There are several types of membrane for RO processes. In order to reach an efficient desalination, membranes should allow a high flux and keep high rejection. The flux is inversely proportional to the thickness of the membrane. The first commercial membrane was cellulose-acetate (CA). One of the disadvantages of using CA membrane is that it can be deteriorated by hydrolysis, for this reason a rigid pH control has to be applied to maintain the pH around the value of 4-5. In addition, at high pressure, CA membranes tend to decrease the overall performance. This kind of membrane is still commercially available but the current trend is to use composite membranes (TFC: Thin Film Composite). These membranes are produced by interfacial polymerization and are made of a thin active layer of polyamide (<1µm), and a porous support of different material (50-100 µm), usually micro- or ultrafiltration membrane made of polysulphone (asymmetric membrane). TFC membranes are physically and chemically more stable than CA membranes: high resistance to bacterial degradation, no hydrolysation, less influence of membrane compaction and stability in a wider range of pH. However TFC membranes are inclined to fouling (thin layer deposits over the

membrane) more than CA membrane; moreover they can be deteriorated by a small amount of chlorine. In Table 2.1 the main differences between CA and TFC membranes are summarized (Fritzmann *et al*., 2007).

Table 2.1. *Membrane characteristics (modified from Fritzmann et al., 2007 and Norman, N., 2008).*

	Cellulose acetate (CA)	**Thin-Film-Composite (TFC)**
pH value	4 - 5	3 - 11
Continuous free chlorine	< 1mg/L	200 – 1000 ppm/h tolerance
Bacteria	not resistant	resistant
Free oxygen	resistant	resistant
Hydrolysis	yes	no
Salt rejection	up to 99.5%	> 99.6%
Net Driving Pressure (NDP)	15-30 bar	10-15 bar
Surface charge	neutral	anionic
Cleaning frequency	months to year	weeks to month
Pre-treatment	low (SDI(1) < 5)	high (SDI < 4)
Organics removal	relative lower	high

(1)Silt Density Index (SDI).It is a measure of the potential of fouling.

A possible future alternative to TFC membrane is ultrahigh-permeability membranes. These types of membranes allow a very high flux, reducing the pressure needed to drive permeation. However there are no experimental studies that demonstrate, for these membranes, an adequate salt rejection for the desalination processes (Elimelech, *et al*., 2011).

There are two main types of membrane module used in RO desalination plants: hollow fibre and spiral wound modules (SWM). Hollow fibre reverse osmosis membranes have an optimal membrane area to volume ratio. Figure 2.4 shows a hollow fibre module. It is formed by millions of asymmetric fibres contained in a cylindrical vessel and both ends are epoxy sealed. The feed flows in a perforate plastic tube and distributes radially around the fibres. The permeate flows from outer side to inner side of hollow fibre core or vice versa. Product water recovery per element is about 30%.

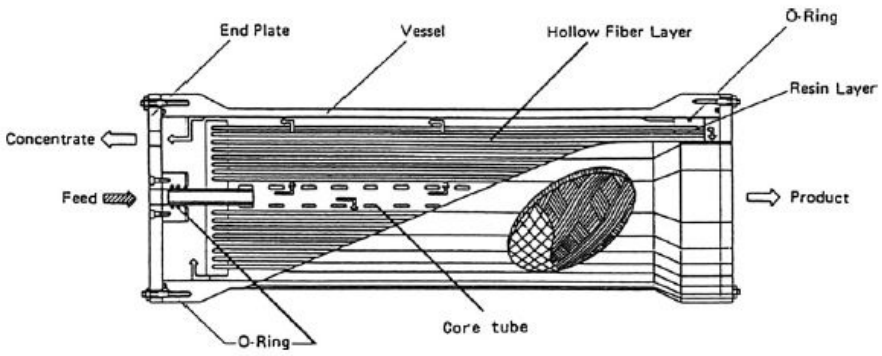

Figure 2.4. *Flow through a hollow fiber module (Kumano et al., 2008).*

This type of membrane is available in the market; however the most installed membranes in recent RO plants are spiral wound modules. SWMs offer a good equilibrium in terms of permeability, fouling control, packing density and ease of operation. In Table 2.2 there are the main advantages and disadvantages of SWM.

Table 2.2. *Advantages and disadvantages of SWM (Fritzmann et al., 2007).*

Advantages	**Disadvantages**
Cheap and relatively simple production	High feed side pressure loss
High packing density <1000 m^2/m^3	Susceptible to fouling
High mass transfer rates due to feed spacers	Hard to clean

In Figure 2.5 the flow through a spiral wound module is described. SWM are formed of several flat sheet membranes glued and rolled up in order to form a cylinder with feed channels and permeate spacer between each sheet. The permeate passes through the membrane from the feed channels to the permeate channels and flows in these spaces from the edge to the centre where it is gathered by a collector tube. Instead, the concentrate brine is rejected from membrane and leaves the membrane module on the opposite side. Feed channels create eddies which reduce concentration polarization (accumulation of dissolved and particulate matter in front of the membranes) and consequently increase mass flow through the membrane. On the contrary, feed channels raise the necessary hydrostatic pressure. An optimal dimension for feed channel was found to be between 0.6 and 1.5 mm, and for permeate channels between 0.5 and 1 mm. Generally a single SWM has a recovery of 5% to 15% and 0.5 bar of head pressure loss. Usually 4 to 8 elements are placed in series in a pressure vessel (Fritzmann *et al.*, 2007).

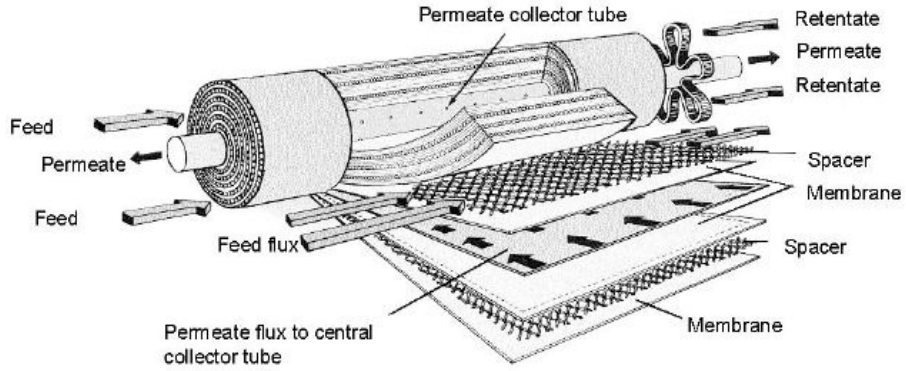

Figure 2.5. *Flow through a spiral wound module (Fritzmann et al., 2007).*

2.2.2 Mass transfer

In any membrane processes the characteristic of the flow are functions of the membrane polymer. For instance different membranes have different area and thickness and consequently a diverse set of RO parameters is applied. The flux of water across the membrane has to face a series of resistances: the intrinsic material of the membrane and the concentration polarization resistances (Figure 2.6).

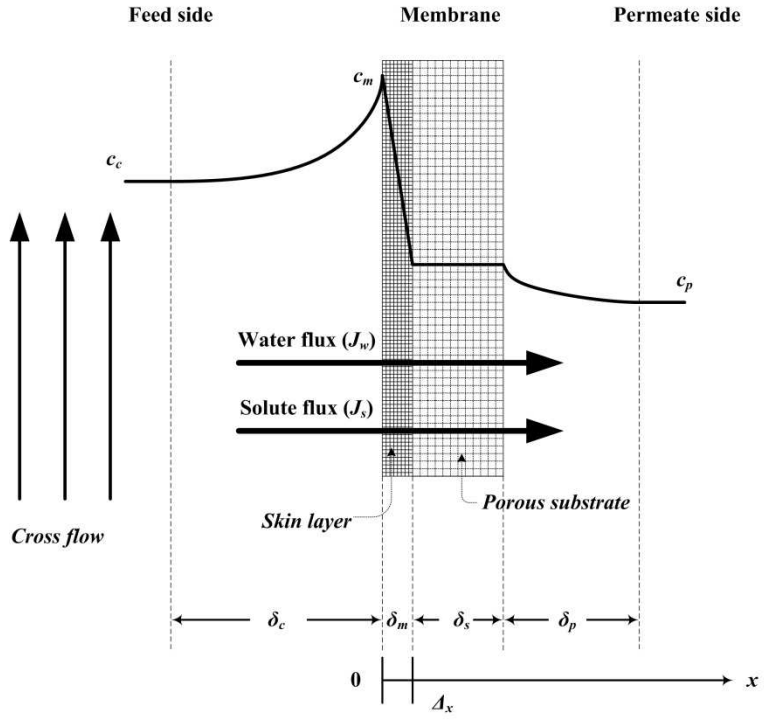

c_c : salt concentration in the feed-concentrate bulk side

c_m : salt concentration at the membrane interface in the feed side

c_p : salt concentration in the permeate bulk side

δ_c : concentration boundary layer thickness feed side δ_s : pouros substrate layer thickness

δ_p : concentration boundary layer thickness permeate side δ_m : active skyn layer thickness

Figure 2.6.*Concentration profile through a RO membrane.*

The concentration polarization (CP) is an accumulation of dissolved and particulate matter in front of the membrane. This phenomenon generates a thin highly concentrate layer liable of the resistance outside of the membrane: the boundary layer. Thus, lead to a diffusive back flow from the membrane to the bulk. Usually, also a thin permeate side boundary layer could occurs, when the solute flux is considerable. However, this resistance can be neglected in the mass transfer calculation. Concentration polarization has several negative aspects (Fritzmann *et al.*, 2007): (1) rejection decrease; (2) possibility of salt precipitation; (3) water flux decrease because osmotic pressure increases; (4) possibility of cake formation on the surface of the membrane. Concentration polarization is induced by high permeate fluxes and low velocity in the feed channels.

The extent of concentration polarization can be calculated with the following equation:

$$\frac{c_m - c_p}{c_c - c_p} = \exp\left(\frac{J_w}{k}\right) \quad , \tag{2.4}$$

where c_m is the concentration at the membrane surface, c_p and c_c the concentration on the permeate and the feed bulks, respectively, and k is the mass transfer coefficient. k values can be estimated by a Sherwood correlation (Fritzmann *et al.*, 2007):

$$\mathrm{Sh} = \gamma_1 Re^{\gamma_2} Sc^{\gamma_3} \quad . \tag{2.5}$$

It is possible to discriminate two different mass transfer involved in RO process: one inside the membrane and one outside it. There are a lot of different models that relate the permeate flux and the rejection to the main process variables (pressure, temperature and solute concentration) for a given membrane. Each model considers only the dense skin layer and ignores the small resistance of the porous substrate. In this paragraph only a brief description of the general principles of mass transfer models is given.

As regards mass transfer inside the membrane models, they can be divided in two main categories (Soltanieh& Gill, 1981):

- models based on non-equilibrium or irreversible thermodynamics (IT): there is no need of membrane structure information because membrane is bypassed, it is like a black-box in which slow processes take place near equilibrium;
- structural models: it is assumed a mechanism of transport, the flux is related to the forces of the system, the physicochemical properties of the membrane and the characteristics of the solution are involved in the transport model, and the membrane performance can be predicted without experimental data. It is possible to distinguish homogeneous model from porous model. In homogeneous model the membrane is assumed to be non-porous and the

transport takes place between the interstitial spaces of the polymer chains by diffusion. On the contrary in porous models the transport takes place through the pores by both convection and diffusion.

As regards the mass transfer models outside the membrane, it is possible to use the boundary layer theory. The boundary layer is idealized as a thin liquid film in which eddy motion is assumed to be negligible and therefore mass transport takes place by molecular diffusion alone. The concentration profile outside the membrane is shown in Figure 2.6. The bulk concentration (c_c) is assumed to be constant, without any gradient, because of the turbulence of the bulk feed. Concentrations gradient are present only in the boundary layer: all the mass transfer resistances are due to the laminar film.

Currently know models for mass transfer in RO system separate the transport phenomena inside the membrane from those outside the membrane. Thus, the interaction between the membrane phase and the fluid phase is mostly disregarded. In order to solve this problem a new model is being tested: the Solution-Diffusion Pore-flow Fluid-Resistance (SDPFFR) model. This model is intended to describe the whole system and provide an alternative at the classical CP models (Toffoletto, M., 2010).

2.2.2.1 Solution Diffusion Model

The most commonly model used to predict salt and water flows through the membrane in RO processes is the Solution Diffusion Model (SDM). This model is based on the following assumptions (Fritzmann *et al*., 2007):

- the active membrane layer is dense and without pores, the permeate dissolve in membrane phase;
- in steady-state conditions there is chemical equilibrium at the phase interface (membrane-feed and membrane-permeate side);
- salt flux depends on concentration gradient, not on pressure;
- water and salt flux are independent each other;
- water concentration and water diffusion coefficient across the membrane are constant.

According to SDM assumptions, the driving force of the process can be divided in two parts: the concentration gradient and the pressure difference between the permeate side and the feed side. At low salt concentration the pressure gradient is negligible, furthermore only a pressure difference (Δp) between the two sides causes a water flux through the membrane, because the water concentration inside the membrane is assumed to be constant.

The salt flux (J_s) and the water flux (J_w) can be determined as following:

$$J_w = A_w(\Delta p - \Delta\pi) \ , \tag{2.6}$$

$$J_s = B_s(c_{s,f} - c_{s,p}) \ , \tag{2.7}$$

$$\Delta \mathrm{p} = \frac{P_f + P_c}{2} - P_p \ , \tag{2.8}$$

$$\Delta \pi = \frac{\pi_f + \pi_c}{2} - \pi_p \ , \tag{2.9}$$

where $c_{s,f}$ is the salt concentration in the feed, $c_{s,\mathrm{p}}$ is the salt concentration in the permeate, A_w and B_s are model parameters that involve mass transfer coefficients (respectively solvent and solute membrane's overall permeability) to be determined by experiments, $\Delta \mathrm{p}$ is the average of the trans-membrane hydraulic pressure difference, $\Delta \pi$ is the osmotic pressure difference, and the subscripts f, c and p refer to the feed, concentrate and permeate stream, respectively. $(\Delta p - \Delta \pi)$ is called the Net Applied Pressure (NAP). The solute rejection can be expressed as:

$$\frac{1}{R} = 1 + \left(\frac{B_s}{A_w}\right) \frac{1}{\Delta P - \Delta \pi} \tag{2.10}$$

Proper result is given by SDM models at low concentration of salt. At high concentration is necessary to use models which consider the interactions between solute and solvent (e.g. ESDM: Extended solution diffusion model).

2.3 Reverse osmosis plants

Nowadays, over 17,000 desalination plants are in operation worldwide, and approximately 50% of those are RO plants (Greenlee *et al.*, 2009). In Figure 2.7 is shown a general flow sheet of a RO plant. It consists typically in several key components (Fritzmann *et al.*, 2007): (1) water abstraction, (2) pre-treatment, (3) pumping system, (4) membrane separation unit, (5) energy recovery system, (6) post treatment and (7) control-system.

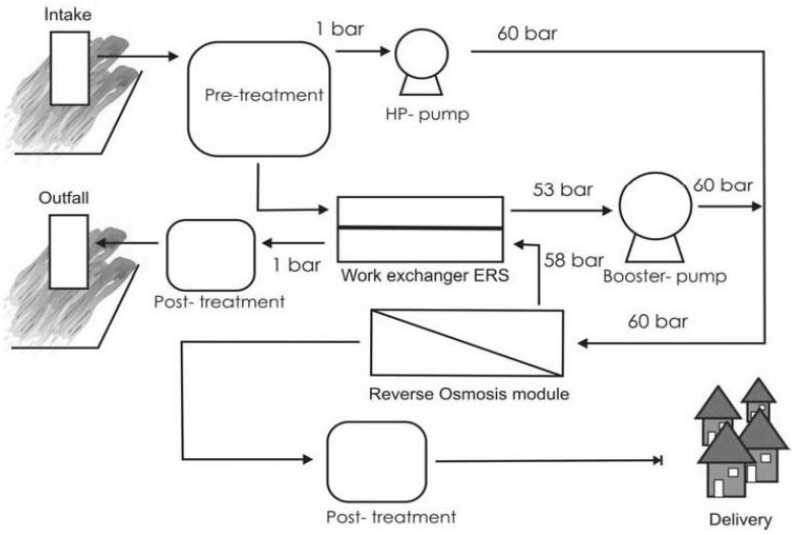

Figure 2.7. *Schematic flow sheet of a RO desalination plant (Fritzmann et al., 2007).*

(1) Water abstraction.

The abstraction of the seawater can be realized through coast or beach wells, or open seawater intake. The quality of the water in terms of turbidity, algae and total dissolved liquid is better in coast or beach wells because of the slow sand filtration. However seawater intake requires less space and is usually used for large plants. In brackish water desalination plants, wells are utilized to abstract the feed water. Generally brackish water sources are ground waters, low particulate and colloidal contaminants are suspended, and the salinity is lower than seawater.

(2) Pre-treatment.

A high general performance of RO plants can be reached if membrane fouling is prevented or at least restricted. The aim of pre-treatment system is to provide to membrane separation units a high quality feed water in order to maintain high performance levels, to reduce fouling potential (thin layer deposits over the membrane), and to minimise scaling (formation of a thin layer of precipitated salts on the membrane surface). A high quality feed water is characterized by a value of the Silt Density Index (SDI) minor than three. SDI is a measure of the potential of fouling produced by fine suspended colloids. There are two possible types of pre-treatment system: conventional pre-treatment and membrane pre-treatment. The conventional pre-treatment consists in chemical and physical pre-treatment without the use of any membrane technology. Generally it involves: chlorination to disinfect the water, coagulants and flocculants addition, pH adjustment consistently with the type of membrane, media filtration, cartridge filtration, antiscaling agent addition and dechlorination to prevent membrane

degradation. However fluctuations of feed water quality, difficulties to reach a constant SDI<3.0, difficulties to remove particles smaller than 10-15 µm, large footprint due to slow filtration velocities and negative influence of coagulants agent on membrane performance are the reason why the new trend in pre-treatment system is to use membranes. MF and UF membrane are used in pre-treatment system after a rough filtration by mechanical screen. This kind of pre-treatment is becoming very competitive for the following reason: no fluctuation of feed water quality; particles, bacteria, colloidal materials are rejected by MF and UF membrane producing a feed water with SDI<2 and turbidity less than 0.5 NTU (Nephelometric Turbidity Units), and reducing the frequency of RO membranes cleaning and replacement (Greenlee *et al.*, 2009 and Fritzmann *et al*., 2007).
In Table 2.3 the chemicals used in pre-treatment are summarized.

Table 2.3. *Chemical used in pre-treatment (Fritzmann et al., 2007).*

Pre-treatment	Purpose	Chemicals added	Fate of chemicals
pH adjustment	lower carbonate concentration, protect membrane from hydrolysis	acid (H_2SO_4)	sulphate stays in concentrate, pH decrease
antiscalants	prevent formation of membrane scaling	sequestering agent dispersants	complexes formed stay in concentrate
coagulation-filtration	prevent membrane fouling and clogging	coagulants-flocculants	flocs settle, removal by filtration
disinfection	prevent biological fouling	chlorine (or UV)	forms hypochlorite, chlorination by-products
dechlorination	protect chlorine sensitive membranes	sodium bisulphate	sulphate and chloride generated stay in concentrate

(3) Pumping system and (4) membrane separation unit.

The pumping system is the main energy using step in a RO plant. Figure 2.8 shows qualitatively how energy consumption is spilt in each step of the process. The power required to the membrane separation unit depends on feed pressure, salt concentration and flow rate. The higher these parameters are the greater is the pumping power required to produce the desired permeate flux. Moreover, as the recovery increases, the osmotic pressure and also the pumping energy requirement increase. However, as the recovery increases, the feed flow required decreases and consequently also the pumping

power. Thus, a minimum energy requirement exists, generally at a recovery between 45 and 55% (Figure 2.9, Greenlee *et al.*, 2009).

Furthermore, the feed pressure required fluctuates due to the degree of membrane fouling and scaling, feed water salinity, membrane compaction and temperature. Thus, a flexible pumping system with a variable frequency drive is recommended in order to keep to pressure of the system at the same optimum level.

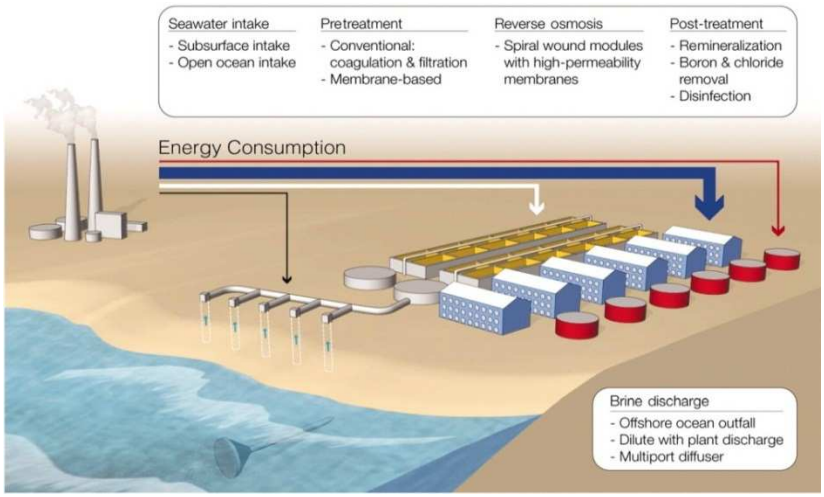

Figure 2.8. *Energy consumption distribution in a RO plant (Menachem, 2011).*

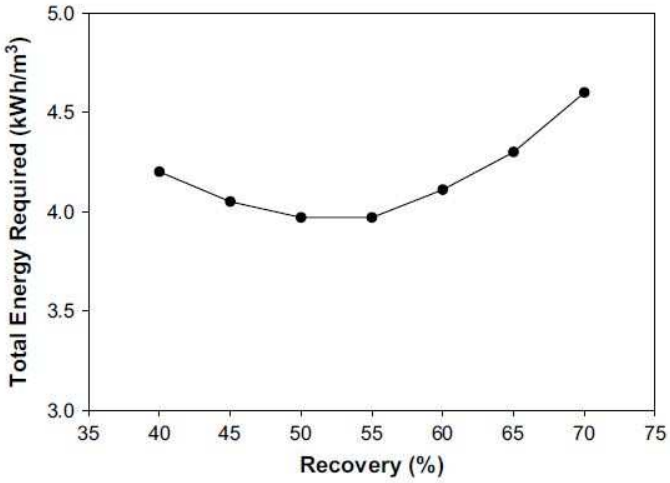

Figure 2.9. *Total energy required per volume of permeate produced as function of RO system recovery (Greenlee et al., 2009).*

A comparison of typical parameter values of SWRO and BWRO is shown in Table 2.4. The parallel system of pressure vessels is often called skid or train. RO desalination plants usually operate using 1-4 passes (the permeate of a RO skid is the feed of the next one in the series) or stages (the concentrate of a RO skid is the feed of the next one in the series). Each pass or stage is formed by multiple pressure vessels operating in parallel. In every pressure vessel there are 6-8 membrane elements. The choice between passes, stages and their number is not simple and depends on several factors as: energy

cost, plant cost, feed water characteristic (temperature, composition and TDS), desired characteristics of product water and desired recovery. For example, generally temperature can vary between 12°C to 35°C; an increase of 1°C can increase the salt permeability of 3-5%. Thus, if high feed water temperature are expected, multiple passes may be necessary to reach the desire water product.

Table 2.4. *A comparison of typical parameter values for seawater RO and brackish water RO (Greenlee et al., 2009).*

Parameters	Seawater RO	Brackish water RO
RO permeate flux [L/(m^2 h)]	12-15 (open water intake) 15-17 (beach well)	12-45 (groundwater)
Hydrostatic pressure [bar]	55-80	6-30
Membrane replacement	20% per year Every 2-5 years	5% per year Every 5-7 years
Recovery [%]	35-45	75-90
pH	5.5-7	5.5-7
Salt rejection [%}	99.4-99.7	95-99

Seawater desalination plants are often operated with one or two passes; each pass could be formed by one or more stages. Most of RO plants are designed to product fresh water with less than 500 mg/L TDS for potable water production. If the TDS required is lower (for instance for industrial production purposes) (300-400 mg/L) at least two passes are necessary; in the second pass the recovery increases because the feed is the permeate of the first one. Seawater RO plants are the 25% of total RO plants and various design options are available for a multi-pass seawater RO system (Greenlee *et al*., 2009):

- two-pass system: the first pass is a high-pressure seawater RO membrane (35-45% recovery) and the second is a low pressure brackish water RO membrane (85-90% recovery). Usually the concentrate of the second pass is recycled to the front of the first pass to minimizes the waste and increase water quality;
- alternative two-pass system: a portion of high salinity permeate (take at the end of the membrane element where salt flux through the membrane is higher due the higher concentration of the feed) is taken as the feed of the second pass; while the other low salinity portion is collected directly as product water. The overall power consumption is lower because only a portion of permeate is pumped to the second pass;
- four-pass system: one plant exists in Ashkelon (Israel); that is the world's largest RO desalination plant. Four passes permits to obtain high quality permeate.

Brackish water RO plants are the 48% of the total number of RO plants, and tend to be smaller in production capacity than seawater RO plants. The basic system design is different from seawater RO plants because usually in BWRO plants, stages are used. Brackish water has lower TDS concentrations than seawater and this allow reaching higher recoveries, by recovering other permeate from the concentrate stream of the first stage. Several design alternatives are (Greenlee *et al*., 2009):

- two-stage system: each stage has a recovery of 50-60% for an overall system recovery of 70-85%;
- three-stage system: the third stage is used to increase the recovery or to remove recalcitrant contaminant (e.g. boron);
- NF membrane in series following the RO system to treat the RO concentrate and increase the overall recovery. Then RO and NF permeate are then blended together.

One of the limiting factors of BWRO plants is the cost of concentrate disposal in inland desalination plants. Thus, some new technologies have been studied and proposed to solve this problem, recovering more product water (Greenlee *et al*., 2009):

- pre-treatment through compact accelerated precipitation softening (CAPS) which removes most of the calcium and allows an high recovery;
- interstage precipitation between two RO units to avoid scaling;
- seawater RO membrane treatment of brackish water RO concentrate;
- crystallizer-UF treatment of brackish water RO concentrate;
- treatment of the concentrate for specific salt recovery using pH changes and salt precipitation.

Figure 2.10 shows schematic array configurations for an RO process. The simplest plant design is based on the series array configuration, which is limited by feed fouling potential and restrictions on pressure head loss. For higher plant through-put, multiple housings are utilized in parallel. If feed side flow rates are considerably reduce by permeation and fall below the minimum requirements, the tapered array configuration can be applied to maintain a similar feed/concentrate flow rate per vessel through the length of the system.

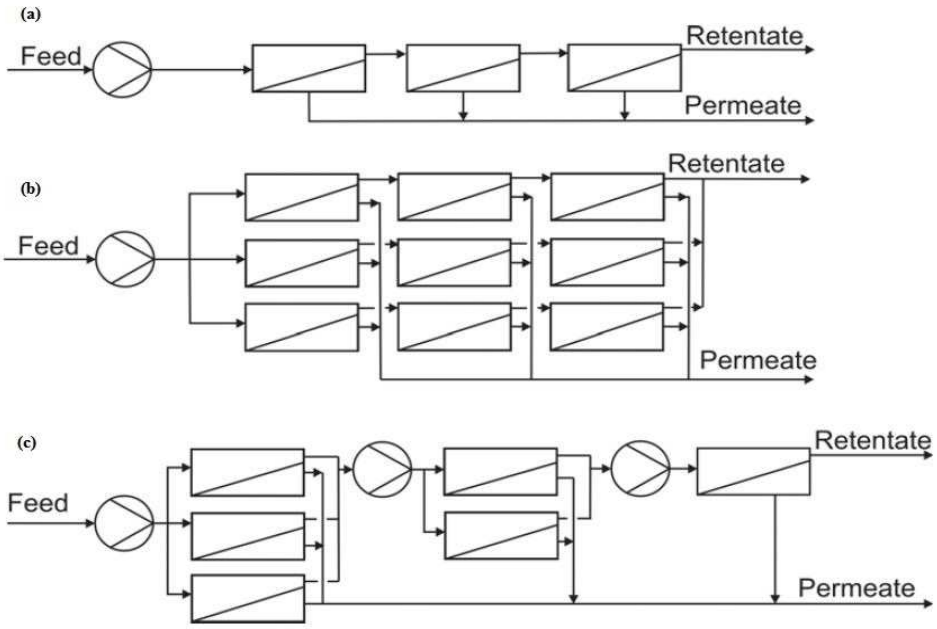

Figure 2.10. *Reverse osmosis plant configurations: (a) series array, (b) parallel array, (c) tapered array (Fritzmann et al., 2007).*

Along a membrane element, flux decreases and salt concentration of the feed side increases. The reverse osmosis driving force is reduced by the pressure losses along the vessel and by the increasing of the salt concentration of feed side. Thus, interstage pumps (booster pumps) are necessary. The number of parallel housing of a specific pass and the number of elements per housing depend on the maximum allowed pressure, the maximum and minimum flow rate, and the target recovery. Very high flux along a pressure vessel can damage the membrane because of the high pressure drop. Very low flow does not provide sufficient turbulence and may result in a predominant concentration polarization phenomenon (Fritzmann *et al*., 2007). A concentrate recycle is generally used in smaller RO plants, to increase the cross-flow velocity and decrease the risk of fouling.

(5) Energy recovery system.

The main way to decrease seawater RO desalination costs is the development of energy recovery systems. Generally, Energy Recovery Devices (ERD) are used to recuperate the remaining energy of the concentrate stream, which otherwise would be wasted, to apply part of the necessary pressure to the feed. The two main groups of EDR are: pressure exchangers and turbine system. Pressure exchangers (or work exchanger) directly transfer pressure from the concentrate stream to the feed, with an efficiencies of 96-98%. In Figure 2.11(a) a schematic process scheme shows how a pressure exchanger operates in a RO process: only part of the feed is pressurized in the high pressure pump.

Turbine system are mostly Plenton wheel or turbocharger systems, which convert potential energy from the concentrate stream to mechanical energy to supply the feed pump or directly to pressurize the feed water with an efficiency of 90%. Figure 2.11(b) and Figure 2.11(c) show respectively how a Plenton turbine and a turbocharger operate in a RO process. In the first case the turbine supplies part or the necessary energy to the pump; on the contrary in the second case the turbocharger pressurizes the feed from an intermediate step to the desired pressure.

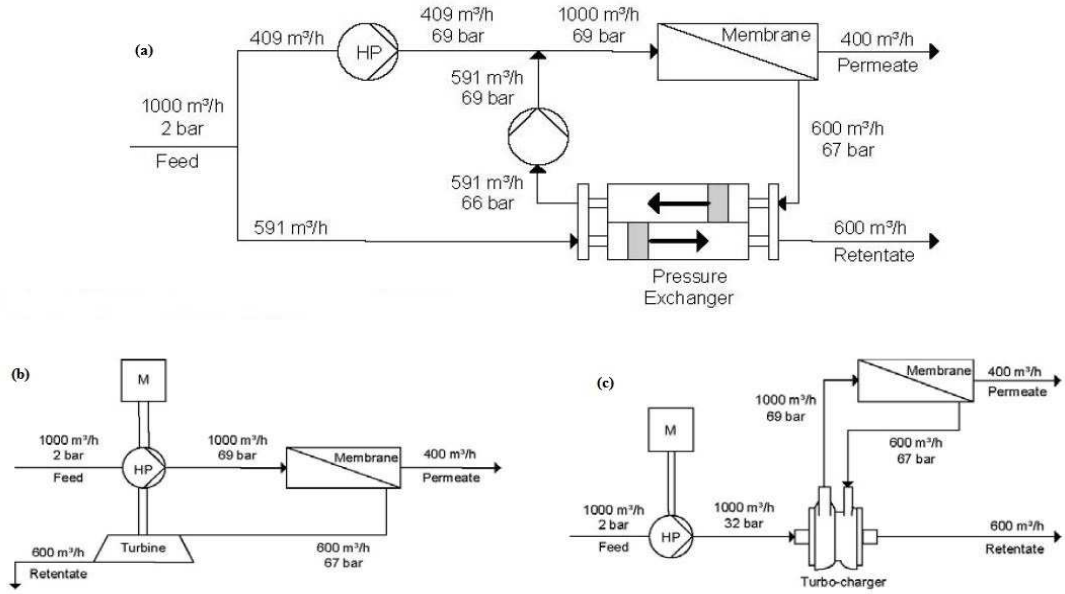

Figure 2.11. *RO process energy recovery schemes with (a) turbo exchanger, (b) Pelton turbine, and (c) turbocharger (Fritzmann et al., 2007).*

Turbochargers are the mostly used technology for energy recovery systems despite the fact that their efficiency is lower than pressure exchangers. The reasons are that pressure exchangers need expensive equipment and increase the salinity of the permeate stream. However, pressure exchangers do not suffer stronger reductions in efficiency if operated outside the design point as turbine system.

EDR are designed and used also for brackish water RO plant even if the energy recovered is lower than SWRO application, due to higher water recoveries and lower operating pressure (Fritzmann *et al*., 2007 and Norman, N. Li., 2008).

(6) Post-treatment

The permeate stream of RO plants is not drinkable because it does not conform to drinking water standard such as the World Health Organization (WHO). It has to be treated, before to be stored or distributed, with the following usages:

- re-hardering in order to produce a Langelier Saturaton Index (LSI) slightly positive to have a fine precipitation layer of calcium carbonate for protection.

The LSI is a measure of the corrosivity of the water: if LSI is zero the water is non-aggressive, if it is negative the water is corrosive. The aim of re-hardering post-treatment is to increase alkalinity and pH to give the water its typical taste and to prevent pipe corrosion. There are several methods for re-hardering (Fritzmann *et al*., 2007): dissolution of lime or limestone by carbon dioxide, dosage of chemical solution based on calcium chloride or bicarbonate, blending of RO permeate with treated water from a saline source and addition of calcium chloride or sodium bicarbonate;

- disinfection to protect the consumer from any pollution. Chlorine, chlorammines or sodium hypochlorite can be used;
- boron removal: boron is typically present in seawater as boric acid and it is suspected to be dangerous for people and agriculture. The WHO limit of boron in drinking water is 0.5 mg/L and typical boron concentration in seawater can be as high as 7 mg/L (Fritzmann *et al*., 2007). Boron is not rejected by RO membrane in standard conditions because the pH is too low. High pH value permits a boron rejection about 99%. However, there are lots of problematic aspects such as fouling and scaling working at high pH in RO processes. The main solutions for boron removal are (Figure 2.12): (a) single-pass SWRO with high rejection RO membranes; (b) SWRO followed by BWRO: the permeate close to the feed entry of the first pass is blended with the permeate of the second pass operating at high pH value; (c) SWRO followed by a Boron Selective ion exchange Resin (BSR): the selective resin permits a boron rejection of 99 to99.9%; (d) SWRO followed by a hybrid process of BSR and BWRO: the second stage decrease both salinity and boron concentration.

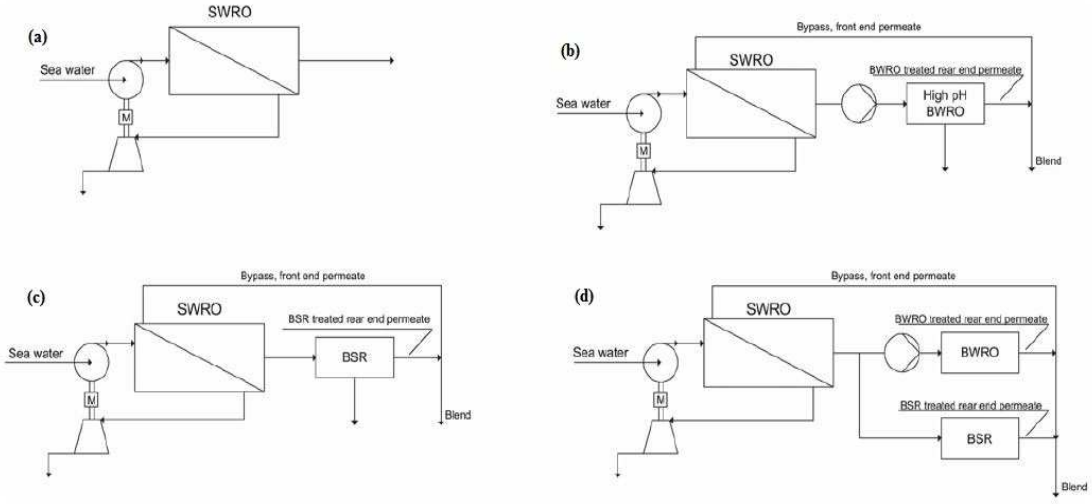

Figure 2.12. *Boron removal process schemes: (a)single-pass SWRO, (b)SWRO followed by BWRO, (c)SWRO followed by a boron selective ion exchange resin (BSR), and (d)SWRO followed by a hybrid process of BSR and BWRO (Fritzmann et al., 2007).*

In Table 2.5 the main chemicals used in post-treatment are shown.

Table 2.5.*Chemical used in post-treatment (Fritzmann et al., 2007).*

Post-treatment	Purpose	Chemicals added	Fate of chemicals
removal of dissolved gases	remove gases (CO_2, H_2S, radon)	aeration, degasing	air emission
pH adjustment to 7	protect aquatic life at discharge point	NaOH, soda ash, lime	increased sodium/calcium level, pH
disinfection	prevent grow in distribution system	chlorine	chlorine stays in produced water
reduction of chlorine level	eliminate chlorine and other oxidisers	sodium bisulphite	increases sulphate and chloride levels
oxygenation	increase dissolved oxygen	aeration	increase DO in concentrate
removal of other species	decrease pollutants in produced water and/or concentrate	depends on species	

2.3.1 Limiting factors

There are some limiting factors that have to be considered when a RO process is operated (Figure 2.13). The first one is the increasing of the osmotic pressure due the concentration polarization; this is described in paragraph §2.2.2. The other limits are discussed here.

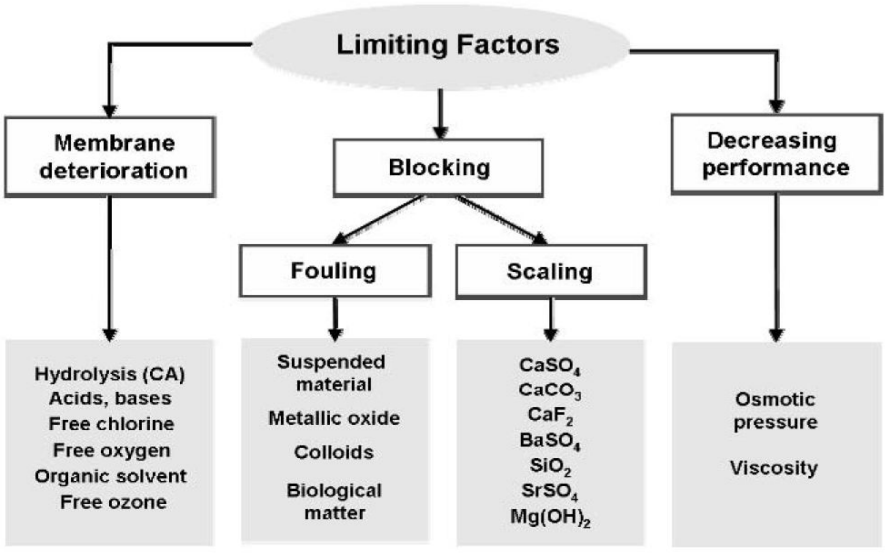

Figure 2.13.*Limiting factors to RO desalination (Fritzmann et al., 2007).*

Membrane deterioration

Several chemicals can damage irreversibly the active layer of the membrane. Even traces of oxidant used during pre-treatment or cleaning chemicals are very dangerous for the membrane. Moreover, also very low or very high pH can damage polymeric membranes.

Membrane blocking

The loss of performances of the membrane is also caused by the surface deposition of substances called foulants. These contaminants include non-dissolved, colloidal or biologic matter. Depending on the mechanism of precipitation and formation of a cake on the surface of the membrane, it is possible to distinguish two kinds of membrane blocking: fouling and scaling.

Scaling is caused by super-saturation of inorganic compounds on the feed side and it is characterized by the formation of a thin layer of precipitated salts. This phenomenon is easier to be found in BWRO and in the downstream of all RO stage, where the concentration of the feed solution is higher. Scaling can be prevented in pre-treatment by pH adjustment and addition of antiscalants agents or reducing recovery to reduce the overall salt concentration (Fritzmann *et al*., 2007).

Fouling is caused by convective and diffusive transport of foulants: a thin layer deposits over the membrane, increasing the overall resistance to mass transfer and decreasing the total performance of the process. There are some methods to limit fouling, but it can never be fully prevented:

- *modules and process conditions*: the higher the cross flow velocity parallel to the membrane surface, the lower rate of fouling;
- *membrane properties*: the most performance membrane is characterized by a neutrally charged surface in order to minimized the attachment of charged foulants and by a high surface area in order to decrease flux and increase cross-flow velocity;
- *pre-treatment of the feed solution*: there are a lot of possible pre-treatment to be applied in a RO process in order to reduce membrane fouling. Each type of foulant requires some specific treatments from the following list: coarse strainer, chlorination, clarification with or without flocculation, final removal of suspended particles using cartridge filters, clarification and hardness reduction using lime treatment, reduction of alkalinity using pH adjustment, media filtration, addition of scale inhibitor, water sterilization using UV radiation, reduction of free chlorine using sodium bisulphite or activated carbon filters.

  Inorganic precipitates. The fouling tendency of a given feed water is valued using LSI for brackish water and the Stiff and Davis Stability Index (S&DSI) for

seawater; they give an indication of the concentration of calcium carbonate saturation (Fritzmann *et al*., 2007):

$$\mathrm{LSI} = \mathrm{pH} - \mathrm{pH}_s \ (\mathrm{TDS} < 10{,}000\ \mathrm{mg/L}),\ pH_s = pCa + pAlk + pK_2 - pK_s \ , \quad (2.11)$$

$$\mathrm{S\&}DSI = pH - \mathrm{pH}_s \ (\mathrm{TDS} > 10{,}000\ \mathrm{mg/L}),\ pH_s = pCa + pAlk + K \ , \quad (2.12)$$

where pH_s= pH level at which the water is in equilibrium with calcium carbonate, pCa = negative log_{10} of calcium concentration [mol/L], $pAlk =$ negative log_{10} of total alkalinity [mol/L], pK_2 = negative log_{10} of ionization constant of HCO_3, pK_s = negative log_{10} of the solubility product of calcium carbonate, and K = the ionic strength constant at 25°C. Another key parameter is the Solubility Product (SP) (Fritzmann *et al*., 2007):

$$\mathrm{SP} = c_A^n c_B^m \ , \quad (2.13)$$

where c_A is the concentration of the negative ion and c_B is the concentration of the positive ion, at saturation conditions.

Precipitation of carbonate is avoided by keeping the pH value around 4-6, maintaining LSI and S&DSI smaller than 2-2.5 and using antiscalants agents such as organic polymers, surface active agents, organic phosphonates and phosphate.

Organic precipitates. Degradation of organic matter such as plants produces macromolecules called humid acids, with polymeric phenolic structure. These acids chelate with metal ions and form a fouling gel layer over the membrane. Humid acids are removed by pre-treatment: flocculation, coagulation with hydroxide flocs, ultrafiltration or adsorption on activated carbon.

Biofouling. It is caused by bacteria, algae, fungi, viruses and biotic debris such as bacteria cell wall fragments. The RO membrane is an ideal substrate for microorganism grown, which creates a biofilm. It is difficult to remove a biofilm due to the gel layer. Therefore is necessary to reduce biofouling by effective pre-treatment such as chlorination.

Particulates. Particulates matters can be divided in four categories depending on particle size (Fritzmann *et al*., 2007): (1) settable solids (>100 µm), (2) supra-colloidal solids (1-100µm), (3) colloidal solids (0.001-1 µm), (3) dissolved solids (<10 Å). Particles larger than 25 µm can be easily removed by screens, cartridge filters and media filters; for smaller particles is necessary to use

coagulants or flocculants agents. The Silt Density Index (SDI) is used to estimate the presence of suspended solids (Greenlee *et al*., 2009):

$$SDI = 100\% \frac{\left(1-\frac{t_1}{t_2}\right)}{t}, \tag{2.14}$$

where t is the total time elapsed and t_1,t_2 are the times (s) required to filter 500 mL of water, initially and after t minutes, respectively.

SDI is recommended to be <3-5, while the turbidity, measured in NTU (Nephelometric Turbidity Units), is recommended to be <0.2. There are other indexes that better correlate flux decline, particles concentration and membrane fouling, for instance: MFI (modified fouling index) and MFI-UF;

- *Membrane cleaning*: membrane fouling can never be totally avoided; thus membrane cleaning at definite intervals permits to restore membrane performance. Figure 2.14 shows a typical membrane cleaning process: (1) make-up of the cleaning solution (e.g. acids), (2) low flow pumping of the cleaning solution, (3) recycling of cleaning solution, (4) turning off the pumps and soaking of the membrane for 1-15 hours, (5) high flow operation, (6) flush-out.

  Direct osmosis is used as a novel procedure for membrane cleaning. A high salinity solution with an osmotic pressure that overcomes the pumps pressure permits to RO to shift in direct osmosis.

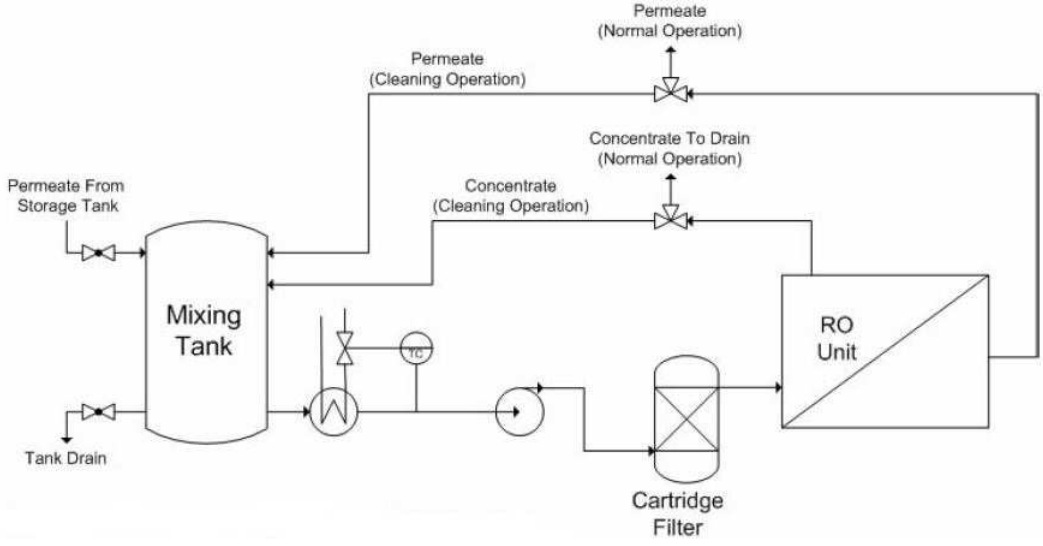

Figure 2.14. *Membrane cleaning equipment (Fritzmann et al., 2007).*

Membrane compaction

If a membrane is exposed to high pressure, it increases its density (compaction) because of a mechanical deformation of the polymer. Membrane compaction decrease the rate of

diffusion and consequently the permeate flux. This phenomenon is more evident in asymmetric cellulose membranes and in SWRO than in BWRO.

2.3.2 Factors affecting performance

There are several key parameters that can influence RO performance, the main ones are the following: pressure, temperature, recovery, and feed water salt concentration. In Table 2.6 the effects of these key parameters are summarized.

Table 2.6. *Factors influencing reverse osmosis performance (modified from American Water Works Associations, 1999).*

Factor	Permeate Flow	Salt Passage
Increasing effective pressure	increases	decreases(1)
Increasing temperature	increases	increases
Increasing recovery	decreases	increases
Increasing feed water salt concentration	decreases	increases

(1) It depends on salt ions type

Figure 2.15a shows the effect of increasing pressure on permeate flux and salt rejection: as pressure increases more water is forced across the membrane thus the permeate flux increase. Furthermore, salt passage is increasingly overcome as water is pushed through the membrane at a faster rate than salt can be transported. Thus, salt rejection increase. However an upper limit for the increasing of salt rejection exists above a certain pressure level.

The effect of temperature is shown in Figure 2.15b. As temperature increases, water flux increases almost linearly, due to the higher diffusion rate of water through the membrane. Moreover, an increase of the feed water temperature results in a higher diffusion rate for salt, consequently in a higher salt passage.

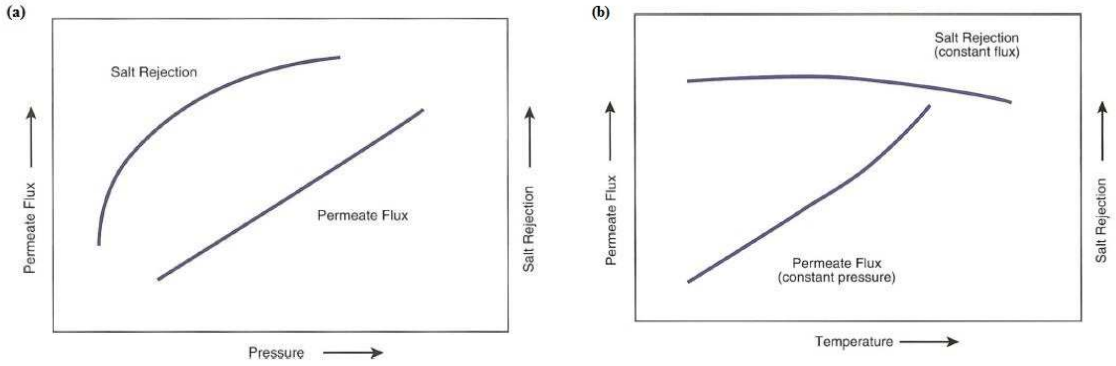

Figure 2.15. *(a) Effect of increasing pressure and (b) temperature on permeate flux and salt rejection (American Water Works Associations, 1999).*

Figure 2.16a shows the effect of increasing recovery (without adjust the feed pressure to keep it constant): the permeate flux and salt rejection slowly decrease and stop if the salt concentration reaches the value in which the osmotic pressure is equal to the applied pressure. This is due to the fact that the salt in residual feed becomes more concentrated. The maximum recovery percentage possible does not depend on a limiting osmotic pressure, but on the concentration of salts in the feed water and their tendency to precipitate on the membrane surface (scaling). The effect of water salt concentration is shown in Figure 2.16b. As salt concentration increases, also osmotic pressure increases, and consequently the process driving force decreases. Thus, permeate flux decreases and the salt passage increase.

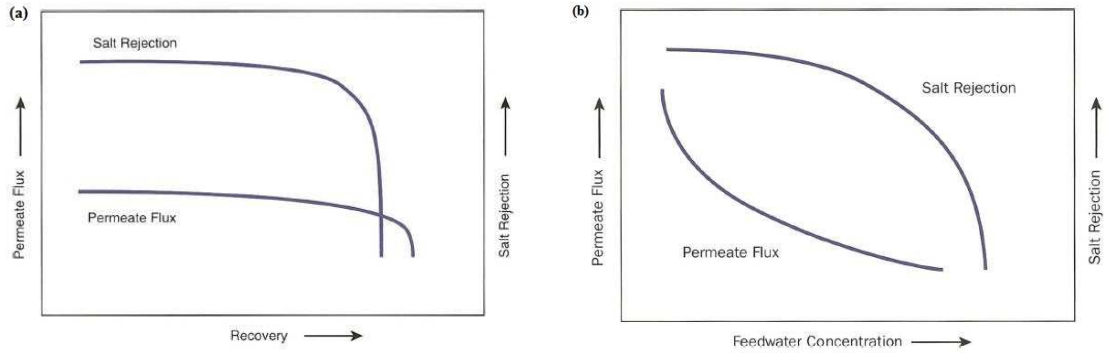

Figure 2.16. *(a) Effect of increasing recovery and (b) feed water salt concentration on permeate flux and salt rejection (American Water Works Associations, 1999).*

2.3.3 Costs

The cost of RO desalination has gradually decreased from the commercial introduction in 1970s until today, despite the fact that prices of energy is rising. Energy is the major cost component in the operation of a RO desalination plants. Figure 2.17 shows how energy cost has been reduced from the late 1970s (20 kWh/m^3) to nowadays (less than 2 kWh/m^3) through the development of more efficient membranes, new membrane materials, improving in pumping and energy recovery systems and more efficient plant designs.

Instead, the energy requirement for BWRO plants is below 1kWh/m^3, due to the lower salinity of the feed water.

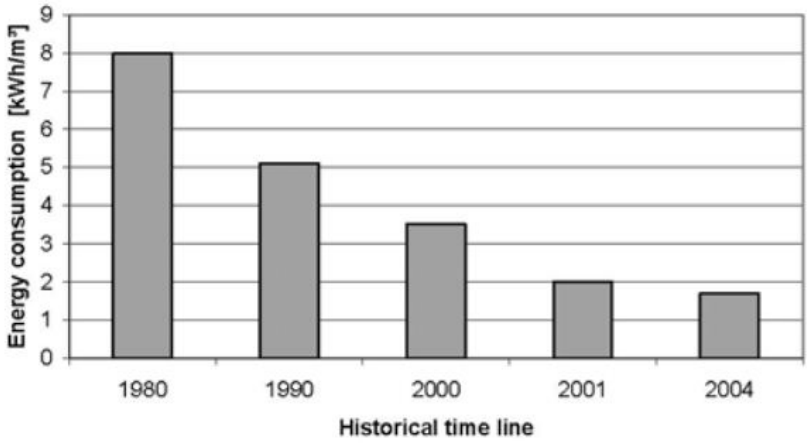

Figure 2.17. *Development of achievable energy consumption in RO desalination processes (Fritzmann et al., 2007).*

The unit water cost for SWRO ranges between US$0.53/m^3 (new plants) and US$1.5/m^3 (plants built in 1990s). Furthermore the unit water price for BWRO ranges between US$0.1/m^3 and US$1/m^3. Thus, it depends on the type of the feed water, as well as the plant size, the energy source and the plant design. The capital and energy costs of SWRO plants are about five times greater than the BWRO plants due to more extensive pre-treatment systems, higher pressures and lower recovery (Greenlee *et al.*, 2009).

Figure 2.18 shows the combination of different costs in a SWRO plant, and the energy consumption contributors in each step of the process.

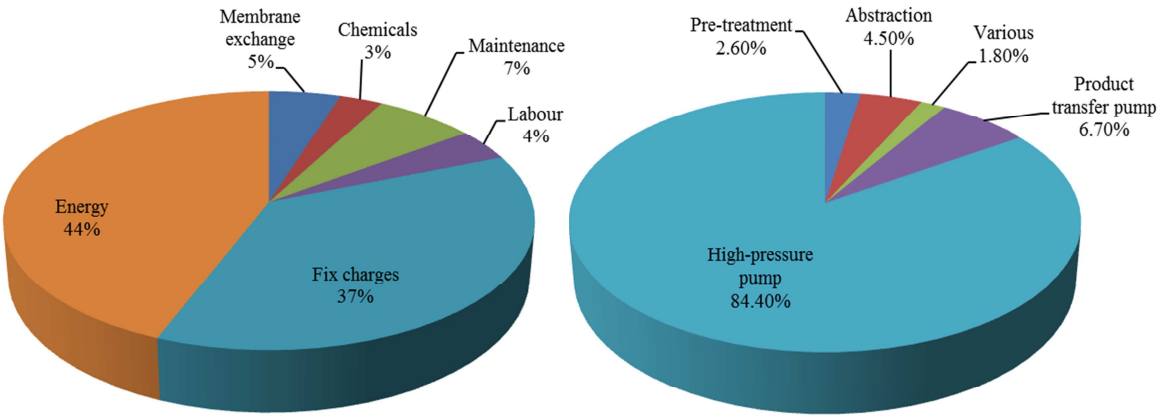

Figure 2.18. *Water distribution costs (left) and energy consumption of different process stages in RO desalination plants (right) (modified from Fritzmann et al., 2007).*

Fixed costs include the purchase of the land and process equipment and plant construction. It decreases with the size of the plant, even if membrane-based

desalination is less affected by economy of scale than other processes due to modular assembly. Membrane replacement costs around 0.11€/m^3 to 0.29€/m^3. Labour cost has a minor impact to overall costs: 1.12 €-cent/m^3. Chemical cost can be reduced with membrane pre-treatment, but it always depends on the quality of the raw water (Fritzmann *et al*., 2007).

2.4 Environmental impacts

Desalination processes have several disadvantages regarding their impact on the environment. The main environmental aspect to be considered are: management of brines, emission of greenhouse gases (1.4 - 1.8 kgCO_2 per m^3 of produced water) (Menachem, 2011), impingement and entrainment of marine organisms during in seawater intakes, high salinity of the brine, the chemicals used in pre-treatment, the noise emitted, waste membrane to be discharged, interference with the marine ecosystem and the meddling with local fishing or tourism.

Most energy for desalination processes results from thermo-electric power generation. Thus, it makes water production highly dependent on fossil oil price. To minimize greenhouse gas emission and to make desalination processes independent of the oil price, renewable energy sources, such as wind or solar energy, could directly power SWRO plants in the future.

As regards the brines management, is possible to distinguish three types of brine: (1) backwash water for physical pre-treatment, (2) saline concentrate stream, (3) membrane cleaning solution. The level of the environmental impact of the brines disposal in the sea depends on the chemical composition, natural hydrodynamics, the discharge point and the kind of marine life presents. The high salinity of the brine may influence the marine biota and expose marine organism to osmotic stress. However, limited research exists about effects of desalination on marine ecosystems. Possible measures to mitigate the environment impact are the following: dilution of the brine with seawater or process water before the discharging, lower recovery rates to reduce brine salinity, multiple discharge points, discharge in area with strong currents or waves and discharge at a larger depth. Furthermore, chemicals can be reduced using membrane pre-treatment and chlorination could be replaced by ultraviolet radiation.

As regards the brine disposal in non-coastal area, some alternative are: discharge into solar evaporation ponds, disposal to wastewater system, injection to deep saline aquifers, disposal into sea through long pipeline systems, disposal on land surface and land application. However, these alternatives are expensive and in some cases may lead to ground contamination (Fritzmann *et al*., 2007).

2.4.1 Life Cycle Assessment

Desalination is a mature technology, nevertheless its environmental impact is not well known yet. One common environmental impacts analysis is the Life Cycle Assessment (LCA). LCA is a systematic, objective and powerful tool to assess environmental incidence of a process, including all stages and impacts. An LCA study normally consists into four stages (Raluy *et al.*, 2006): (1) goal and scope definition, (2) life cycle inventory, (3) life cycle impact assessment (LCIA), (4) interpretation. Unfortunately, at the current state-of-the-art the RO desalination environmental impacts vary due to the different LCIA methods. Hence, different methods give different scores in several impact categories such as acidification, eutrophication, photochemical oxidation and human health (Zhou *et al.*, 2011). For this reason, in this paragraph, just a comparison between RO, MSF and MED scores are presented.

In 2006, Raluy G., compared LCA results of MSF, MED and RO. The studied RO desalination plant produces about 46,000 m^3/day of fresh water, 8000 h of operation per year, average lifetime of 25 years and an energy consumption of 4kWh/m^3. Table 2.7 shows some of the most relevant airborne emission produced by the analysed desalination processes along all their life cycle. It is evident that the RO process is definitely the less polluted compared to MSF and MED.

Table 2.7. *Relevant airborne emission produced by desalination systems (Raluy et al., 2006).*

	MSF	MED	RO
kg. CO_2/m^3 desalted water	23.41	18.05	1.78
g. dust / m^3 desalted water	2.04	1.02	2.07
g. NO_x / m^3 desalted water	28.3	21.41	3.87
g. NMVOC / m^3 desalted water	7.90	5.85	1.10
g. SO_x / m^3 desalted water	27.91	26.48	10.68

The scores obtained for each impact category (EI 99 method) for each desalination technology is represented in Figure 2.19. The fossil fuel effect is the highest contribution to global impact in each process. However, RO scores are approximately one order of magnitude lower than those corresponding to thermal technologies. Furthermore, if an energy consumption of 2kWh/m^3 is considered for the RO plant, the overall score is lower: 0.0448.

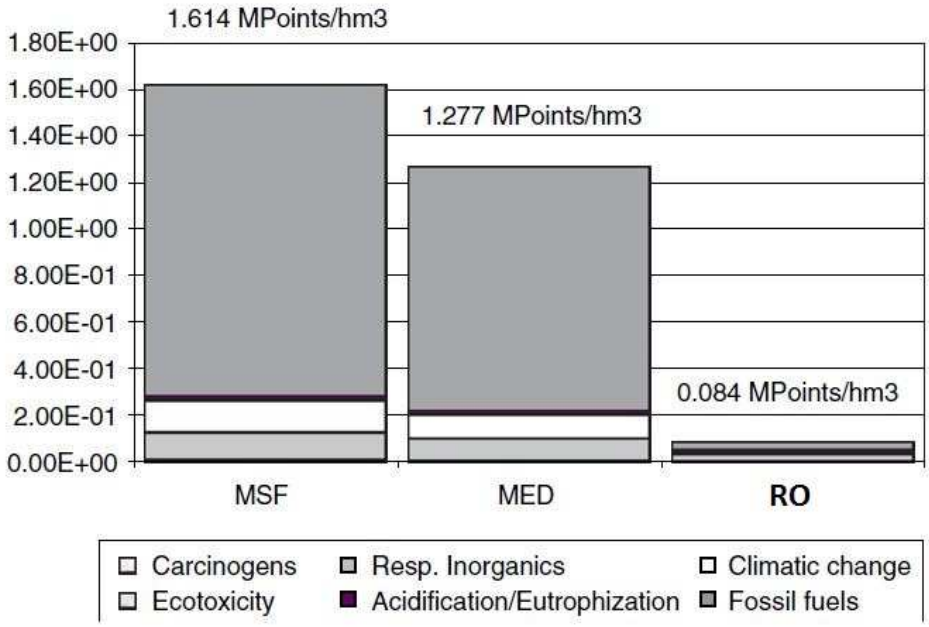

Figure 2.19. *Overall scores obtained in the evaluation phase for each desalination technology. EI 99 method (Raluy et al., 2006).*

Another interesting aspect is about RO energy consumption. Table 2.8 shows how the relevant airborne produced by RO are reduced by about 47% when the energy consumptions are reduced from 4kWh/m^3 to 2kWh/m^3.

Table 2.8. *Relevant airborne emission produced by RO for different energy consumptions (Raluy et al., 2006).*

	RO (4kWh/m^3)	**RO (3.5kWh/m^3)**	**RO (3kWh/m^3)**	**RO (2.5kWh/m^3)**	**RO (2kWh/m^3)**
kg. CO_2/m^3 desalted water	1.78	1.56	1.35	1.14	0.92
g. dust / m^3 desalted water	2.07	1.81	1.55	1.30	1.05
g. NO_x / m^3 desalted water	3.87	3.40	2.95	2.49	2.03
g. NMVOC / m^3 desalted water	1.10	0.97	0.84	0.70	0.57
g. SO_x / m^3 desalted water	10.68	9.52	8.39	7.26	6.10

Independently of the methods used, the materials, the assembly and the final disposal have low load in the analysis; the most environmental load (about 95%) is associated to

the operational stage, due to the high energy consumption. In addition, from the aforementioned data presented, RO emerges as the less aggressive desalination technology for the environment (Raluy *et al.*, 2006).

2.5 Trends in desalination and considerations

The further developments in sea-water and brackish water RO desalination processes aim to reduce the energy consumption and minimize the negative effects of fouling and scaling. Some recent and future innovation of the state-of-the-art of reverse osmosis may involve:

- development of membranes that are less prone to fouling, operate at low pressure and required less pre-treatment of the feed water. For instance surface modification by ultraviolet irradiation can make the membrane more hydrophilic with lower fouling tendencies;
- development of more efficient energy recovery systems and pumps;
- improvement of the desalination plant design;
- use of renewable energies;
- use of different membrane elements in the same pressure vessel (HID: Hybrid RO membrane Interstage Design);
- new RO membrane module design: larger diameter spiral wound, high flux membrane, sulfonate polysulfone composite membrane highly resistant to chlorine attack;
- optimization of antiscalant dosing, pH control, chemical addition;
- new membrane with higher boron rejection to minimize the extent of post-treatment;
- new management in membrane replacement for longer membrane life.

One emerging desalination technology is Forward Osmosis. Water naturally passes through a semipermeable membrane to a draw solution with a lower chemical potential than seawater. The solutes in the draw solution are then recovered to complete the desalination. The main challenge, and also the aim of this thesis, is to find a suitable draw solution that would be cheap, easy to remove, chemically compatible with the membrane and soluble in water. One potentially suitable draw solution is ammonia-carbon dioxide (Menachem, 2011). There are several ways to separate the fresh water from the diluted draw solution (e.g. column distillation, membrane distillation). The use of a pressure-driven membrane step (RO or NF) in the recovering stage characterize the novel Manipulated Osmosis Desalination (MOD) process, developed at the University

of Surrey's Centre for Osmosis Research and Applications (CORA) (Sharif & Al-Mayahi, 2005). Forward Osmosis and MOD process are widely described in Chapter 3.

2.5.1 Hybrid desalination and integrated membrane system

Another possibility today is the integration of different technologies in order to combine their different advantages, resulting in hybrid desalination systems. There are three main types of hybrid system (Fritzmann *et al*., 2007):

- simple hybrid system;
- integrated hybrids;
- power/water hybrids.

Simple hybrid systems involve the integration of a distillation and a membrane process. Usually the combination of MSF and RO is used: common seawater intake and outfall, and blending of permeates. These respectively reduce capital investment and permit RO plants to work at a higher TDS. Thus, preserving membrane life permits lower energy consumption due to high recovery rate and reduces severe requirements on boron concentration.

Integrated hybrids MSF/RO plant is designed to be more energy efficient, using all waste heat of MSF and waste pressure energy of RO to control water temperature and de-aeration of the feed water.

Finally, *power/water hybrids* take advantage from the storage of water. Electricity is difficult to be stored and desalination plants are a reliable and constant costumer of electricity. Thus, larger desalination plants can use over-capacities of the network.

Furthermore a *hybrid integrated membrane* process is possible: the low pressure reverse osmosis involves a nanofiltration stage as pre-treatment and a second RO stage operated at 20 bar (Van der Bruggen *et al.,* 2003). The NF pre-treatment step uses ion-selective membranes and has two main advantages: the sieving effect and the electrostatic effect. This means a high rejection of uncharged species (depending on the size) and a high rejection of divalent ions, so that the recovery can be increased in the RO stage. However, at current state-of-the-art, water cost for a NF/RO process in still higher than a double pass RO (Fritzmann *et al*., 2007).

2.5.2 Considerations

Reverse Osmosis has lots of advantages: the process and the modular installation is simple, plants have a high space/production capacity ratio, seemingly unlimited and reliable water sources. However membranes are sensitive to abuse, pre-treatment is always required, brine must be carefully disposed and there is risk of bacterial contamination of the membrane. Despite the high costs compared to conventional

technologies for the treatment of fresh water such as groundwater extraction or rainwater harvesting, advances in technology have seen reverse osmosis become the most popular desalination process in the world. From 2005 to 2008 the annual RO capacity increased from 2 million to 3.5million m^3/day and the 61.1% of the worldwide capacity is attributable to RO (Penãte *et al.*, 2011). Basically, R&D is continuing to improve the process; for instance the first plants operated with a pressure of 120bar, nowadays plants operate at 60bar. The energy demand for SWRO desalination processes by state-of-the-art is only 25% higher than the practical minimum energy for desalination for an ideal RO stage (Menachem, 2011). Hopefully future research could decrease the energy demand and increase the energy efficiency, focus on pre-treatment and post-treatment, yet too extensive in the process. Hence, it involves the development of fouling-resistant membranes and the improving of hydrodynamic mixing in membrane modules.

Seawater offers the prospective for a stable and abundant source of fresh water, but further researches and studies has to be done to improve and develop this necessary technology.

Chapter 3

Manipulated Osmosis Desalination process

The aim of this chapter is to describe the novel Manipulated Osmosis Desalination process developed at the University of Surrey's Centre for Osmosis Research and Applications (CORA) (Sharif & Al-Mayahi, 2005). In order to do this, forward osmosis principles and technology is firstly given in Section 3.1, and MOD process is explained in Section 3.2.

3.1 Forward osmosis

Forward Osmosis (FO) principles are unfolded in the following paragraphs in order to have the necessary elements to understand MOD process. As RO, FO uses a semipermeable membrane, which acts as a barrier that allows the passage of small molecules like water, and rejects bigger molecules such as salts and bacterial species. FO is a net flow of water through the membrane due to the natural osmotic pressure. Water moves from a region of higher water potential, lower solute concentration, lower osmotic potential and lower entropy to a region of lower water potential, higher solute concentration, higher osmotic potential and higher entropy (see Figure 3.1). It results in concentration of a feed stream and dilution of a highly concentrate stream (Cath *et al.*, 2006).

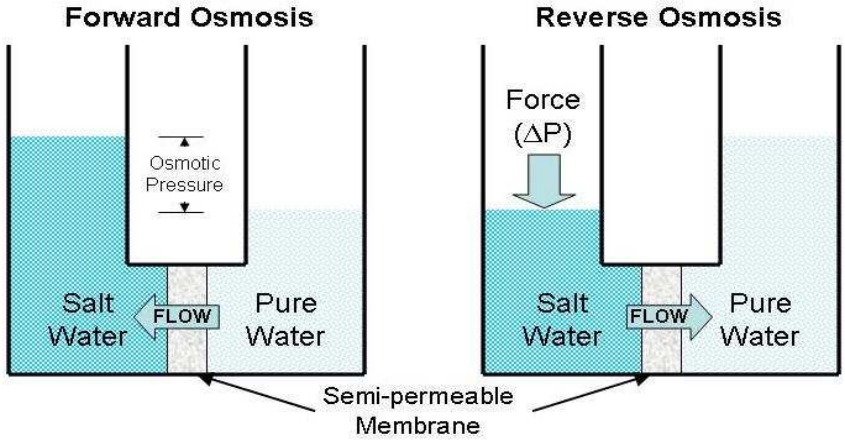

Figure 3.1. *Schematic representation of the osmosis phenomena in reverse osmosis and forward osmosis.*

Forward osmosis is used in emerging desalination processes, wastewater treatment, water purification, hydration bags, food processing, brine concentration and dehydration of pharmaceutical products. It is also used to generate power (Pressure Retarded Osmosis PRO). In order to produce electricity, the osmotic pressure difference between fresh water and sea water is converted into hydrostatic pressure. Theoretically, 1.7 or 2.5MJ energy can be produced respectively from $1m^3$ of river water and $1m^3$ or more of sea water (Zhao *et al.*, 2012). In the following paragraph the desalination application of FO is described.

3.1.1 Forward osmosis desalination process

Forward osmosis is currently been studied as an emerging desalination process, and represents a challenge for the future technology improvements. Most previous literature on FO desalination processes is in patent form. From 2005, technical papers began to appear in the international scientific world.

In recent studies, it was demonstrated that when using a suitable FO membrane (e.g.FO-asymmetric cellulose triacetate) and a high osmotic pressure draw solution (e.g. highly soluble ammonia and carbon dioxide gases), seawater can be efficiently desalinated (Cath *et al.*, 2006). In Figure 3.2 the FO desalination process is shown.

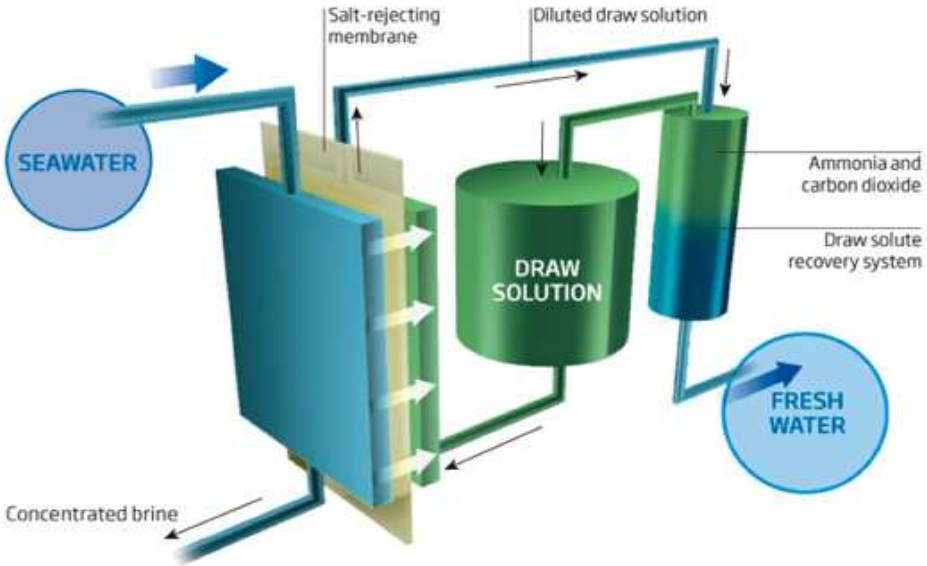

Figure 3.2. *Schematic representation of the FO desalination process.*

Water is extracted from the sea and passes the FO membrane, due to the osmotic pressure. It results in the dilution of the draw solution. Upon moderate heating (close to 65 °C), the dilute draw solution decompose to ammonia and carbon dioxide. Generally speaking, the separation of the fresh product water and the dilute draw solution can be obtained in several ways (e.g. column distillation, ion exchange, electrodialysis, crystallization, rapid spray or membrane distillation). The separated draw solution is

then recycled to the FO unit. In a FO process, the rate of permeate water through the membrane is approximately proportional to membrane area and osmotic pressure difference. Bench-scale FO data demonstrated that ammonia-carbon dioxide FO process with CTA membrane is a possible desalination process: salt rejection is about 95% and flux is 25 L/m^2h, with a calculated driving force of more than 200 bar (Cath *et al.*, 2006). The flux is lower than expected, due to internal CP (see § 3.1.1).

The only pressure to be applied is due to the flow resistance in the membrane module (few bars). Thus, the equipment to be used is very simple and membrane support is not a problem.

FO desalination process operates with some advantages if compared to RO desalination process (Chung *et al.*, 2010 and Zhao *et al.*, 2012):

- low hydraulic pressure which leads low fouling, low energy and reduced cleaning;
- high osmotic pressure, which leads to high water flux and high recovery (over 75%);
- high rejection, which leads to high quality product and less contaminants;
- no need of chemical pre-treatment;
- less brine discharge;
- no membrane compaction.

Thus, it can be summarized as a potentially less operation energy, low cost technology.

However the lack of high performance membranes, which minimize fouling, concentration polarization and reverse diffusion, and the necessity for a simply separable draw solution, have limited the assertion of FO desalination process.

3.1.1.1 Membranes

The desired FO membrane should have mechanical and performance stability, high density of the active layer for high salt rejection, resistance to a wide range of pH, high water flux, and low concentration polarization (Chung *et al.*, 2010). Cellulose acetate (CA), cellulose triacetate (CTA), polybenzimidazole (PBI) and aromatic polyamide membranes have been developed for FO process. In the last decade also asymmetric cellulosic osmotically driven membranes, thin film composite (TFC) membranes and chemically modified membranes have been investigated (Zhao *et al.*, 2012).

In pressure-driven membrane processes as RO or NF, solutes and particles can accumulate close to the membrane surface (concentration polarization). It could be on the feed side of the membrane (concentrative CP) and/or in the permeate side (dilutive CP). Also in osmotic-driven membrane processes as FO, both concentrative and dilutive concentration polarization (CP) reduce the effective osmotic driving force. This phenomenon can be minimized by increasing flow velocity and turbulence at the

membrane surface. Unfortunately, because of the low flow in FO process, the ability to reduce external CP is limited. Luckily, due to the low hydraulic pressure applied, the influence of external CP in fouling induction is minimal. The main problem with FO membrane technology is to overcome the internal concentration polarization (ICP). This phenomenon is similar of the external CP, except for the fact that it takes place within the porous layer. It can be minimized by higher cross-flow and higher temperatures. In FO applications for desalination, the active layer of the membrane faces the feed solution and the porous layer faces the draw solution, because the feed solution has a higher fouling tendency (Zhao *et al.*, 2012, see Figure 3.3).

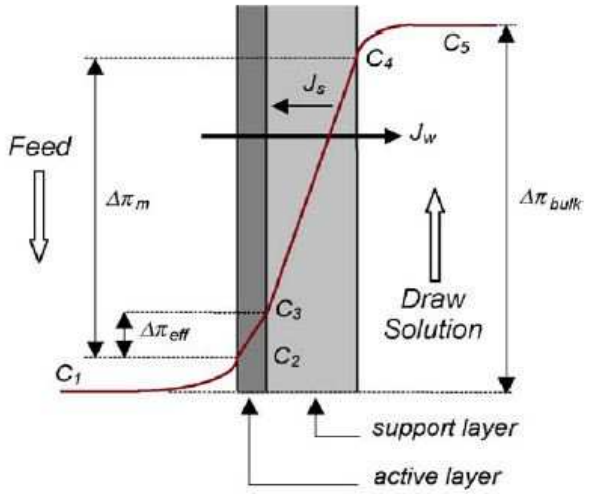

Figure 3.3. *Schematic representation of the concentration polarization across an asymmetric membrane in FO (Cath* et al.*, 2006).*

It can be evidently seen in Figure 3.3 that the osmotic pressure difference between the bulk draw solution and the bulk feed ($\Delta\pi_{bulk}$) is higher than the osmotic pressure difference across the membrane ($\Delta\pi_m$), due to the external CP. The effective osmotic pressure driving force ($\Delta\pi_{eff}$) is even lower, due to the internal CP within the porous layer. Furthermore, if feed and draw solutions flow tangential to the membrane, but in opposite directions, the driving force is almost constant along the membrane module; this makes the process more efficient.

As regards membrane module, different configuration can be used (Cath *et al.*, 2006): flat sheet or tubular/capillary membranes are studied in laboratory-scale; whereas flat sheet membranes in plate-and-frame configurations are used in larger-scale application. Spiral-wound membrane elements cannot usually be operated in FO applications because the draw solution cannot be forced to flow inside the envelope formed by the membranes. Plate-and-frame is the simplest flat sheet configuration. However the lack of adequate membrane support limits operation to low pressure, and the low packing density leads to larger system footprint and consequently higher capital cost. The use of

tubular elements (similar to hollow fiber element, see § 2.2.1) for FO continue applications is more practical because: tubular membrane are self-supported, packing density is relatively high and liquids flow freely on both sides of the membrane. The main different between tubular membranes and hollow fiber is the bigger internal diameters of the membranes, which modifies the flow regime from laminar to turbulence. Thus, CP, fouling and scaling are reduced.
To clean the membranes, backwash may be enough to remove the deposited particles. This could be done simply replacing the draw solution with pure water, or reducing the concentration of the osmotic agent (OA) in order to generate a net water flux in the opposite direction. Similar results can be obtained by increasing the salt concentration in the feed side, or by fluctuating the operating pressure.
Significant progress has to be made as regard membranes efficiency in order to make FO competitive with other desalination processes.

3.1.1.2 Draw solutions

One of the main current challenges of FO desalination technology is to find out an effective draw solution (DS). DS is usually a water solution of a high molecular weight salt (osmotic agent, OA). The extent of OA diffusion depends on its molecular weight (diffusion decreases as the OA molecular weight increases) and on membrane type (Merdaw, 2009). The draw solution is the source of the driving force of the process and it should have these characteristics (Chung *et al.*, 2010 and Zhao *et al.*, 2012): high osmotic pressure (solute with a low molecular weight), zero toxicity, stability at or near natural pH, minimum ICP, easy recovery and low cost. For the draw solution, lower viscosities, higher diffusion coefficients, and smaller molecules/ion sizes will minimize ICP. Thus, better permeate fluxes will be obtained. In Table 3.1 an overview of the investigated draw solutions is reported.
The first draw solution used in 1965 by Batchelder was sulphur dioxide; it could be removed by stripping operation. However, the patent is vague, and only demonstrates that a positive water flux takes place. Later, also aqueous aluminium sulphate and many sugars, such as glucose and fructose, were explored as draw solution. Kravath, in 1975, described a FO desalination process using glucose as draw solute; while concentrate fructose was used by Stache in 1989 to produce a drinkable sugar-water. In 1992, Yaeli, continued to test sugar, and described a continue FO/RO process with sucrose as draw solute. In the early 2000's water soluble mixture of ammonium bicarbonate (NH_4HCO_3) was discovered as draw solute (McCutcheon, Yale University). It can be recovered, in carbon dioxide and ammonia, heating upon 65 °C. Current R&D is focused on studying highly hydrophilic nano-size particles as draw solutes in integrated FO-UF process. Where a UF step is used to split the product water from the dilute draw solution and

recover the draw solution (Chung *et al.,* 2010). Furthermore ultrasonication and magnetic separators could recover a draw solution with magnetic hydrophilic nano-size particles. However, the problem of particles agglomeration during the recycling is a limiting factor. One of the last tested draw solute is a polymer hydrogel, which draws water from the saline water feed when swelling, and releases the water during the process of deswelling caused by heating, or hydraulic pressure. Moreover a gel-like mixture composed of positively charged $Al_2(SO_4)_3$ and $CaSO_4$, with special negatively charged nanoparticle and an external magnetic field, has been investigated as a novel draw solution that could potentially make FO desalination process eco-sustainable (Zhao *et al.,* 2012).

Table 3.1. *Overview of the draw solutes/solutions used in FO investigations and their recovery methods (Zhao et al., 2012).*

Year	Draw solute/solution	Recovery method
1965	Volatile solution (e.g. SO_2)	Heating or air stripping
1965	Mixture of water and another gas (SO_2) or liquid (aliphatic alcohols)	Distillation
1972	Al_2SO_4	Precipitation by doping $Ca(OH)_2$
1975	Glucose	None
1976	Nutrient solution	None
1989	Fructose	None
1992	Sugar	RO
2002	KNO_3 and SO_2	SO2 is recycled through standard means
2005-2007	KNO_3 and SO_2 (NH_4HCO_3)	Moderate heating (~ 60°C)
2007	Magnetic nanoparticles	Captured by a canister separator
2007	Dendrimers	Adjusting pH or UF
2007	Albumin	Denatured and solidified by heating
2010	2-Methylimidazole-based solutes	FO-MD(1)
2010-2011	Magnetic nanoparticles	Recycled by a magnetic field
2011	Stimuli-responsive polymer hydrogels	Deswelling the polymer hydrogels
2011	Fertilizers	Unnecessary
2011	Hydrophilic nanoparticles	UF

(1) Membrane Distillation

3.1.1.3 Considerations

Internal concentration polarization, reverse solute diffusion, membrane characteristic, draw solute properties and membrane fouling are the main key challenges of FO applications. These factors are not isolated but closely linked to each other. Figure 3.4 shows the relationship between the key challenges. The membrane support layer should have high porosity in order to decrease ICP, and the membrane active layer should be highly selective in order to reduce reverse solute diffusion. As reverse solute diffusion decrease, membrane fouling can further decrease. If draw solute particles are small, the ICP will be reduced. However both reverse solute diffusion and membrane fouling could increase. Thus, the criteria for the choice of the right solution is more critical. Generally, high reverse solute diffusion may produce stern membrane fouling and vice versa.

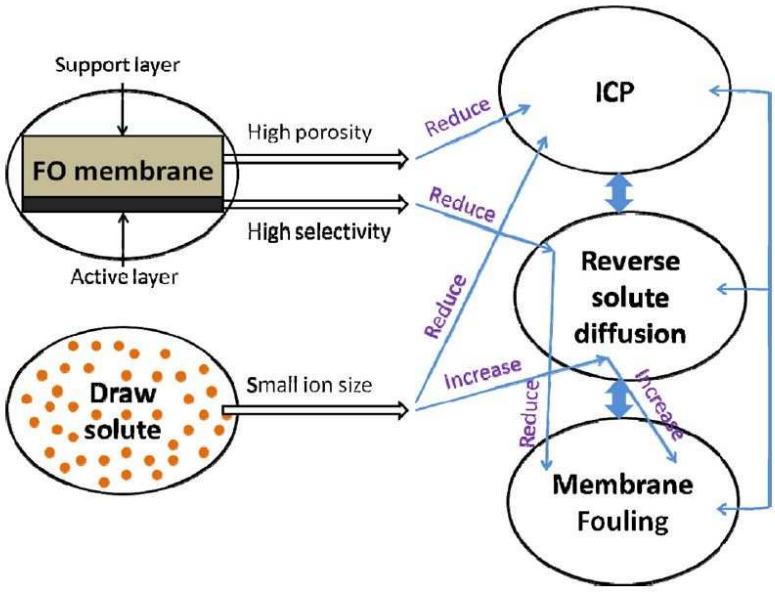

Figure 3.4. *Relationship between ICP, membrane fouling, reverse solution diffusion, membrane characteristic and draw solute properties in FO (Zhao et al., 2012).*

Forward osmosis is growing as an alternative to RO desalination process because of its advantages compare to pressure-driven membrane processes. However, to scale up FO from research applications to industrial plants, significant improvements of both FO membrane performance and draw solute have to be made.

Another important criterion is the selection of a suitable process for re-concentrating the draw solution and obtaining the fresh product water. There are several different technological solutions such as column distillation, membrane distillation, heating and stripping. The use of a pressure-driven membrane step (low-pressure RO or high-

permeability NF) in the recovering stage, characterized the novel Manipulated Osmosis Desalination (MOD) process, developed at CORA (Sharif & Al-Mayahi, 2005).The aim of this thesis is to test, in a RO element, a solution of water and ethanol, as draw solution in a MOD process.

3.2 Manipulated Osmosis Desalination process

The innovations of CORA in the area of desalination and renewable power generation have been commercialised through a university spin-out company, Surrey Aquatechnology Ltd, which was merged with the AIM-listed company Modern Water plc in 2007, and since then three commercial plants have been installed in Southern Europe and the Middle East. Some patent have been done to protect the novel technology (MOD is based on Patent number US7879243, Solvent removal process). MOD is a relatively new process to replace the RO one, which is based on the manipulation of the osmotic potential between two solutions to permit fresh water to diffuse in the wanted direction.

3.2.1 MOD process

Manipulated Osmosis Desalination process is shown in Figure 3.5. The difference from the FO schematic representation of Figure 3.2 is in the regeneration unit: MOD process involves a NF or RO step to regenerate the draw solution (concentrate osmotic agent).

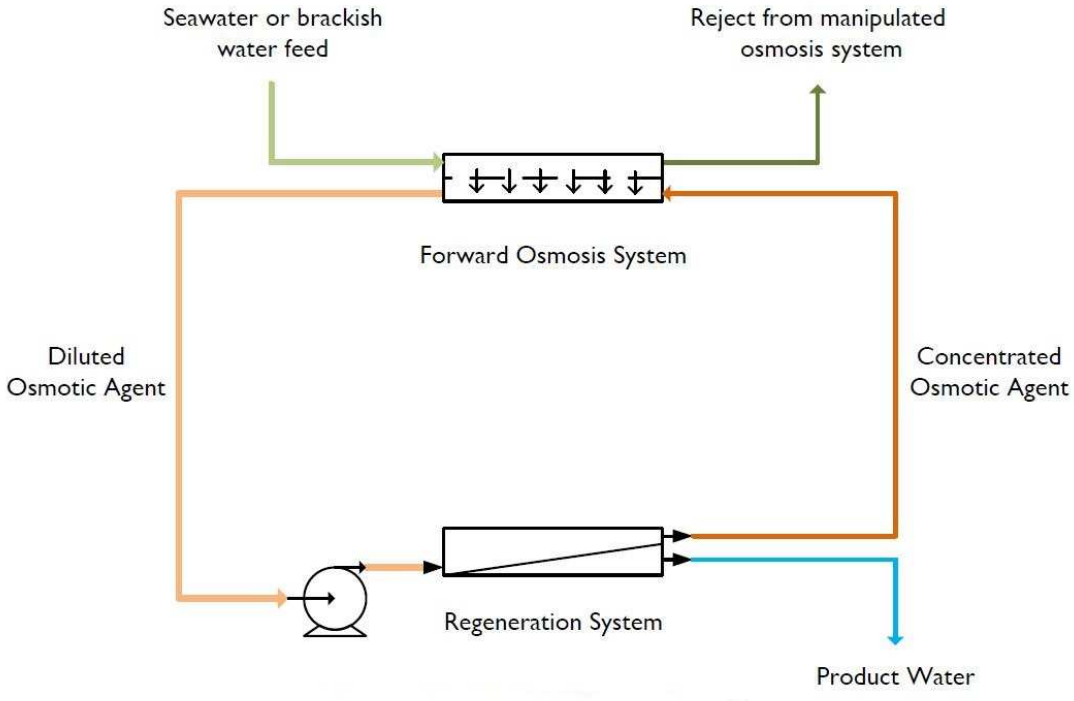

Figure 3.5. *Simplified MOD process diagram (Thompson, 2011).*

The process description is the same of a normal FO desalination process as described in paragraph § 3.1.1. The first step is a FO unit that drives out fresh water from a concentrated salt solution, by manipulating the osmotic energy potential through the use of a proper draw solution. The regeneration system is a low-pressure RO or high-permeability NF pressure-membrane based unit. In this regeneration step, water is driven through the membrane by hydraulic pressure, in order to overcome its natural tendency. Hydraulic pressure consumes energy, but, a careful selection of the osmotic agent (OA) and the operating conditions may minimize the energy requirement.

Key benefits of the MOD process, which have been demonstrated studying the MOD plants in operation, include (Thompson, 2011):

- lower fouling propensity and consequently lower operating cost;
- lower energy consumption than conventional RO, particularly with difficult feed waters (30% lower than RO);
- fewer replacements of the membrane, which results in a reduced membrane whole life cost;
- provision of a double membrane barrier between feed water and desalinated water;
- reducing of problematic seawater contaminants such as boron;
- lower cost and easier fabrication due to the use of low pressure pipework and fittings;
- possibility of modifying the properties of the OA in order to modify the product quality.

The membranes used are, unlike RO membrane, chlorine resistant. The OA is based upon a low cost, non-toxic, commodity chemical. The details of Modern Water's proprietary OA, and the type of the membrane are commercially sensitive and so are not presented here.

New semi-empirical models have been developed and verified in order to describe mass transfers in MOD process (Merdaw, 2009):

- Dynamic Equilibrium-Chemical Capacitance (DECC) model has been applied to describe the mass transfer in the FO process. Accordingly, the dynamic equilibrium is used to explain the relationship between water and solute flux, the electrical capacitance is dealt with to estimate the solution resistance and permeability, and two resistances in series are considered (membrane and solution);
- Solution diffusion-pore flow-fluid resistance (SDPFFR) model had been investigated for the mass transfer in RO process. Accordingly, water permeability is used as an alternative to CP. Furthermore, a better description of membrane-fluid interaction is reached;

- two new analytical models have been developed to link membrane micro-structural parameters, solution molecular properties and operational condition: Analytical-Solution Diffusion-Pore Flow (ASDPF) model, and Molecular Trap (MT) model.

Furthermore, a new theoretical definition of the specific energy consumption, based on mechanical energy balances, is used to assess the performance of each unit and of the whole MOD process.

3.2.2 MOD facilities

MOD process has been investigated initially through planned separate investigation of bench-scale FO and RO unit. The results of individual RO and FO experiments have been used to select the optimal operational conditions of the MOD process. For instance the draw solution dilution has to equate the value of the recovery rate at the RO unit. Then, a MOD pilot plant has been operated. After data collection, models investigation and validation, scale-up has been done to test MOD process out of laboratories, and to have enough long-time data to optimize all process (Merdaw, 2009).

Laboratory test rig

MOD process has been investigated at CORA. The CORA team used a laboratory test rig to examine the performance of several membrane units and procedure to develop the concept of Manipulated Osmosis Desalination.

Trial facility

In September 2008, Modern Water commissioned the first implementation of a MOD plant outside a laboratory environment. The plant was located at Gibraltar, and it was used as a trial FO/RO facility. Then, this plant has been supplying drinkable water to the local system since 1 May 2009. The feed water, after a shared pre-treatment, enters to the FO unit with SDI between 3 and 4. Typically, the product water has a TDS of less than 200 mg/L and boron level of less than 0.6 mg/L. The Gibraltar plants was used to: confirm the accuracy of mathematical models, demonstrate the stable operation of MOD cycle, optimise the entire process gathering long-term operational data, test the duration of the membrane, and identify real-world issues that may not be apparent in the laboratory-scale.

Production facility

In July 2009, a production plant with a design capacity of $100 m^3/d$ was planned and deployed to a site in the Sultanate of Oman. The site is owned by the Public Authority for Electricity and Water (PAEW) and, prior to Modern Water's arrival, contained a SWRO plant with a nominal capacity of 100 m^3/d. MOD plant was designed to share both pre- and post- treatment equipment on the site with the existing facility, in order to

demonstrate the benefits of MOD compared with the RO plant. The plant has been fully operational since November 2009. Modern Water's experience on the site has been challenging, due to the hard ambient conditions and the low quality of the feed water. Despite the difficulties, the product water typically has TDS of less than 200mg/L and a boron level between 0.6 and 0.8 mg/L, with a recovery of 35% and a feed water SDI of 5. The output of FO system, over the course of 2010, remained relatively the same. Contrarily, over the same period, SWRO output, despite the repeated cleaning, had a decline of 30%. Furthermore, the energy consumption of MOD plants is lower than SWRO. For instance, the specific energy consumption per unit of product is 4.9kWh/m^3 for MOD plant, instead of 8.5kWh/m^3 for the SWRO plant. MOD process is seen to be operated at about 60% of the energy consumption of the SWRO plant (Thompson, 2011). A third desalination plant is being built at Al Naghdah in the Al Wusta region of Oman for PAEW. The plant is designed to produce 200m^3/d of drinkable water which will be supplied to the local community.

3.2.3 Considerations

The success of MOD is highly dependent on the proper selection of RO and FO membrane, and the draw solution. Moreover membrane micro-structure, fluid properties and operation conditions need efficient models in order to obtain excellent design equations.

Modern Water has successfully taken MOD process from the laboratory to a full-scale commercial facility, investigating the aforementioned issues. Key advantages have been proven and MOD technology is ready to become mature. It could save the 90% of the energy requirement compared to current thermal desalination processes and the 30% (up to 60% in Sultanate of Oman's facility) compared to SWRO process. If RO was considered a revolutionary technology in desalination processes 30 years ago, now MOD process can further reduce costs and save energy. The Water Desalination Report (WDR) of Global Water Intelligence (19 November 2010) rated MOD technology 8.9 out of 10, the highest rate in desalination processes. Nevertheless, membrane technology and the optimization of the process have to be improved because there are still areas of amelioration, so that minimized MOD Specific Energy Consumption (SEC) would make the process more commercially attractive. Furthermore, the discovery of a better draw solution could make the process more efficient. The aim of this thesis is exactly to test one possible draw solution make of ethanol and water.

Chapter 4

Experimental work

The experimental work involves two types of RO flat-sheet thin film composite commercially available membrane: polyamide TFC®-ULP, and aromatic polyamide RO98pHt® (previous name: HR98PP) membranes. Experiments are carried out in a bench-scale cell using a solution of water and ethanol at different concentration as feed solution. In the Section 1 a brief discussion about water-ethanol solution is given, while in Section 2 the bench-scale experiments are described.

4.1 Ethanol as an osmotic agent

Ethanol is a 2-carbon alcohol with chemical formula CH_3CH_2OH. It is a volatile, flammable and colourless liquid. Solutions of ethanol and water form an azeotrope at about 89% ethanol and 11% water by mole, or about 95.6% of ethanol by mass. This azeotropic composition strongly depends on temperature and pressure. In Table 4.1 a comparison between water and ethanol properties is shown.

Table 4.1. *Ethanol and water properties.*

Property	Ethanol	Water
Melting point	-114.1°C	0.0°C
Boiling point	78.5°C	100 °C
Density (25°C)	787.00 Kg/m^3	997.05 Kg/m^3
Molecular weight [u]	46.07	18.015

Water-ethanol solution could potentially be a suitable draw solution for the following reason:

- high available osmotic pressure gradient over a wide range of composition (see Table 4.2);
- ethanol has a low molecular weight;
- high ethanol solubility in water;
- ethanol is relatively cheap;

- enough vapour-liquid equilibrium data in the literature to precisely describe the chemical potential of aqueous-ethanol solutions to design the separation process.

In Table 4.2 the osmotic pressure of ethanol in water at different concentrations is shown. Low concentrations generate a solution with high osmotic pressure. This confirms the aforementioned reason why ethanol could potentially be a suitable osmotic agent. The data has been obtained by using OLI's software.

Table 4.2. *Water-ethanol osmotic pressure at different concentrations (25°C, 1bar).Values calculated using OLI's software (OLI System Inc., 2006).*

Ethanol concentration [mol/L_{H2O}]	Ethanol concentration [% m/m]	Osmotic pressure [atm]
0.2	0.92	4.83
0.4	1.81	9.55
1	4.42	23.12
3	12.17	62.79
5	18.77	92.58
6	21.71	109.92
8	26.99	135.05
10	31.60	156.13
15	40.94	194.29
20	48.03	214.96
25	53.60	220.04

Several simulations of water-ethanol solutions, have been done by using OLI's software in order to evaluate:

- the change of osmotic pressure with pressure at constant ethanol composition;
- the change of osmotic pressure with temperature at constant ethanol composition.

In Figure 4.1 the dependence of water-ethanol osmotic pressure at different concentrations as a function of pressure is shown. It is clear that pressure does not affect the osmotic pressure of the system. For instance, the osmotic pressure of a 20 mol/L_{H20} ethanol solution in water slightly increases from 214.96atm to 215.14atm with increasing the pressure from 1 to 30atm. Besides, the osmotic pressure of a 0.65mol/L_{H20} ethanol solution in water slightly increases from 15.31atm to 15.32atm with increasing the pressure from 1 to 30atm. The changes, for this two aforementioned concentrations are only about +0.084% and +0.065% respectively, totally negligible for our purpose.

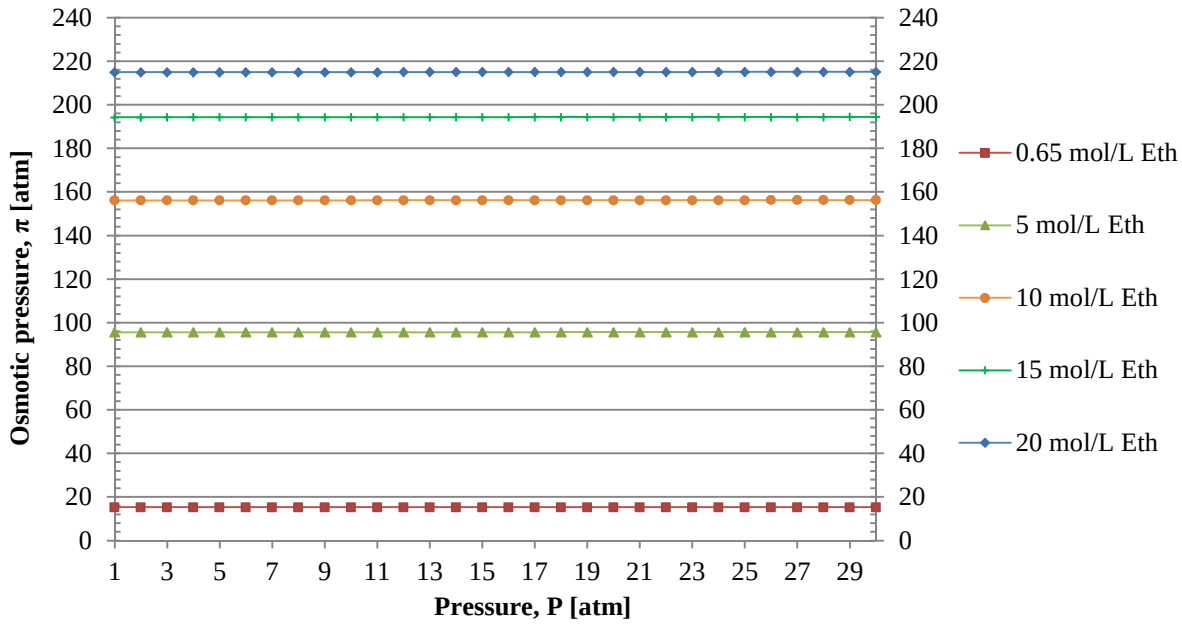

Figure 4.1. *The osmotic pressure π, of a solution of water and ethanol at different concentrations, as a function of the pressure. Values calculated using OLI's software (OLI System Inc., 2006).*

Figure 4.2 shows the dependence between osmotic pressure and temperature. It is clear that at low concentration of ethanol in water, the osmotic pressure increases as the temperature increases, with an approximate linear dependence. At around 9-10mol/L this trend begins to be reverse: as temperature increases, osmotic pressure decreases. At higher concentration it is more evident. For instance, the osmotic pressure of a 0.65mol/L_{H20} ethanol solution in water increases from 14.63atm to 16.37atm (+11.9%), when the temperature of the system is increased from 10 to 50 °C. On the contrary, the osmotic pressure of a 20mol/L_{H20} ethanol solution in water decreases from 237.20atm to 182.23atm (-23.17%) in the same temperature gap. These results can be explained considering the non-ideal behaviour of water-ethanol solutions. At low concentration of ethanol, even though the solution is not ideal, according to van't Hoff relationship (see paragraph § 1.2.1, equation 1.11) the osmotic pressure increases as temperature increases. On the contrary, at higher concentrations other factors seem to overcome the effect of the temperature in increasing the osmotic pressure, and the van't Hoff relationship it is not followed.

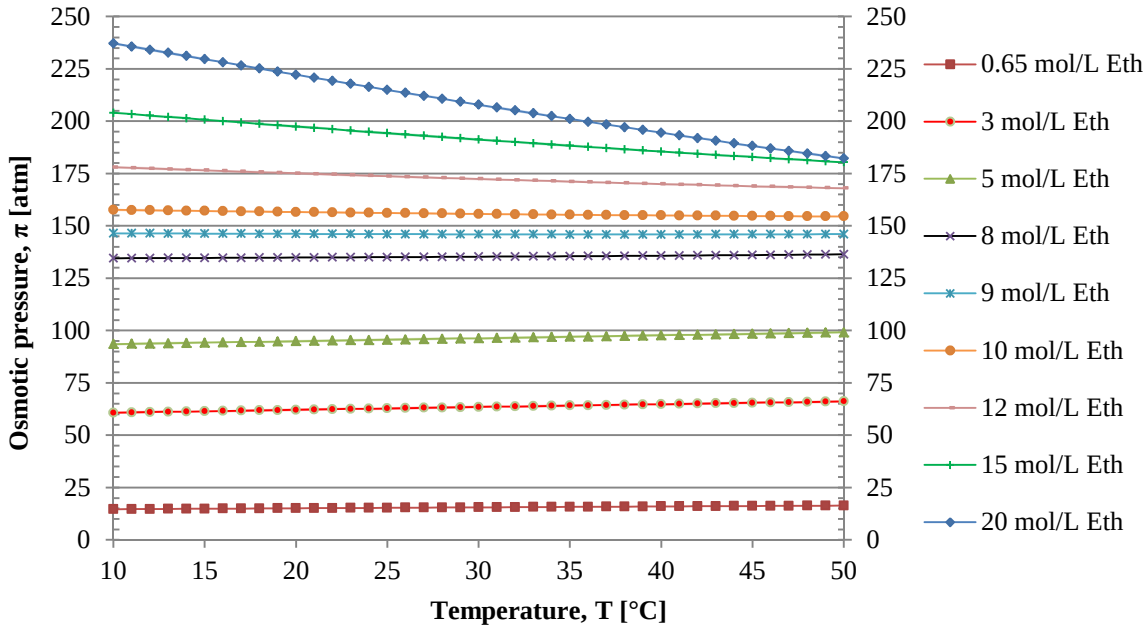

Figure 4.2. *The osmotic pressure π, of a solution of water and ethanol at different concentrations, as a function of the temperature. Values calculated using OLI's software (OLI System Inc., 2006).*

The experiments are carried out at room temperature (22±2°C). An accuracy analysis about the temperature influence on the osmotic pressure results is given in paragraph § 4.2.4.

Solutions of water and aliphatic alcohols have been investigated in the past (see § 3.1.1.2), but the membranes were not enough developed to reach significant results. Recently, an aqueous ethanol solution has been investigated as a draw solution in a FO process by McCormick (2008) for different types of membranes, in order to find out the right membrane to minimize the loss of ethanol (McCormick *et al.*, 2008). However, no recovery methods are considered in McCormick investigation. Theoretically ethanol is a perfect osmotic agent for MOD process, but also in this case there are no enough data about the DS recovery step.

There are several different processes to separate water and ethanol; which are described in the following paragraph. However, the aim of this Thesis is to evaluate the separation efficiency of a RO unit, which is the recovery step of the MOD process. In Figure 4.3 the investigated MOD process with ethanol as the osmotic agent is shown.

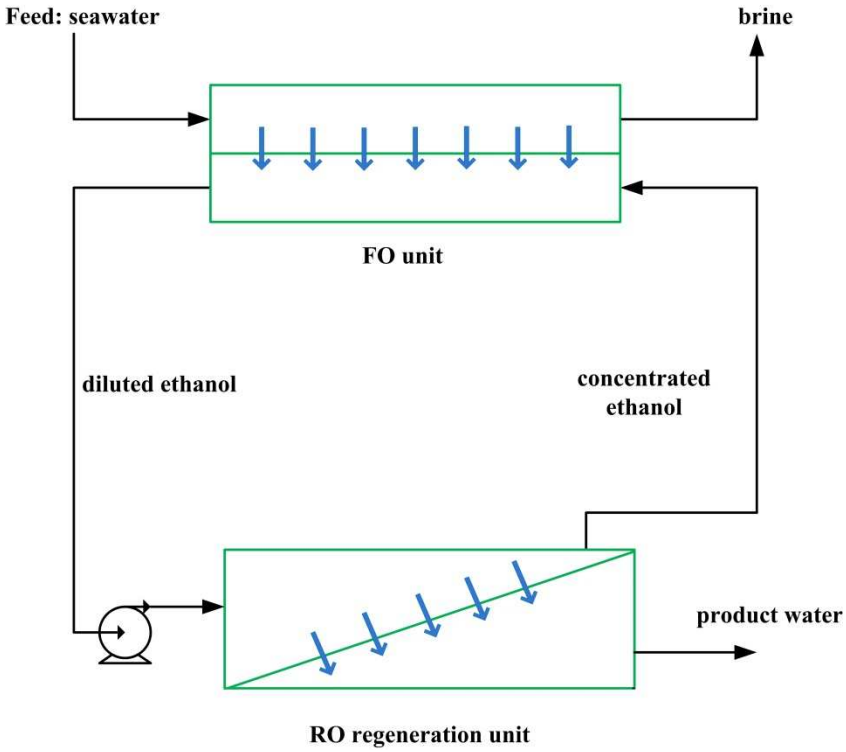

Figure 4.3. *MOD process with ethanol as osmotic agent.*

In the FO unit, water selectively permeates trough the membrane from the feed side (lower water osmotic pressure) to the permeate side due the osmotic pressure difference, diluting the draw solution of ethanol and water. The resulting water + draw solution is then separated into a fresh water stream and the draw solution is recycled back to the FO unit.

4.1.1 Water-Ethanol separation processes

Ethanol dehydration is an energy intensive process due to the presence of the azeotropic point. Ethanol and water can be separated by several techniques (Haelssig, *et al.*, 2011): extractive distillation, pressure swing adsorption of water on molecular sieves and pervaporation/vapour permeation of water through hydrophilic membrane. Furthermore a hybrid process named Membrane Dephlegmation has been investigated.

Distillation

The conventional separation process uses several distillation steps combined with a dehydration process (normally extractive distillation) to go over the azeotropic point. Ethanol is first passed through a “beer” column. This column performs as a steam stripping column and produces a vapour stream with a composition between 40% and 60% of ethanol by mass. This stream usually enters an enriching column to obtain a

distillate close to the azeotropic point, which needs to be dehydrated in order to overcome the azeotropic point and produce anhydrous ethanol (Haelssig *et al.*, 2012).

Pressure swing adsorption of water on molecular sieves

The vapour stream of ethanol and water is pumped and passed in some vessels, containing specific molecular sieves. This can separate ethanol and water because, under pressure, the absorbent bed inside the vessels tends to adsorb water and allow at the ethanol to pass through. Special adsorptive materials (e.g., zeolites) are utilized as a molecular sieve, specially adsorbing the target gas species at high pressure. The process then swings to low pressure to desorb the adsorbent material.

Pervaporation/vapour permeation of water through hydrophilic membrane

In vapour permeation the feed is a vapour, there is no phase change or substantial temperature difference across the membrane. Separation is realized by the different grades to which components are dissolved in and diffuse through the polymer of the membrane. The driving force is proportional to the partial pressure difference of the components in the feed. The main key factor of the process is the membrane material and characteristics (Bolto *et al.*, 2012). Hydrophilic organic polymers are generally used to separate water from water/organic mixtures, due to their attraction of water molecules: water sorption on the membrane surface, diffusion through the membrane matrix and desorption into the permeate bulk phase.

In pervaporation process the concepts are the same of vapour permeation, but the feed is a liquid. Thus, an energy-demanding phase transition from the liquid to the vapours occurs.

Both vapour permeation and pervaporation work according to the solution-diffusion model.

Compare to pervaporation, vapour permeation requires lower membrane area and provides higher flow rate.

Membrane Dephlegmation

Another recent possibility to separate ethanol and water is to use a hybrid distillation – pervaporation process: Membrane Dephlegmation (Haelssig, *et al.*, 2011). This hybrid process replaces the enriching column and dehydration system in the ethanol separation process, combining both distillation and pervaporation within the same unit: a vertically oriented pervaporation membrane, with counter current vapour-liquid contacting on its surface. The pervaporation membranes are NaA zeolite type. They are not limited by vapour-liquid equilibrium, in order to break the azeotropic point, reaching concentration of ethanol greater than 99% by mass. These kinds of membranes, compared with the

polymeric alternatives, have higher water fluxes and higher separation factors. This leads to lower separation costs, absence of concentration polarization, less swelling of the membrane and higher energy efficiency.

Membrane Dephlegmation is not the only possible hybrid separation process that has been investigated. In Figure 4.4 the most promising hybrid separation process configuration involving distillation are shown, pressure swing adsorption and vapour permeation, and the benchmark process (Roth *et al.*, 2010). The hybrid processes could overcome existing limitations and offer a more energy efficient and economic process.

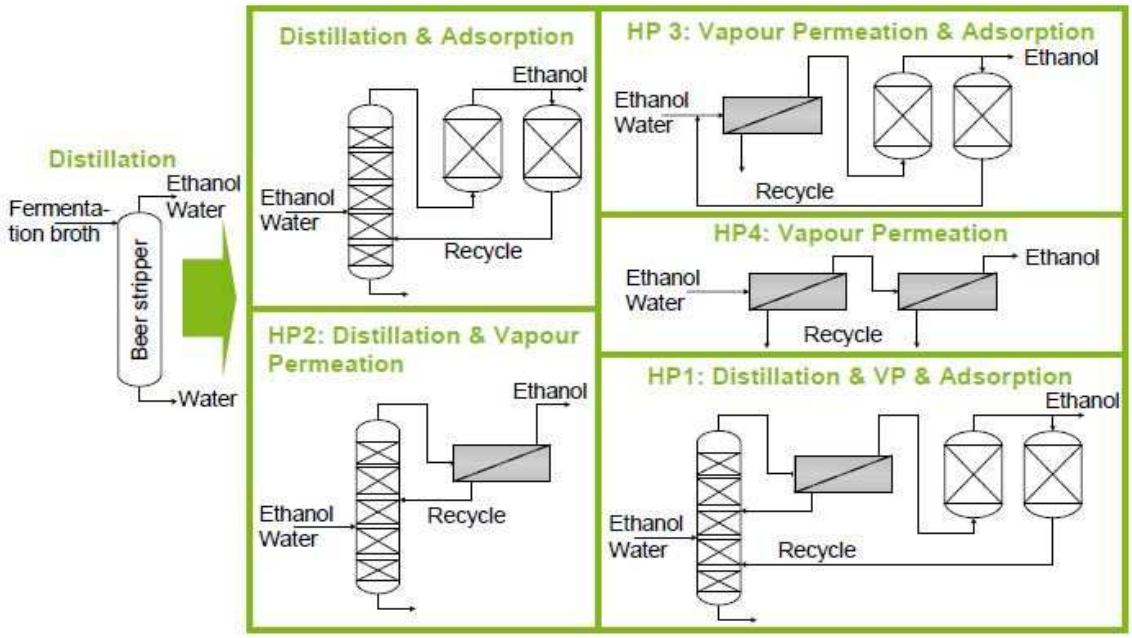

Figure 4.4. *Promising hybrid separation processes for ethanol dehydration (Roth et al., 2010).*

4.2 Bench-scale experiments

The RO experiments have been carried out with pure water, salt water and aqueous solutions of ethanol as feed in order to investigate the performance of the membranes. The effect of hydraulic pressure, at constant temperature, in water flux and ethanol rejection has been examined.

4.2.1 Laboratory cell

Experiments were carried out using a small static RO laboratory cell supplied by SpinTek Filtration, Inc. (USA) (Figure 4.5). The unit consists in a variable speed high pressure pump with flexible connections, a pressure gauge for the feed and the concentrate line, a digital flow meter and a needle valve at the concentrate line, a 4-

liters feed tank and a flat sheet membrane's cell. The flat sheet membrane is laid horizontally on the lower fixed part of the cell. The membrane is then tightened in-place using a rubber gasket with the upper part of the cell by eight, evenly positioned, screw bolts with nuts. The feed solution flows alongside the lower side of the membrane and discharges through a needle valve as concentrate. The permeate fluid obtained from the upper side of the membrane flows through a small opening in the upper part of the cell. In order to avoid membrane bending towards the porosity permeate side due to the high hydraulic pressure difference, ten layers of high porosity filter paper (Whatman, type 1-Qualitative, filter speed: Medium-Fast) were embedded over the membrane substrate surface (for a total thickness of about 2.2 mm) and then secured by a stainless wire mesh of 1 mm thickness.

The upper hydraulic pressure used for the experiments was 20bar, which is the maximum operating hydraulic pressure allowed by the unit. The flow diagram of the reverse osmosis test set-up is depicted in Figure 4.6.

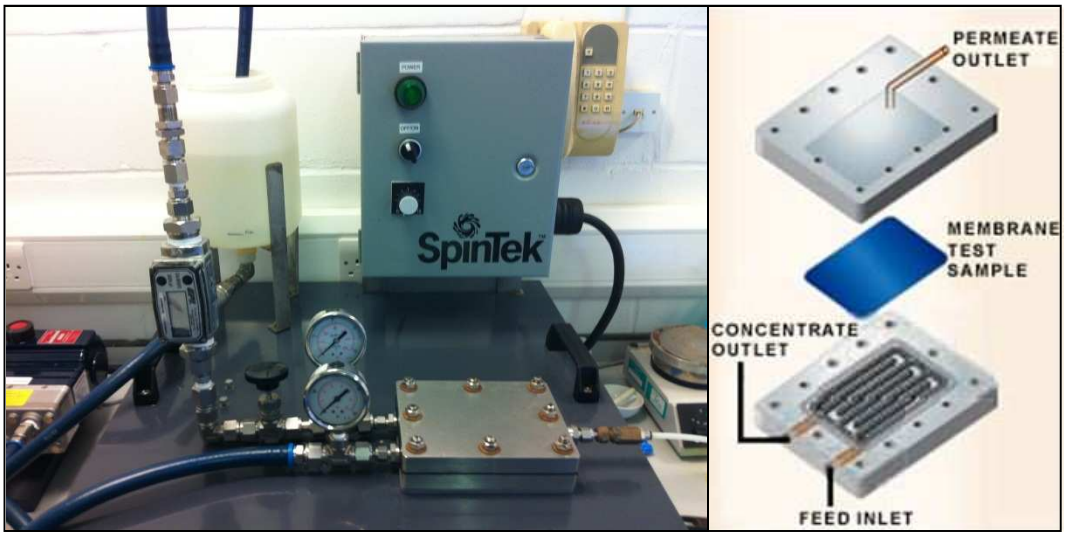

Figure 4.5. *Reverse osmosis bench-scale cell named Static Test Cell (STC (SpinTek Filtration, Inc., USA)).*

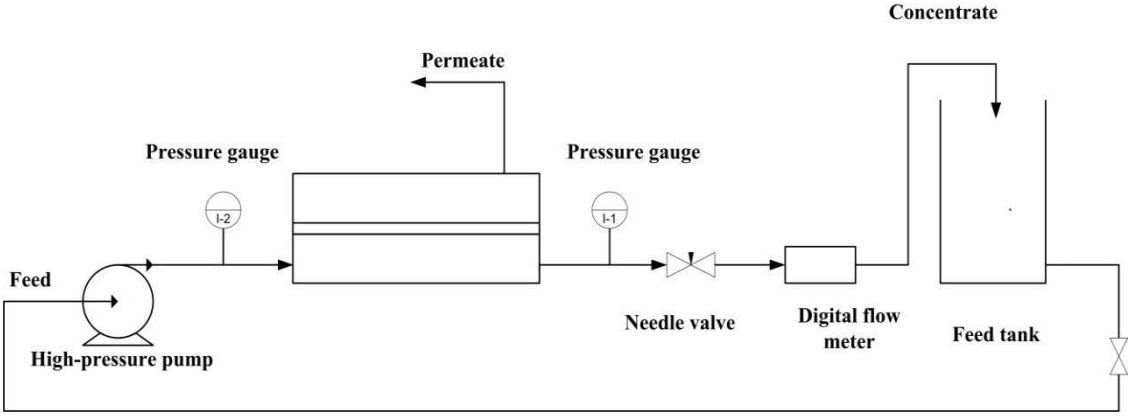

Figure 4.6.*Flow diagram of the reverse osmosis test set-up.*

The filter paper layers force the feed fluid to pass through the grooves of the zigzagged path of the lower part of the cell, as shown in Figure 4.7. The membrane active area is calculated from the path geometry; it is about 45cm^2 (A_m).

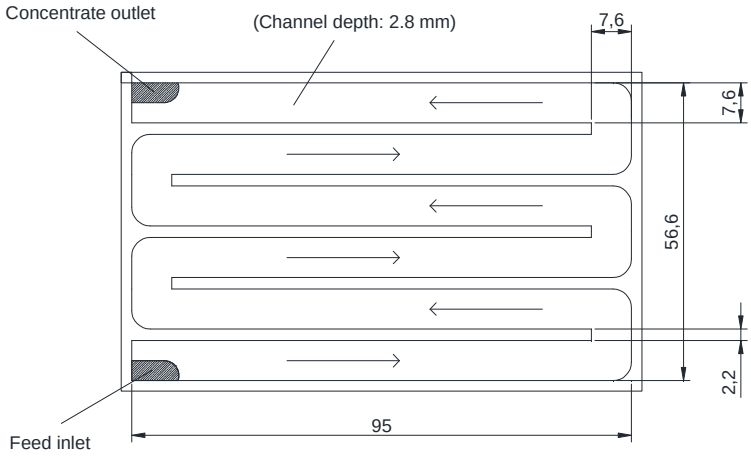

Figure 4.7. *Top view of the lower fixed part of the RO cell, showing the feed flow path. The channel cross section is about 21.3 mm^2.The dimensions are expressed in mm.*

4.2.2 Membranes

The first membrane used is TFC®-ULP. It is manufactured by Koch Membrane System, Inc. (USA), and it was commercialized from 1995 as a new generation of the TFC membranes with polyamide active layer. It is usually used for brackish water desalination by RO process with ultra-low pressure (ULP). About 20-33 % lower energy consumption can be achieved using TFC®-ULP membrane in a brackish water application (Filteau *et al.*, 1997).

Table 4.3 lists some operation and design data about the membrane as specified by the manufacturer, and Table 4.4 lists some micro-structural properties.

Table 4.3. *Manufacturer's operating and design data of TFC®-ULP membrane referred to the 4014 spiral wound model (test conditions: 700 ppm TDS, 13.8 bar, 25°C, pH 7, 15% recovery).*

	TFC®-ULP
NaCl rejection [%]	99.0
Permeate flux [L/(m^2 h)]	46.57
Specific permeate flux [L/(m^2 h bar)]	6.14
Maximum operating temperature [°C]	45
Maximum operating pressure [bar]	24.20
Maximum free chlorine @ 25°C [mg/L]	<0.1
Allowable pH – continuous operation	4-11

Table 4.4. *Micro-structural properties of TFC®-ULP membrane.*

	TFC®-ULP
Pure water permeability @ 25°C [L/m^2.d.kPa]	1.95[(1)]
Molecular Weight Cut Off (MWCO) [Da]	< 180[(3)]
Mean pore diameter [nm]	< 0.64[(2)]
Contact angle [°]	38[(1)]
Mean roughness [nm]	42[(1)]
Charge @ pH 6	Negative[(1)]

[(1)] (Xu &Drewes, 2006), [(2)] (Xu et al., 2005), [(3)] (Schäfer et al., 2000)

The mean pore diameter of a membrane can be featured by the molecular weight cut-off (MWCO) measured by Dalton (Da), which is a nominal measure of the separation potential of a membrane. It is defined as the molecular weight of the molecule that is 90% retained by the membrane. Commercially, MWCO is used as an indication for the membrane's pore size. However, no industry standard exist, therefore the MWCO ratings of different manufactures are often not comparable. Furthermore, the permeability of a solute is dependent, in addition to molecular weight, also on the shape of the molecule, its degree of hydration and its charge, and the nature of the solvent (solvent pH and ionic strength). Accordingly, MWCO should be used only as a guide, and not as an exact indicator of performance.

The mean pore diameter of a membrane can be calculated approximately from the MWCO data by using the following empirical relationship between the molecular weight and the molecular diameter (Ren et al., 2006):

$$D_p = 0.066\, MW^{0.46} \quad , \tag{4.1}$$

where D_p is the approximate equivalent diameter of the molecule in nanometers and MW is the molecular weight in g/mol.

The wetting and adhesion properties of membranes are affected by the contact angle, which is the angle at which the liquid/vapor interface meets the solid membrane surface. The contact angle is specific for any given system and is defined by the interactions across the interface.

Roughness is a measure of the texture of a surface. The mean roughness is the arithmetic average of the deviations from the center plane of peaks and valleys taken at different equally spaced spots (Hirose et al., 1996).

Initially, the membrane is conditioned by using de-ionized water as feed at 25°C and about 10bar for 3 hours, in order to eliminate any irreversible changes that could affect the following experiments.

The second membrane used was RO98pHt®. It is manufactured by Alfa Laval (Denmark), and it is a high-rejection aromatic polyamide with a polypropylene support. Table 4.5 lists some operation and design data about the membrane as specified by the manufacturer.

Table 4.5. *Manufacturer's operating and design data of RO98pHt®flat sheet membrane (test conditions: 2000 ppm NaCl, 16bar, 25°C).*

	RO98pHt®
NaCl rejection [%]	> 97.0
Typical operating pressure [bar]	46.57
Operating temperature range [°C]	5-60
Maximum operating pressure [bar]	55
Maximum free chlorine @ 25°C [mg/L]	<0.1
Allowable pH – continuous operation	2-11

The membrane is cleaned and conditioned prior the initial use with the following cleaning procedure, as recommended by Alfa Laval Product Specification:

- flushing with de-ionized water as feed for one hour (25°C and about 10bar);
- recirculating the de-ionized water at 30-40°C, standard pressure and flow conditions for 30 minutes;
- adding NaOH to achieve a pH of 8.5-10.5 and recirculating for 30 minutes;
- flushing with de-ionized water as feed (25°C and about 10bar) until achieve neutral pH for both permeate and retentate is achieved.

4.2.3 Feed solutions

The feed fluids were de-ionized pure water, aqueous solutions of NaCl and aqueous solutions of ethanol. All the chemicals used were of laboratory grade with high purity. In Table 4.6 their general specifications are listed.

Table 4.6. *Specifications of the chemical used.*

Chemical	Manufacturer	Grade	Purity	Molecular formula	MW
Sodium chloride	Sigma-Aldrich	Laboratory reagent	>99.5%	NaCl	58.44
Ethanol	Fisher Scientific	Analytical reagent grade	96% v/v	CH3CH2OH	46.07

NaCl solutions were prepared by dissolving the required amounts of salts in pure water of less than 10µS/cm electrical conductivity. Dissolving of salt was carried out at ambient temperature by using a laboratory magnetic stirrer. Measures of concentration during solutions preparation and during experiments were taken by using a digital electrical conductivity meter (model: SevenMulti, manufactured by Mettler-Toledo, Switzerland). The measurement of concentration and conductivity were taken directly from the instrument readings, as it was calibrated for this use.

Ethanol solutions were prepared by pouring the calculated amounts of ethanol in a known-volume holder, and filling the holder with pure water, in order to generate the required solution. Otherwise, if the ethanol is added to the wanted volume of water, the volume of the solution may change, because water-ethanol solutions have excess volumes.

In order to measure the concentration of ethanol in the permeate and concentrate streams, several possibilities have been investigated. The concentration of ethanol in aqueous samples can be measured by:

- the electrical conductivity of the samples and finding out the concentration of ethanol comparing the values generated by OLI's software;
- the density of the samples and calculating out the concentration of ethanol with a mathematical model based from the following equation:

$$\rho_{mix} = \frac{1}{\sum_i \frac{w_i}{\rho_i} + e} \ , \tag{4.2}$$

  where ρ_{mix} is the density of the sample, w_i and ρ_i are respectively the mass fraction and the density of the pure substance, and e is the excess quantity due to the no ideal solution;
- the analysis of samples with Gas Chromatography (GC) or High Performance Liquid Chromatography (HPLC).

As regards the electrical conductivity method, there are several negative aspects: the variation of EC is too small to be measured with accuracy, the EC of de-ionized water slightly changes in every experiment, and ethanol is a very weak electrolyte. As concerns the density method, the density-meter available in the laboratory unluckily was three decimal accurate. Unfortunately, working at such low concentration of

ethanol, a four decimal density-meter would be required. Therefore, both conductivity and density method could not be used to measure the concentration of ethanol in the samples. The most suitable alternatives are to use a GC or HPLC analysis.
In order to analyse the samples, the GC instrument of the Chemistry Department (University of Surrey) has been used (Agilent 6890N with flame ionisation detector).
The ethanol concentrations in de-ionized water, with the corresponding osmotic pressures used to test the performance of TFC®-ULP and RO98pHt®, membranes are listed in Table 4.7. The concentration of ethanol in water is low, in order to generate a solution with an osmotic pressure lower than the maximum operating pressure of TFC®-ULP membrane (24.2 bar) and the maximum operating pressure of the RO unit (20 bar). In addition, the concentration of ethanol in water is appropriate for the aim of this research. The osmotic pressure of the solution is calculated by using OLI's software (OLI System, Inc., 2006).

Table 4.7. *Ethanol concentration and osmotic pressure of the feed solution.*

Ethanol concentration **[mol/L_{H2O}]**	**Ethanol concentration** **[%v/v]**	**Ethanol concentration** **[%m/m]**	**Osmotic pressure** **[25°C, 1atm]**
0.05	0.29	0.23	1.22
0.15	0.87	0.69	3.63
0.25	1.44	1.14	6.01
0.35	2.00	1.59	8.38
0.45	2.56	2.04	10.71
0.55	3.11	2.48	13.02
0.65	3.66	2.92	15.30

4.2.4 Experimental accuracy

Generally, the aim of the experiments is to investigate the relationship between the controllable variables and the observed response. In our case, the controllable variables considered are the solutes concentration and the hydraulic pressure of the feed fluid. The experiments were carried out at constant feed flow rate and cell configuration. The observed variables were the flow rate and the concentration of permeate and concentrate streams, and the hydraulic pressure of the concentrate. The collected data were then used to calculate other process variables: water flux form volume and time data; solute flux from concentration, volume and time data; osmotic pressure difference across the

membrane (by converting concentrations to osmotic pressure by using OLI's software) and solute and water permeability from all aforementioned data.

The experiments were carried out at room temperature of 22±2°C. As described in paragraph § 4.1, the temperature influences the osmotic pressure of the feed. Then, accuracy analysis about the temperature influence on the result is given in the following.

The 0.65 mol/L_{H20} ethanol solution is chosen to do the accuracy analysis, because it is the highest concentration of ethanol used in the experiments, where the temperature effect is higher. The osmotic pressure of the permeate and concentrate streams for each investigated pressure was calculated by using OLI's software firstly at 20°C and then at 24°C. The difference from the calculated $\Delta\pi_{20°C}$ and $\Delta\pi_{24°C}$ is about 1.14% for both the experiments (the first with TFC®-ULP and the second with RO98pHt®membranes). Hence, the effect of the variation of the room temperature on the osmotic pressure is completely negligible in our experimental work.

However, it is clear that the temperature influences also the values of the fluxes through the membrane; for instance a rise in the temperature increases the permeate flux.

Consequently, the effects of temperature variation, between 20°C and 24°C, during the experiments have been considered acceptable for the purpose of this thesis; however in the same time they are a considerable limitation of this works, because the temperature effects on fluxes were not considered.

In addition, some experimental data have been neglected after careful considerations, in order to maximize the correlation index R^2 ($0 \leq R^2 \leq 1$). The model used is linear, thus a linear regression has been used. The neglected data could have been affected due casual errors, ethanol evaporation, increasing of the feed temperature due to the pump or unsteady state measurement.

Finally, the experimental concentration data for the 0.05mol/L ethanol solution are not considered for the ethanol permeability, ethanol flux and ethanol rejection calculation because they fall outside of the calibration curve of the GC used for the samples analysis.

4.2.5 Experimental procedure

In this section a detailed description of the experimental procedure is presented.

The experiments have been performed according to the following procedure:

- the RO unit was completely disassemble, each component is accurately cleaned with a mixture of hot water and a citric acid soap;

- the RO unit was carefully assembled and then widely flushed with a mixture of hot water and a citric acid soap, in order to remove all the salts deposits left from the previous experiments;
- the RO unit was flushed with de-ionized water, in order to remove all the impurities from the pipes and the cell;
- the membrane was cut and positioned in the cell with ten layers of filter paper as described in paragraph § 4.2.1;
- the membrane was cleaned and conditioned as described in paragraph § 4.2.2. Moreover, in between the use of two feed solutions with different solutes, the system was flushed with de-ionized water for 3 hours to remove residuals of the previous solutions;
- the membrane was tested with an aqueous feed solution of NaCl (8.2 g/L), in order to verify the operation of the membrane. The feed solution was prepared as described in paragraph § 4.2.2;
- the pure water permeability was measured with pure water experiments at two different temperatures (26°C and 33°C);
- the feed ethanol aqueous solutions for each membrane were prepared as described in paragraph § 4.2.2;
- the RO unit was flushed with the required feed solution in order to remove all previous substances. The experiments were carried out at room temperature (22±2°C) and at constant feed flow rate and cell configuration. The controllable variables considered are the feed ethanol concentration, the temperature and the hydraulic pressure of the feed fluid. The observed variables are the flow rate and the concentration of permeate and concentrate streams, and the hydraulic pressure of the concentrate. The investigated feed-fluid pressures are: 2, 5, 8, 11, 14, 17 and 20 bar. For each pressure 3 samples of permeate and 3 samples of concentrate were taken. The samples were analysed, to find out the concentration of ethanol, by using GC (see § 4.2.2 for specification). Permeate flow rates have been measured manually for each 5 or 10 mL collected by using a 10 mL measuring cylinder and a digital stopwatch.

Chapter 5

Results and discussion

As described in Chapter 4, several bench-scale experiments have been carried out using two types of flat-sheet membrane: TFC®-ULP and RO98pHt® membranes (see paragraph § 4.2.2 for specifications). These experiments can be divided in three main groups:

1. with pure water as feed to determine the pure water permeability (A_{wm});
2. with salt water as feed in order to verify the operation of the membrane;
3. with aqueous ethanol solutions, to investigate the separation performance of the membranes.

The Solution Diffusion Model (see § 2.2.2.1) is used to elaborate the experimental data. According to its assumption, it is suitable to work out of the experimental data, due to the low concentration of salt and ethanol in the feed.

In the following sections the results of the aforementioned experiments are presented, and a discussion about the experimental work is developed in the last section.

5.1 Pure water experiments

These experiments were carried out with the purpose to determine the pure water permeability (A_{wm}) and the water flux through the membrane (J_w). These two parameters are calculated by using the following equation based on the Solution Diffusion Model:

$$J_w = A_{wm}\Delta p \ , \tag{5.1}$$

$$\Delta \mathrm{p} = \frac{P_f + P_c}{2} - P_p \ , \tag{5.2}$$

where Δp is the average value of the trans-membrane hydraulic pressure difference, and the subscripts f, c and p refer to the feed, concentrate and permeate stream, respectively. Thus, the water flux through the membrane (J_w) is estimated by dividing the amount of water collected in a certain time by the membrane active area, A_m. The pure water permeability is calculated by dividing the water flux by the trans-membrane hydraulic pressure difference.

Pure water has a maximum electrical conductivity of 10µS/cm.

Figure 5.1 shows the values of pure water permeability of both TFC®-ULP and RO98pHt® membranes as a function of the hydraulic pressure difference across the membrane at 26 and 32°C, and at a constant feed flow rate of ~ 107 L/h.

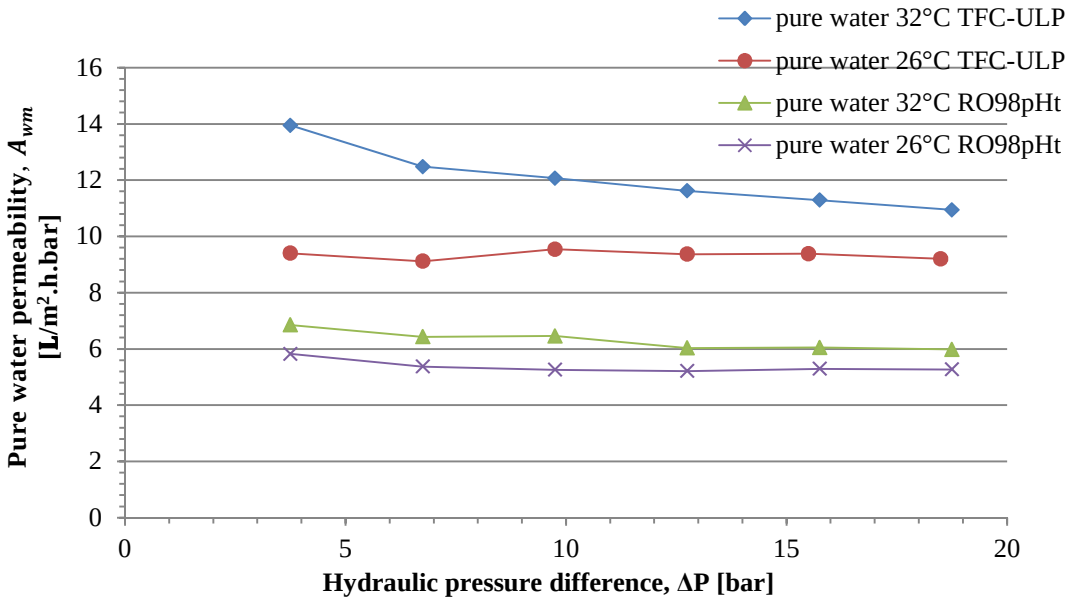

Figure 5.1. *Pure water permeability of TFC®-ULP and RO98pHt® membranes at 26 and 32°C, as a function of the hydraulic pressure difference across the membrane. Feed flow rate constant at ~107 L/h.*

Figure 5.2 shows the results of the water flux through the membrane as a function of the hydraulic pressure difference across the membrane at 26 and 32°C, and at a constant feed flow rate of ~ 107 L/h.

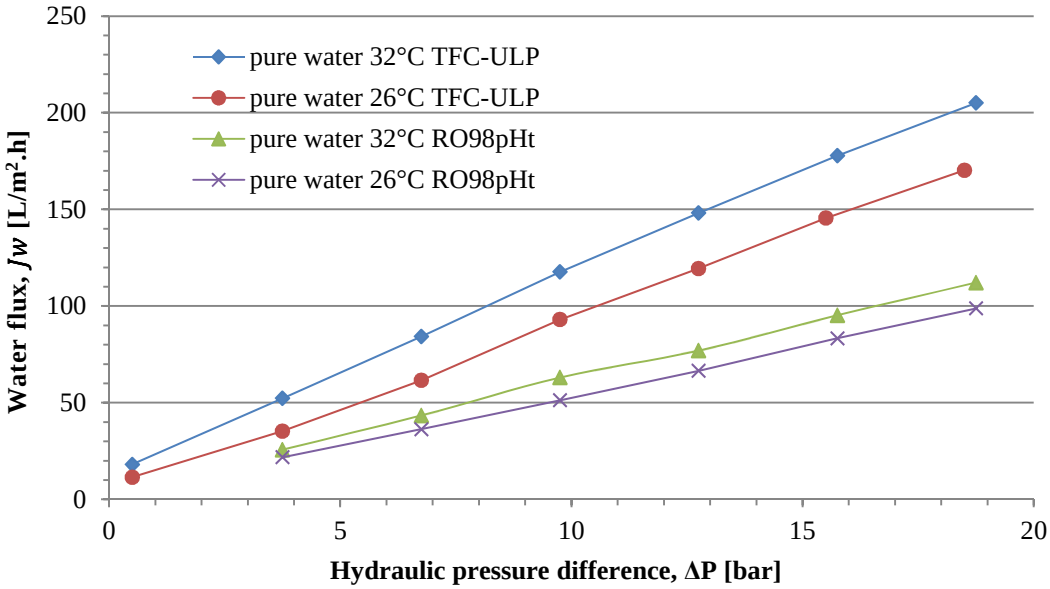

Figure 5.2. *Water flux through TFC®-ULP and RO98pHt®membranesat 26 and 32°C, as a function of the hydraulic pressure difference across the membrane. Feed flow rate constant at ~107 L/h.*

5.2 Salt water experiments

The membranes were tested with a solution of 8.2 g/L of NaCl in order to verify their operation and generate some data to compare with the water-ethanol experiments. In these conditions, the osmotic pressure of the salt solution, calculated with OLI's software, was 6.3atm (25°C, 1atm).

The overall water permeability (A_w) , the water flux (J_w), the salt permeability (B_s), the salt flux (J_s), the salt rejection (R), and the salt passage (P) are calculated with the following equations:

$$J_w = A_w(\Delta p - \Delta\pi) \ , \tag{5.3}$$

$$J_s = \frac{c_p q_p}{A_m} \ , \tag{5.4}$$

$$J_s = B_s\left(c_{s,f} - c_{s,\mathrm{p}}\right) = B_s \Delta_c \ , \tag{5.5}$$

$$\Delta\pi = \frac{\pi_f + \pi_c}{2} - \pi_p \ , \tag{5.6}$$

$$\mathrm{R} = \frac{c_f - c_p}{c_f} \ , \tag{5.7}$$

$$\mathrm{P} = 1 - R \ , \tag{5.8}$$

where c is the salt concentration, π is the osmotic pressure and q the flow rate, the subscripts f, c and p refer to the feed, concentrate and permeate stream, respectively. In addition, A_w and B_s are the overall water and salt permeability, J_s is the salt flux, J_w the water flux, A_m the area of the membrane, P the salt passage, $(\Delta p - \Delta\pi)$ is the Net Applied Pressure (NAP), and R is the salt rejection of the membrane.

Thus, the water flux through the membrane (J_w) is estimated by dividing the amount of water collected in a certain time by the membrane active area, A_m. The overall water permeability (A_w) is calculated by dividing the water flux by the NAP. The values of the osmotic pressure are calculated with OLI's software after the measurement of the salt concentrations. The solute flux through the membrane (J_s) is estimated by using Equation. (5.4), and the solute permeability is calculated by dividing the solute flux by the concentration difference. Eventually, the rejection of the membrane (R) is calculated from Equation (5.7).

Figure 5.3 shows the overall water permeability of both TFC®-ULP and RO98pHt® membranes as a function of the NAP at room temperature and at a constant feed flow rate of ~ 107 L/h.

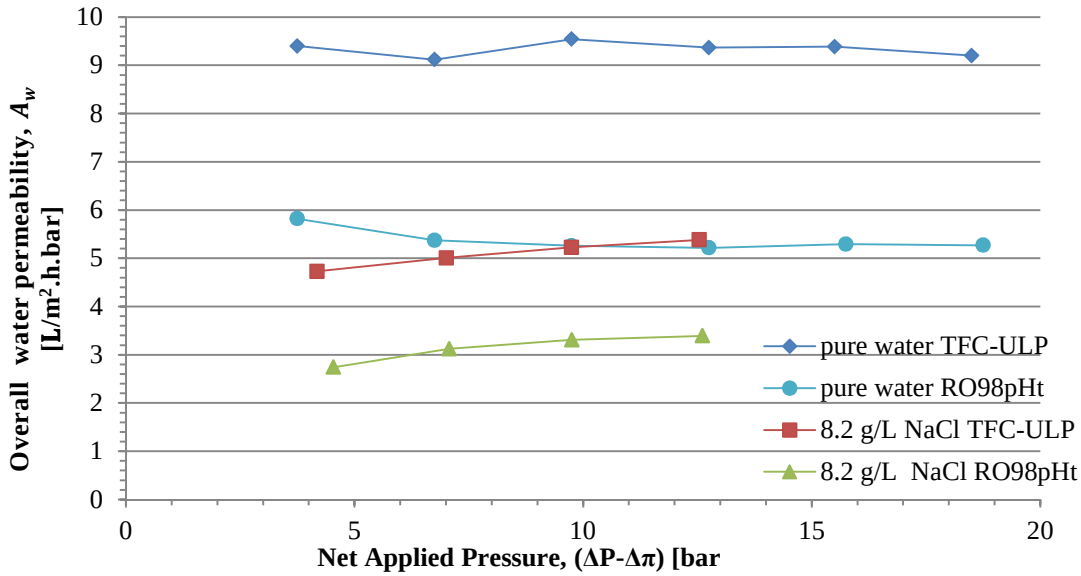

Figure 5.3. *Overall water permeability of TFC®-ULP and RO98pHt® membranesat room temperature, as a function of the NAP. Feed flow rate constant at ~107 L/h.*

Figure 5.4 shows the experimental data of the water flux through the membrane at room temperature, and at a constant feed flow rate of ~ 107 L/h, as a function of the NAP.

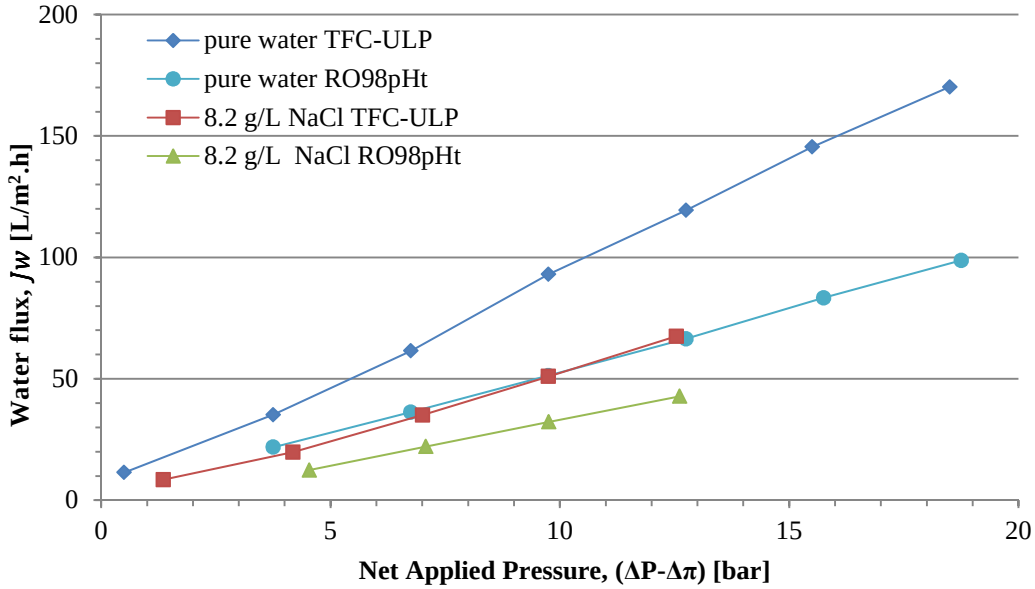

Figure 5.4. *Water flux through TFC®-ULP and RO98pHt® membranesat room temperature as a function of the NAP. Feed flow rate constant at ~107 L/h.*

Figure 5.5 shows the salt permeability of both TFC®-ULP and RO98pHt® membranes at room temperature and constant feed flow rate of ~ 107 L/h, as a function of the NAP.

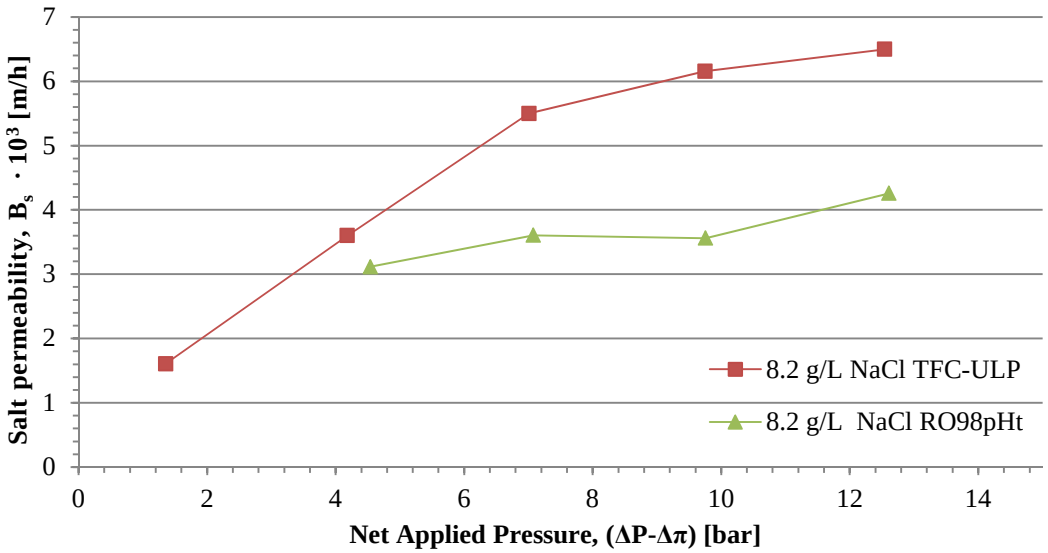

Figure 5.5. *Salt permeability of TFC®-ULP and RO98pHt® at room temperature as a function of the NAP. Feed flow rate constant at ~107 L/h.*

Figure 5.6 shows the experimental data of the salt flux through TFC®-ULP and RO98pHt® membranes at room temperature and constant feed flow rate of ~ 107 L/h, as a function of the NAP.

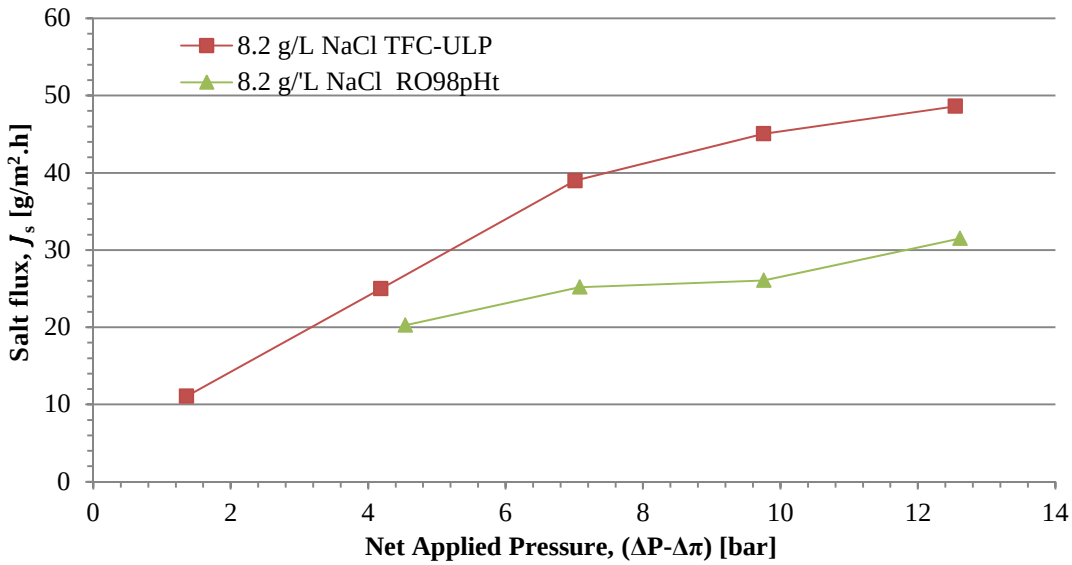

Figure 5.6. *Solute flux through TFC®-ULP and RO98pHt® at room temperature as a function of the NAP. Feed flow rate constant at ~107 L/h.*

The salt rejection of both TFC®-ULP and RO98pHt® membranes is shown in Figure 5.7, as a function of the NAP at a constant feed flow rate of ~ 107 L/h. In addition, Figure 5.8 shows the salt passage of the membrane.

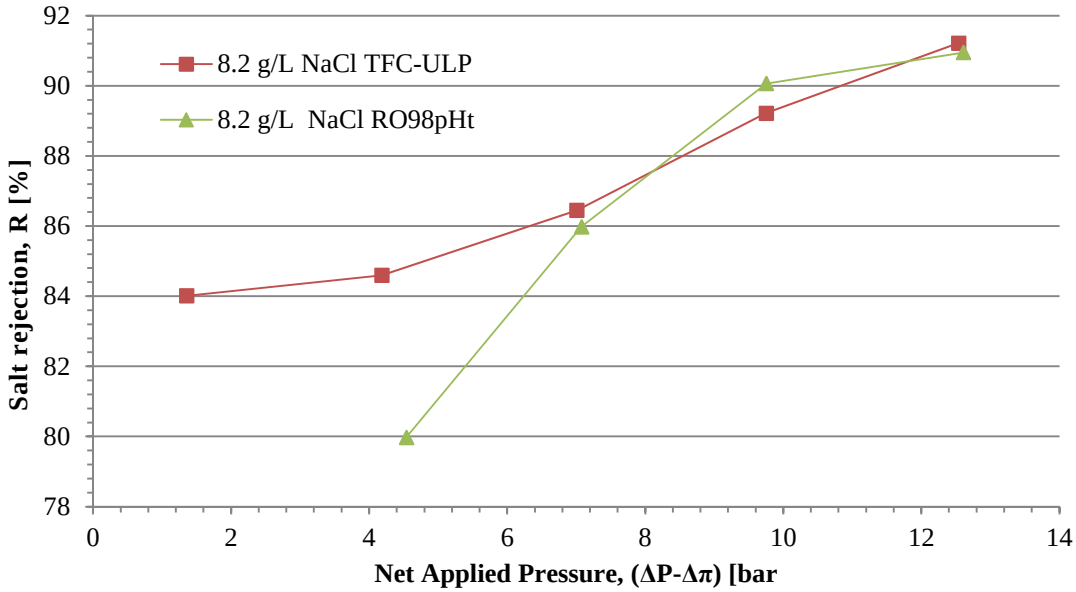

Figure 5.7. *Salt rejection of TFC®-ULP and RO98pHt®membranesat room temperature, as a function of the NAP. Feed flow rate constant at ~107 L/h.*

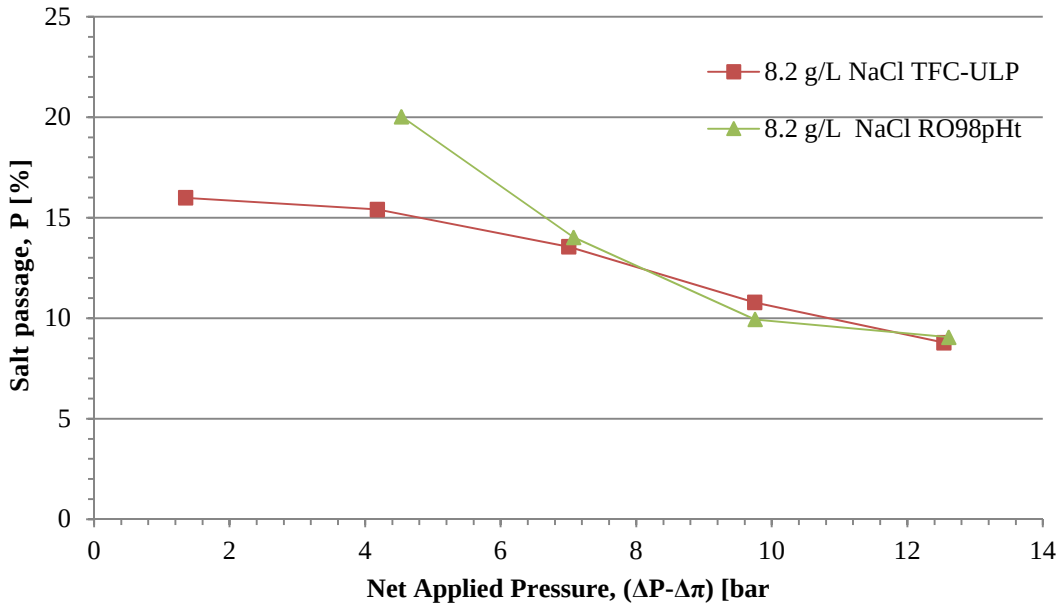

Figure 5.8. *Salt passage of TFC®-ULP and RO98pHt®membranesat room temperature, as a function of the NAP. Feed flow rate constant at ~107 L/h.*

5.3 Water-ethanol experiments

The membranes were tested at room temperature and different concentrations of ethanol, as reported in Table 4.7 (see paragraph §4.2.2), varying the feed pressure at constant feed flow rate (see experimental procedure paragraph § 4.2.4).

The overall water permeability (A_w), the water flux (J_w), the ethanol rejection (R) and the ethanol passage (P) are calculated as described for the salt water experiments in paragraph § 5.2.
The ethanol permeability (B_e), the ethanol flux (J_e) are calculated with the following equations:

$$J_e = \frac{c_p q_p}{A_m} \ , \tag{5.9}$$

$$J_e = B_e\left(c_{e,f} - c_{e,p}\right) = B_e \Delta_c \ , \tag{5.10}$$

where c is the salt concentration and q the flow rate, the subscripts f and p refer to the feed, and permeate stream, respectively. B_e is the ethanol permeability, J_e is the ethanol flux, and A_m the area of the membrane. Thus, the ethanol flux through the membrane (J_e) is estimated by using Equation (5.9), and the ethanol permeability is calculated by dividing the ethanol flux by the concentration difference. The concentration of ethanol in the permeate and concentrate streams are measured by a GC. Instead, the values of the osmotic pressure are calculated with OLI's software.
The author would like to specify that all the concentrations shown in the following diagrams should be considered as mol of ethanol per litre of water.

5.3.1 Effect of concentration

In this paragraph, the effect of varying the concentration of ethanol in the feed on the overall water permeability, ethanol flux, ethanol permeability and rejection is shown.

Overall water permeability

Figure 5.9 shows the overall water permeability of TFC®-ULP membrane, as a function of the NAP at room temperature, constant feed flow rate of ~ 107 L/h, and different concentrations of ethanol feed solution. Besides, Figure 5.10 shows the overall water permeability of RO98pHt®membrane, as a function of the NAP at room temperature, constant feed flow rate of ~ 107 L/h, and different concentrations of ethanol feed solution.

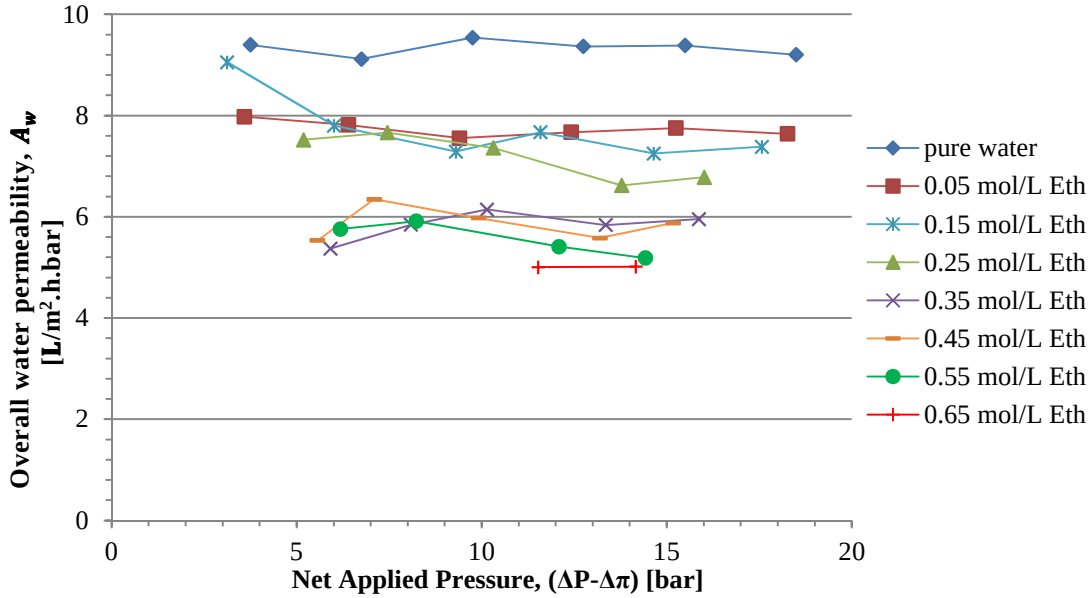

Figure 5.9. *Overall water permeability of TFC®-ULP ®at room temperature and different concentrations of ethanol, as a function of the net applied pressure. Feed flow rate constant at ~107 L/h.*

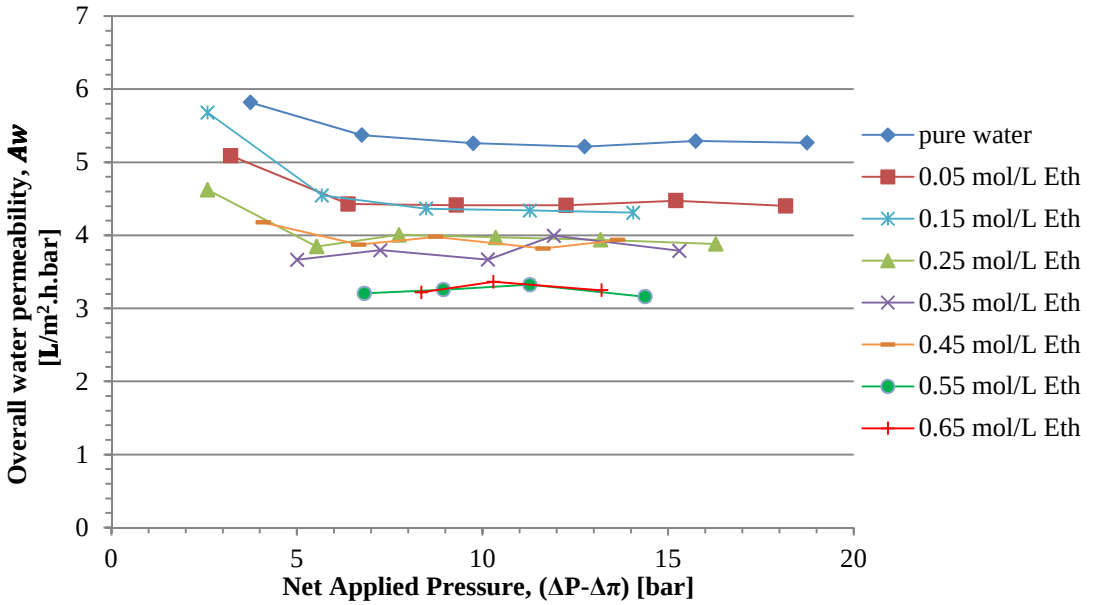

Figure 5.10. *Overall water permeability of RO98pHt®at room temperature and different concentrations of ethanol, as a function of the net applied pressure. Feed flow rate constant at ~107 L/h.*

Water flux

Figure 5.11 shows the experimental data of the water flux through TFC®-ULP membrane, as a function of the hydraulic pressure difference across the membrane at room temperature, constant feed flow rate of ~ 107 L/h, and different concentrations of ethanol feed solution. Besides, Figure 5.12 shows the water flux through TFC®-ULP membrane as a function of the NAP.

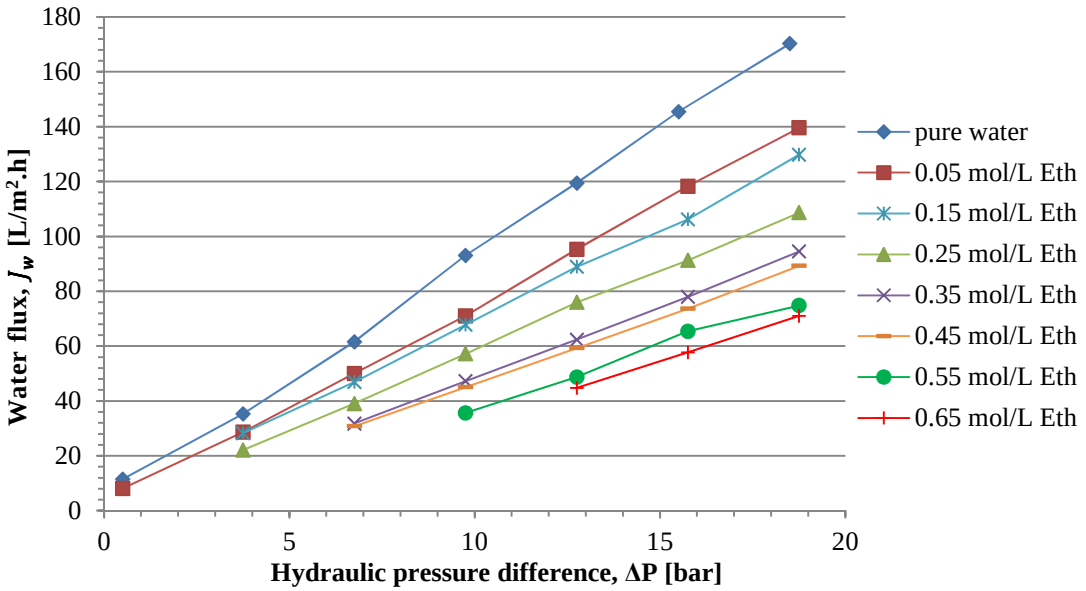

Figure 5.11. *Water flux through TFC®-ULP membrane at room temperature and different concentrations of ethanol, as a function of the hydraulic pressure difference across the membrane. Feed flow rate constant at ~107 L/h.*

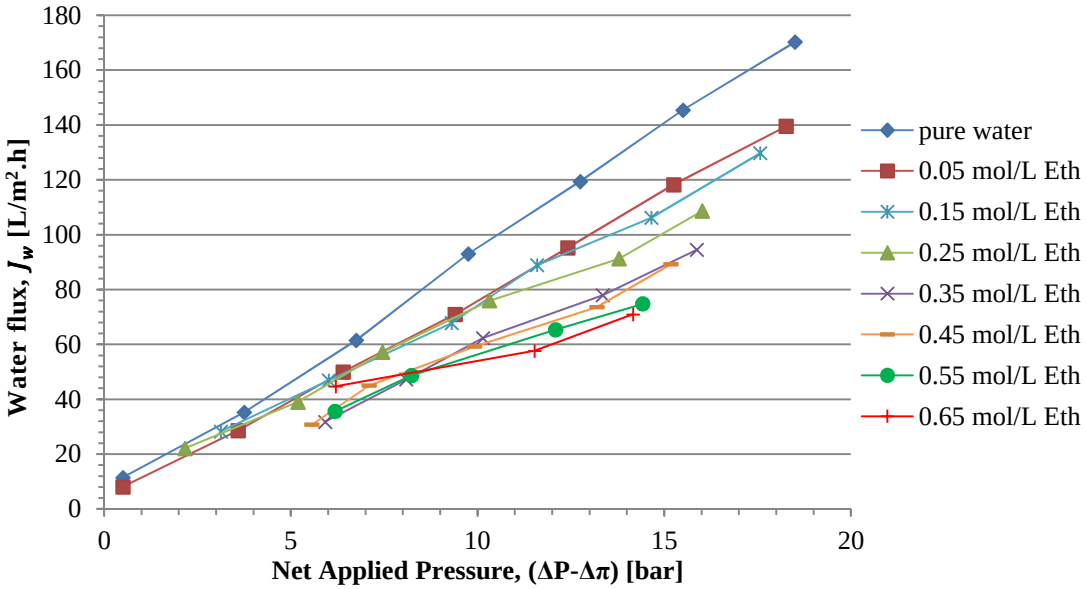

Figure 5.12. *Water flux through TFC®-ULP membrane at room temperature and different concentrations of ethanol, as a function of the net applied pressure. Feed flow rate constant at ~107 L/h.*

Figure 5.13 shows the experimental data of water flux through RO98pHt® membrane, as a function of the hydraulic pressure difference across the membrane at room temperature, constant feed flow rate of ~ 107 L/h, and different concentrations of ethanol feed solution. Besides, Figure 5.14 shows the water flux through RO98pHt® membrane as a function of the NAP.

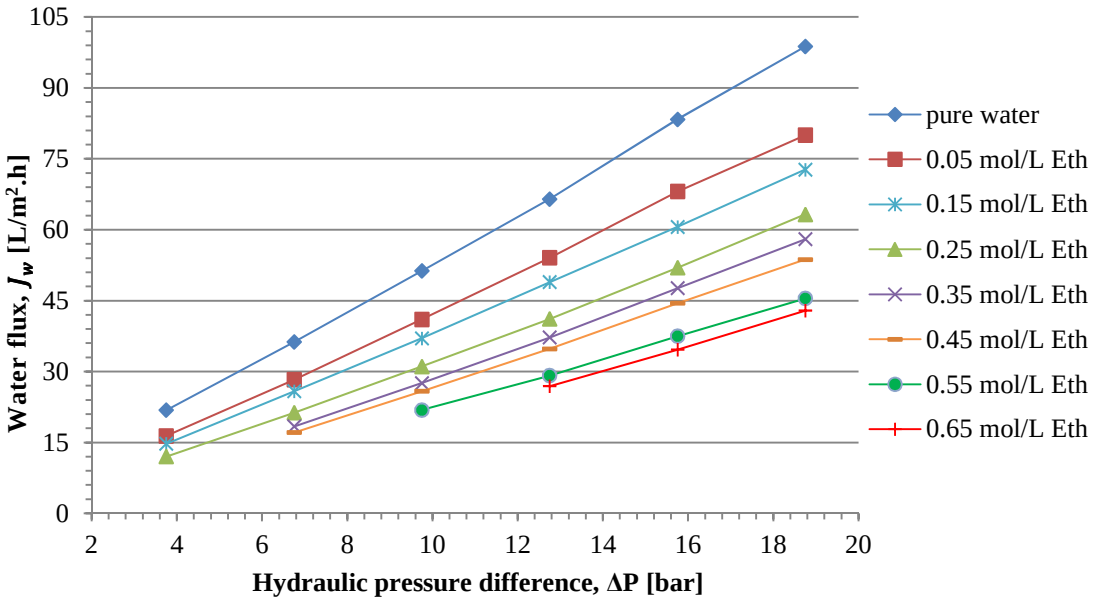

Figure 5.13. *Water flux through RO98pHt® membraneat room temperature and different concentrations of ethanol, as a function of the hydraulic pressure difference across the membrane. Feed flow rate constant at ~107 L/h.*

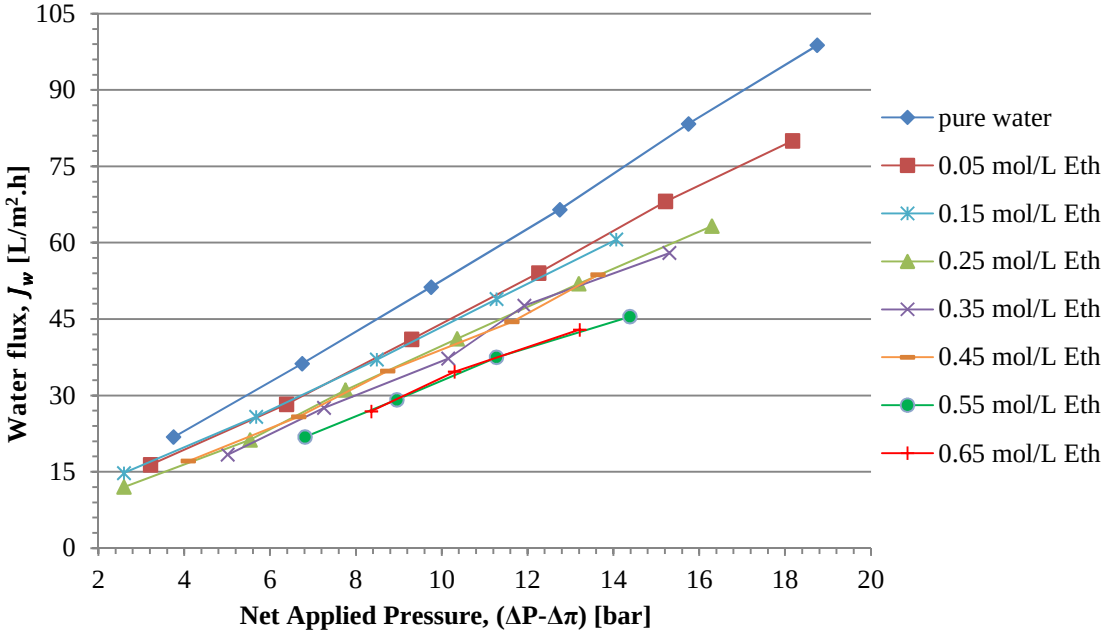

Figure 5.14. *Water flux through RO98pHt® membraneat room temperature and different concentrations of ethanol, as a function of the net applied pressure. Feed flow rate constant at ~107 L/h.*

Ethanol flux

Figure 5.15 shows the ethanol flux through TFC®-ULP membrane, as a function of the net applied pressure at room temperature, constant feed flow rate of ~ 107 L/h, and different concentrations of ethanol. Besides, Figure 5.15 shows the ethanol flux through RO98pHt® membrane.

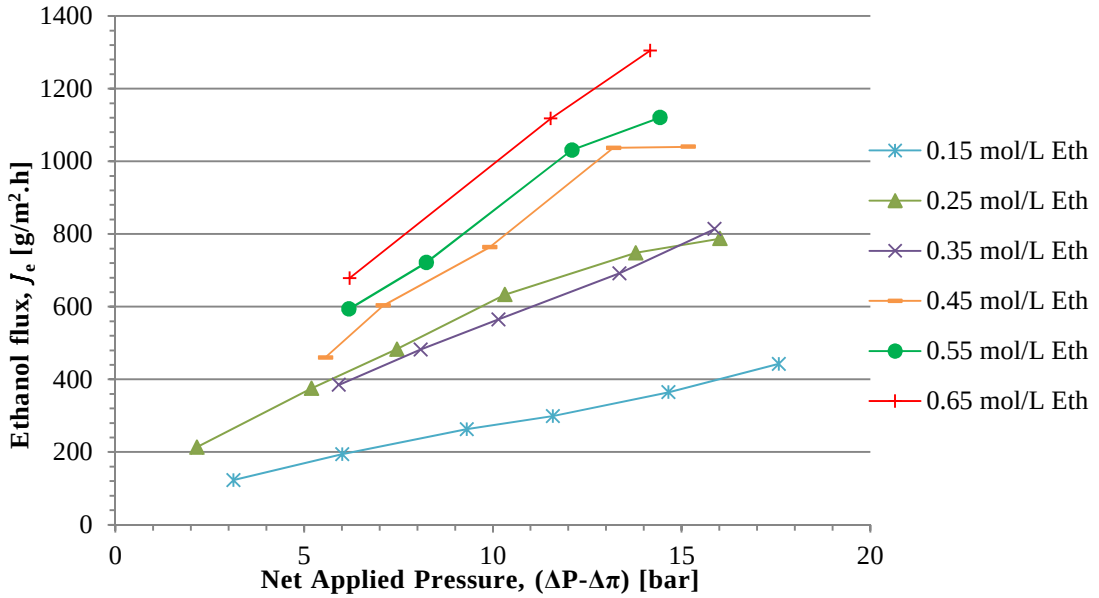

Figure 5.15. *Ethanol flux through TFC®-ULP membrane at room temperature and different concentrations of ethanol, as a function of the net applied pressure. Feed flow rate constant at ~107 L/h.*

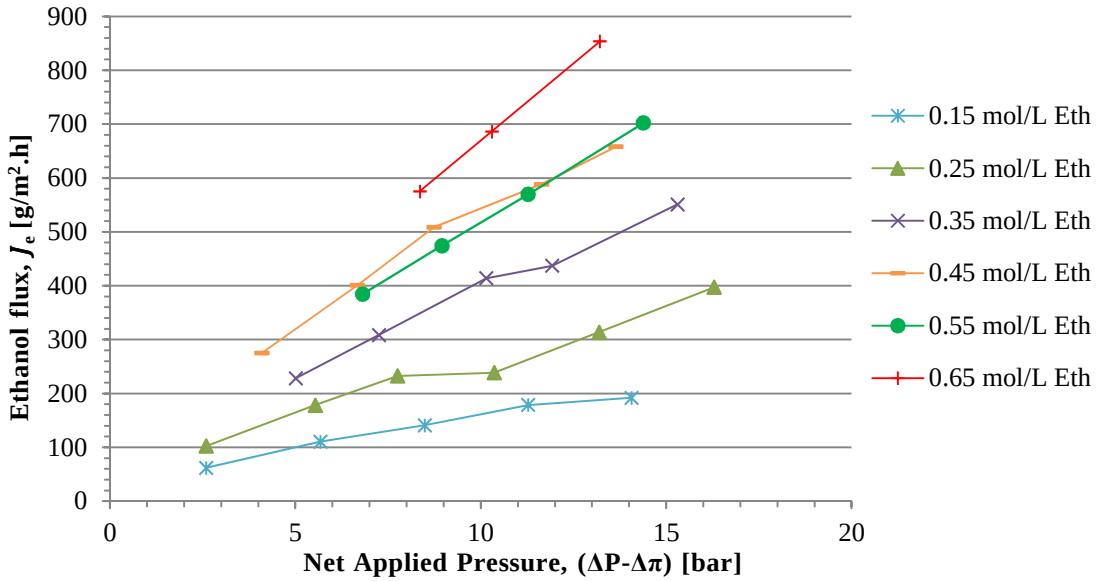

Figure 5.16. *Ethanol flux through RO98pHt® membraneat room temperature and different concentrations of ethanol, as a function of the net applied pressure. Feed flow rate constant at ~107 L/h.*

Ethanol permeability

Figure 5.17 shows the ethanol permeability of TFC®-ULP membrane, as a function of the net applied pressure at room temperature, constant feed flow rate of ~ 107 L/h, and different concentrations of ethanol. Besides, Figure 5.18 shows the ethanol permeability of RO98pHt® membrane.

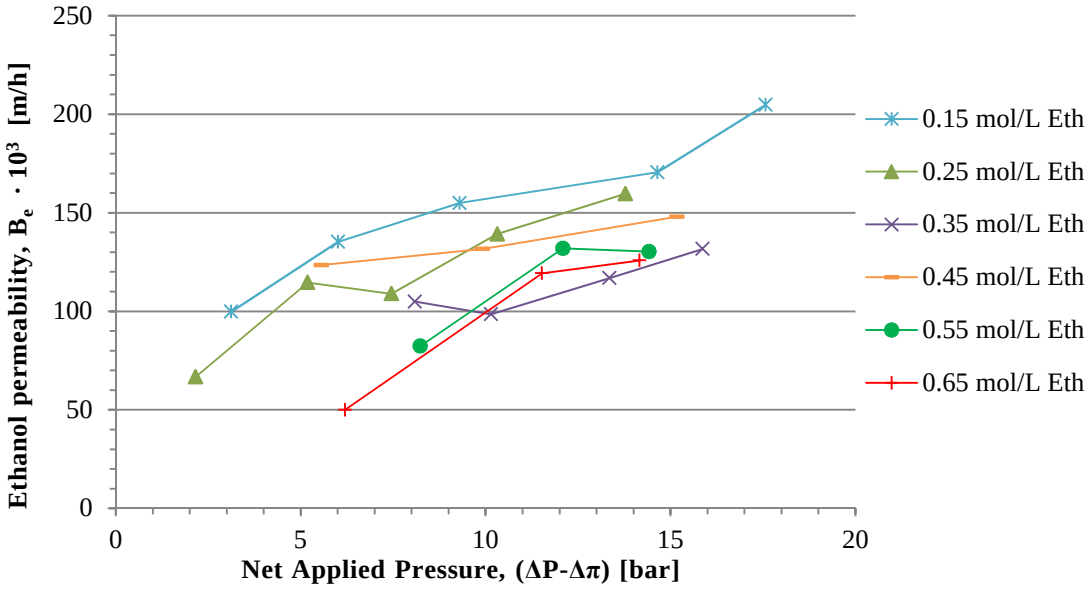

Figure 5.15. *Ethanol permeability of TFC®-ULP membrane at room temperature and different concentrations of ethanol, as a function of the net applied pressure. Feed flow rate constant at ~107 L/h.*

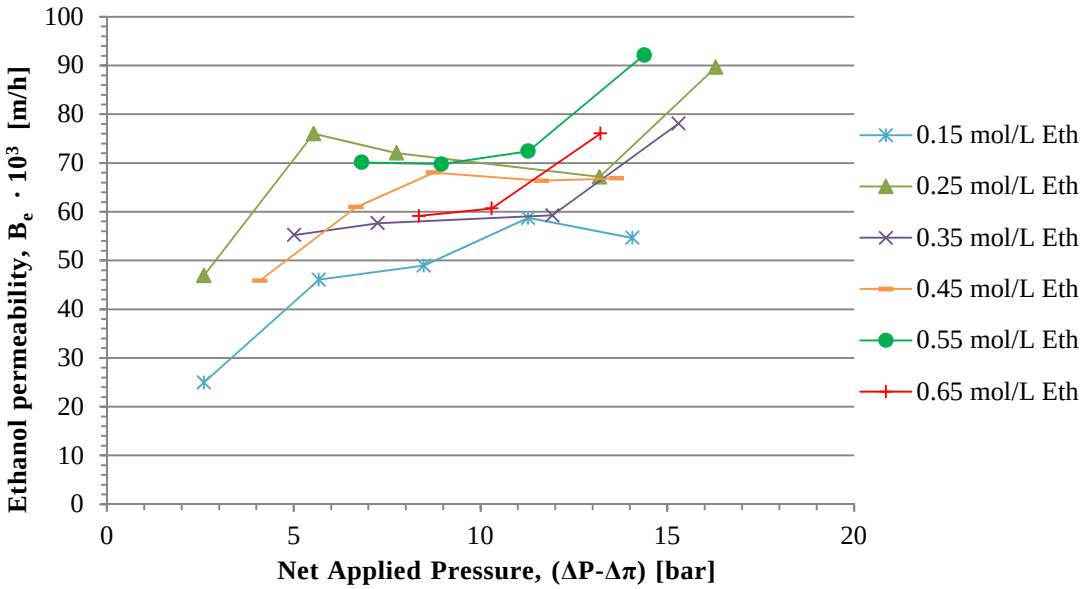

Figure 5.18. *Ethanol permeability of RO98pHt® membrane at room temperature and different concentrations of ethanol, as a function of the net applied pressure. Feed flow rate constant at ~107 L/h.*

Ethanol rejection

Figure 5.19 shows the ethanol rejection of TFC®-ULP membrane, as a function of the net applied pressure at room temperature, constant feed flow rate of ~ 107 L/h, and different concentrations of ethanol. Besides, Figure 5.20 shows the ethanol rejection of RO98pHt® membrane.

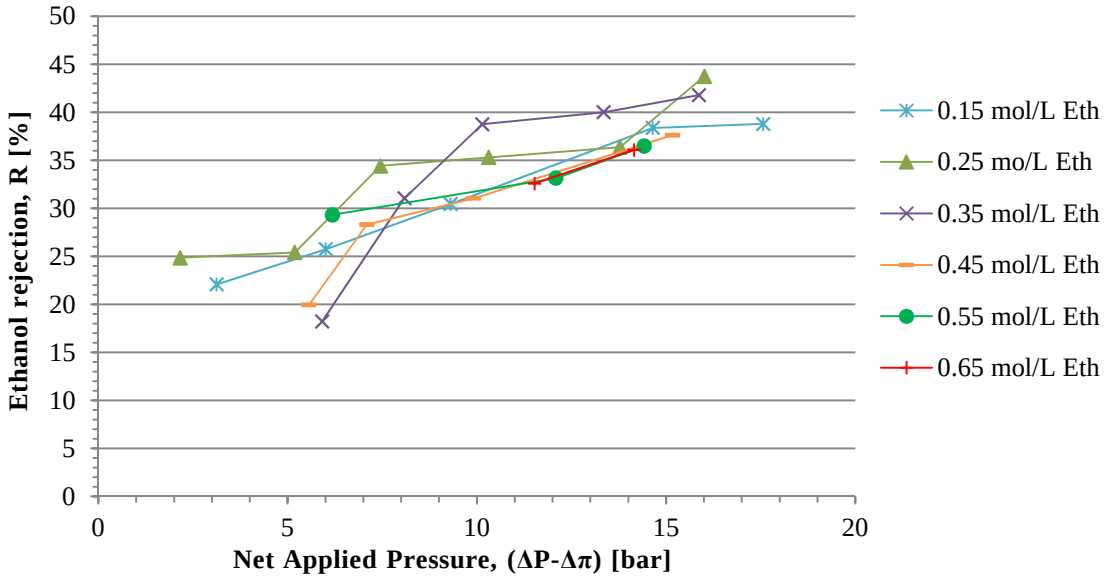

Figure 5.19. *Ethanol rejection of TFC®-ULP membrane at room temperature and different concentrations of ethanol, as a function of the net applied pressure. Feed flow rate constant at ~107 L/h.*

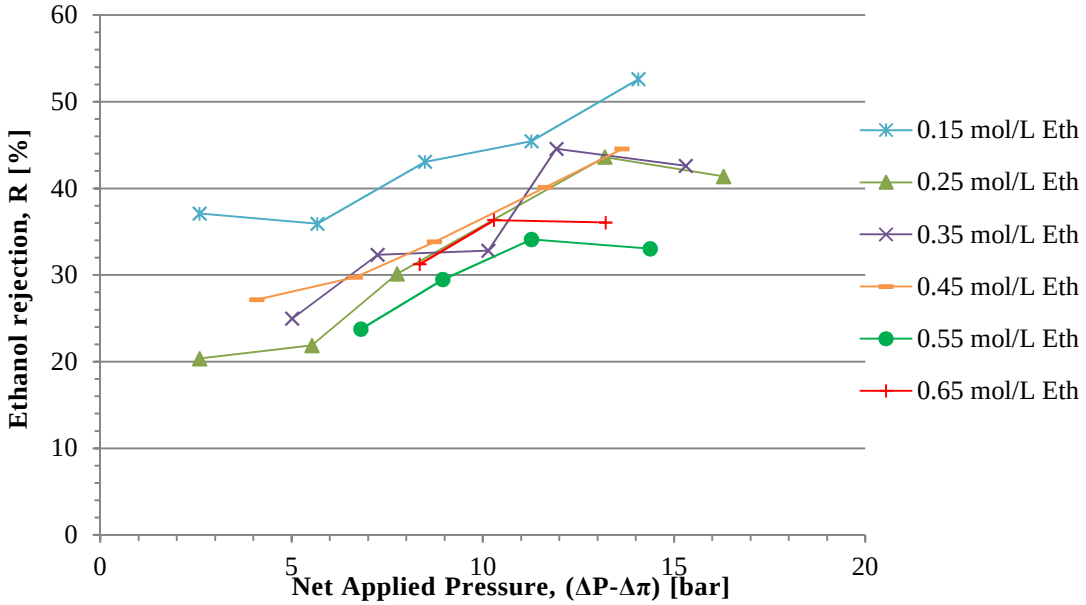

Figure 5.20. *Ethanol rejection of RO98pHt®membrane at room temperature and different concentrations of ethanol, as a function of the net applied pressure. Feed flow rate constant at ~107 L/h.*

Figure 5.21 shows the ethanol passage across TFC®-ULP membrane, as a function of the net applied pressure at room temperature, constant feed flow rate of ~ 107 L/h, and different concentrations of ethanol. Besides, Figure 5.22 shows the ethanol passage through RO98pHt® membrane.

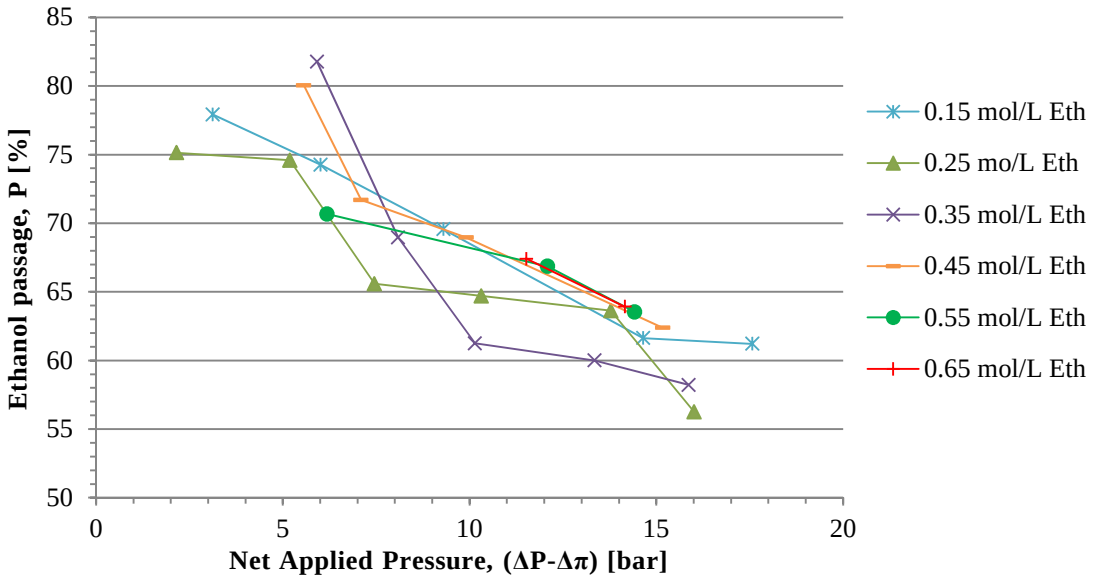

Figure 5.21. *Ethanol passage across TFC®-ULP membrane at room temperature and different concentrations of ethanol, as a function of the net applied pressure. Feed flow rate constant at ~107 L/h.*

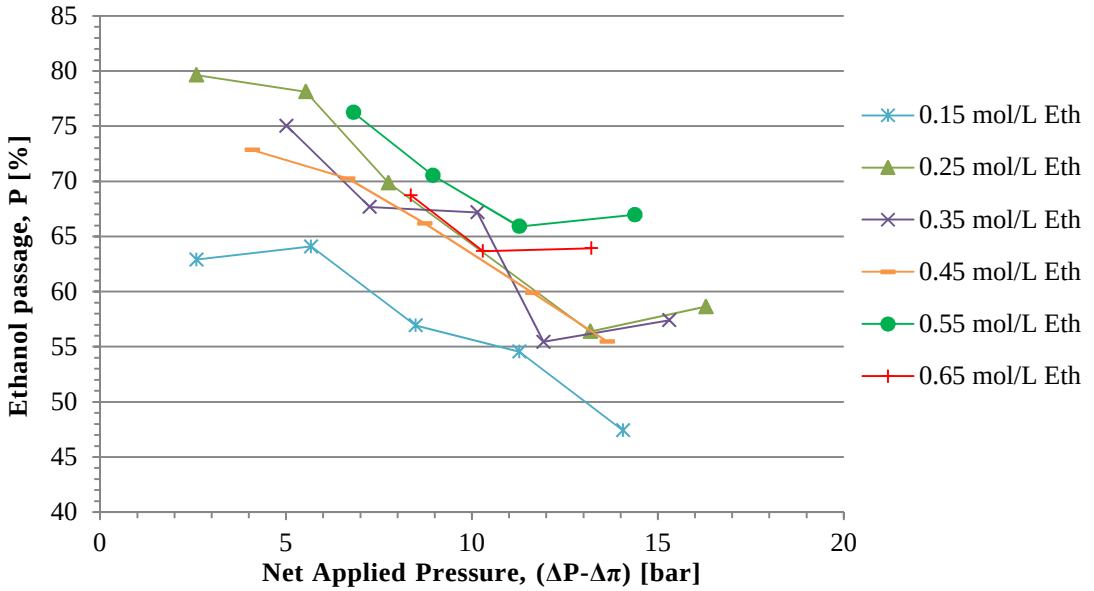

Figure 5.22. *Ethanol passage across RO98pHt® membrane at room temperature and different concentrations of ethanol, as a function of the net applied pressure. Feed flow rate constant at ~107 L/h.*

5.3.2 Effect of membrane

The aim of this paragraph is to compare, through some diagrams, the operability of TFC®-ULP and RO98pHt® membranes. The results of the salt experiments (8.2 g/L Nacl, π = 6.30atm) are compared with the results of the 0.25 mol/L ethanol solution, which has almost the same osmotic pressure (π = 6.01atm), for both the membranes.

In Figure 5.23, a comparison of the overall water permeability for both TFC®-ULP and RO98pHt® membranes is shown.

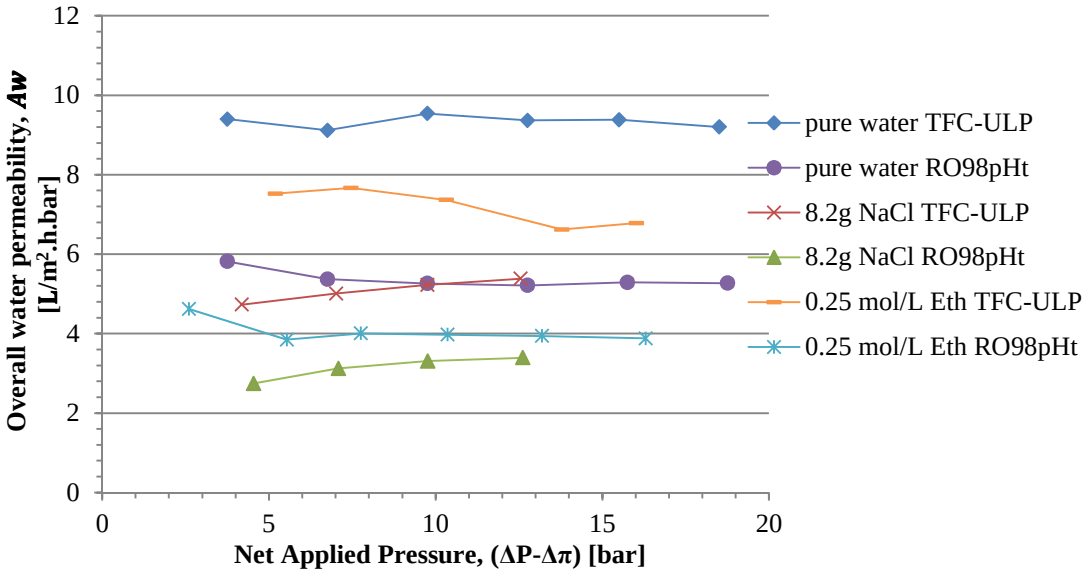

Figure 5.23. *Overall water permeability of TFC®-ULP and RO98pHt®membranes at room temperature for the 0.25mol/L ethanol solution, pure water and 8.2g/L NaCl solution, as a function of the net applied pressure. Feed flow rate constant at ~107 L/h.*

Figure 5.24 shows a comparison of the water flux for TFC®-ULP and RO98pHt® membranes.

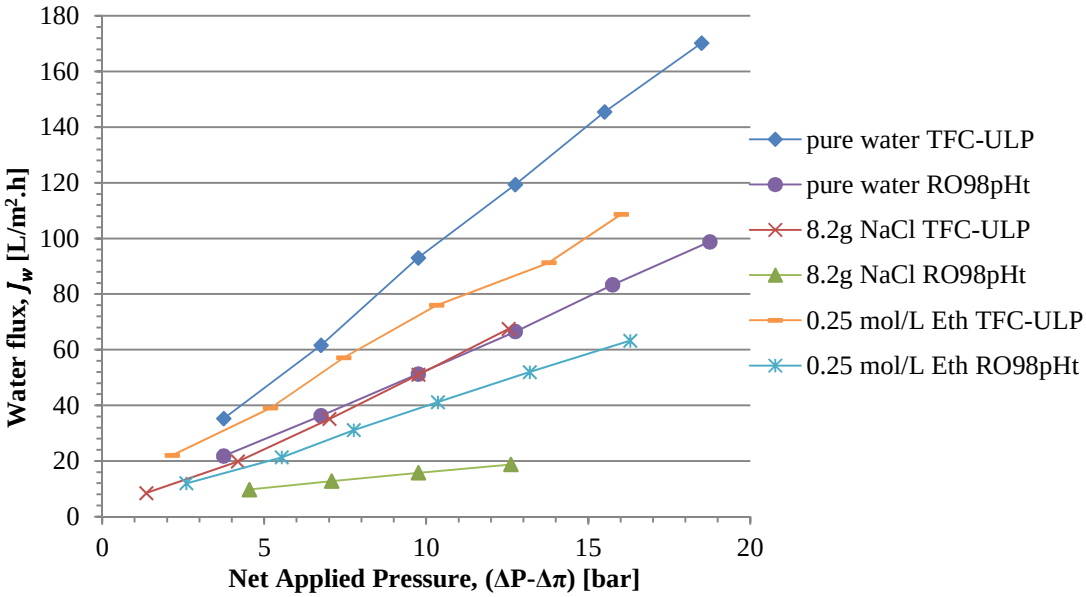

Figure 5.24. *Water flux through TFC®-ULP and RO98pHt®membranes at room temperature for the 0.25mol/L ethanol solution, pure water and 8.2g/L NaCl solution, as a function of the net applied pressure. Feed flow rate constant at ~107 L/h.*

In Figure 5.25, a comparison of the ethanol/salt permeability for both TFC®-ULP and RO98pHt® membranes is shown. Moreover, Figure 5.26 shows a comparison of the ethanol/salt flux through TFC®-ULP and RO98pHt® membranes.

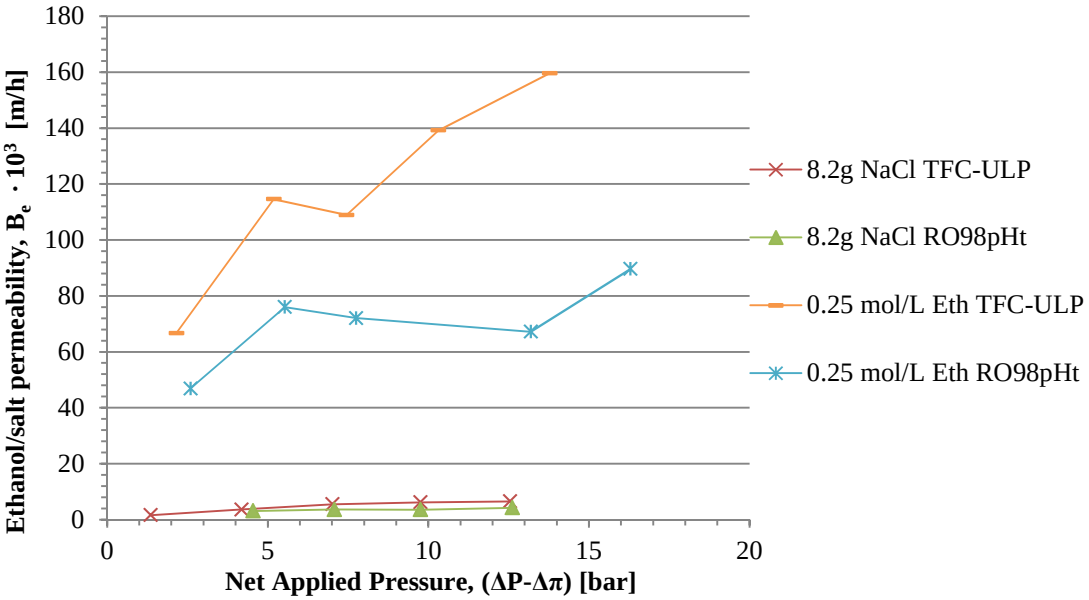

Figure 5.25. *Ethanol/salt permeability of TFC®-ULP and RO98pHt®membranes at room temperature for the 0.25mol/L ethanol solution and 8.2g/L NaCl solution, as a function of the net applied pressure. Feed flow rate constant at ~107 L/h.*

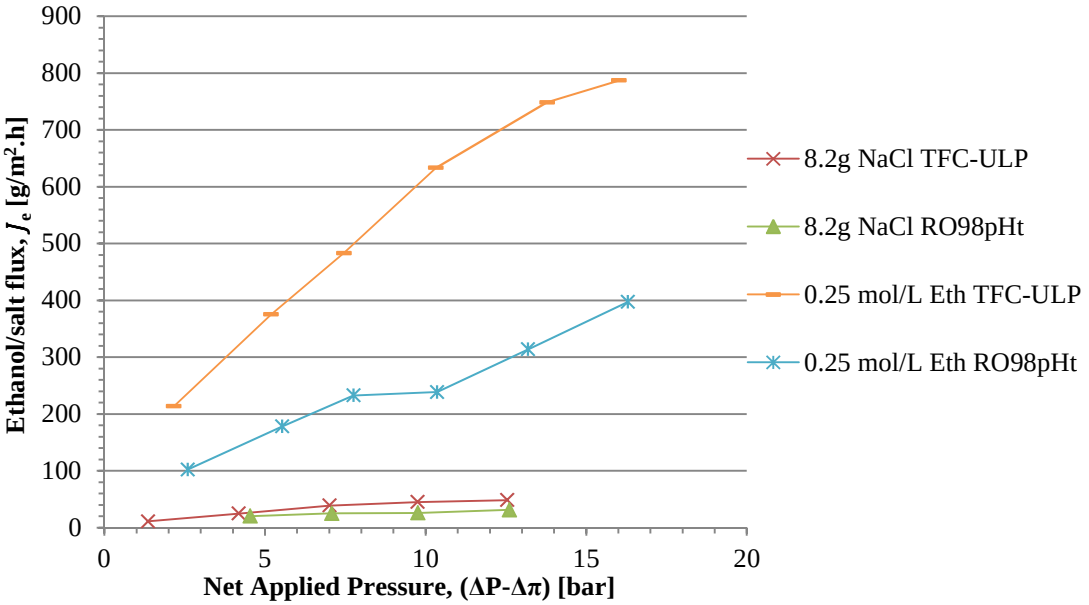

Figure 5.26. *Ethanol/salt flux through TFC®-ULP and RO98pHt®membranes at room temperature for the 0.25mol/L ethanol solution and 8.2g/L NaCl solution, as a function of the net applied pressure. Feed flow rate constant at ~107 L/h.*

5.3.3 Relationship between ethanol and water fluxes

In this paragraph the relationships between ethanol and water flux with the feed concentration is estimated. Furthermore, the connection between the permeate concentration and the net applied pressure is shown.

The concentration values of the permeate flux, c_p, are plotted against the net applied pressure in Figure 5.27 and 5.28 for TFC®-ULP and RO98pHt® membranes, respectively.

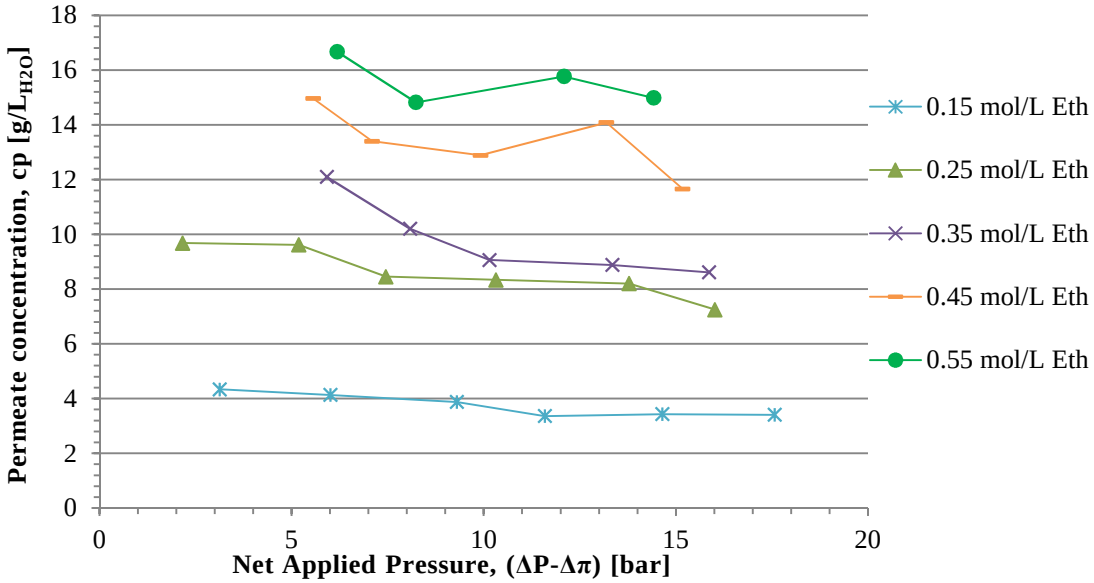

Figure 5.27. *Permeate concentration of TFC®-ULP membrane at room temperature and different feed ethanol concentrations, as a function of the net applied pressure. Feed flow rate constant at ~107 L/h.*

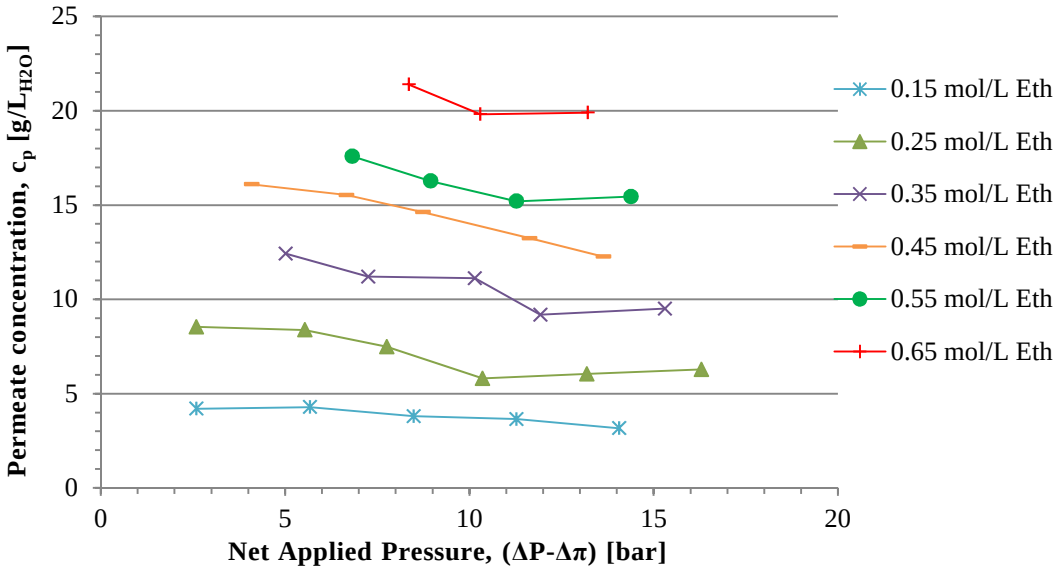

Figure 5.28. *Permeate concentration of RO98pHt®membraneat room temperature and different feed ethanol concentrations, as a function of the net applied pressure. Feed flow rate constant at ~107 L/h.*

Figure 5.29 and Figure 5.30 shows the ethanol flux at room temperature and different feed pressure, as a function of the feed ethanol concentrations, for TFC®-ULP and RO98pHt® membranes respectively.

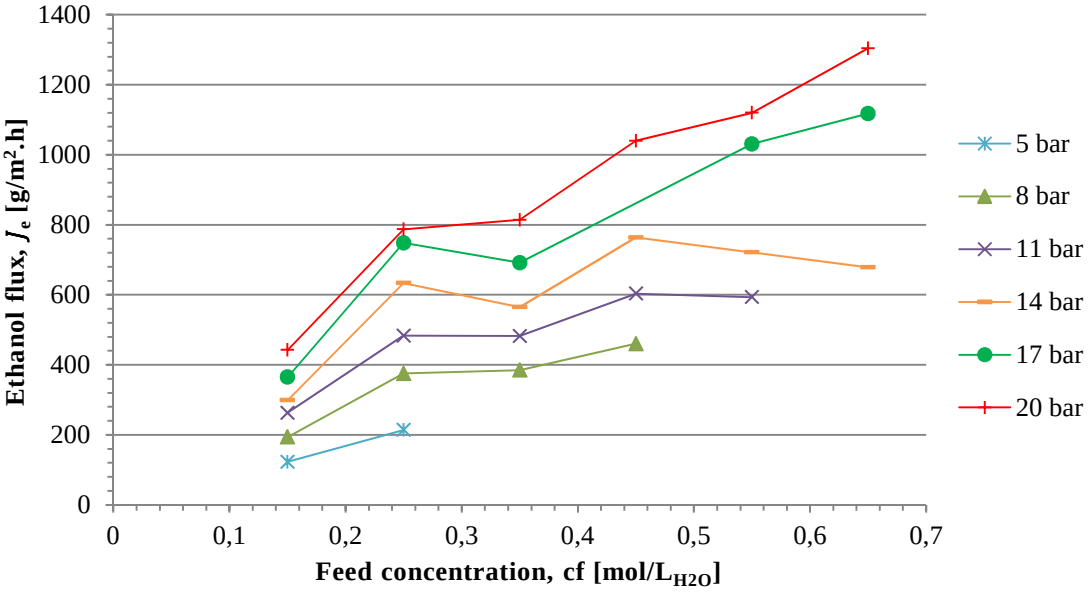

Figure 5.29. *Ethanol flux through TFC®-ULP membrane at room temperature and different feed pressure, as a function of the feed concentration. Feed flow rate constant at ~107 L/h.*

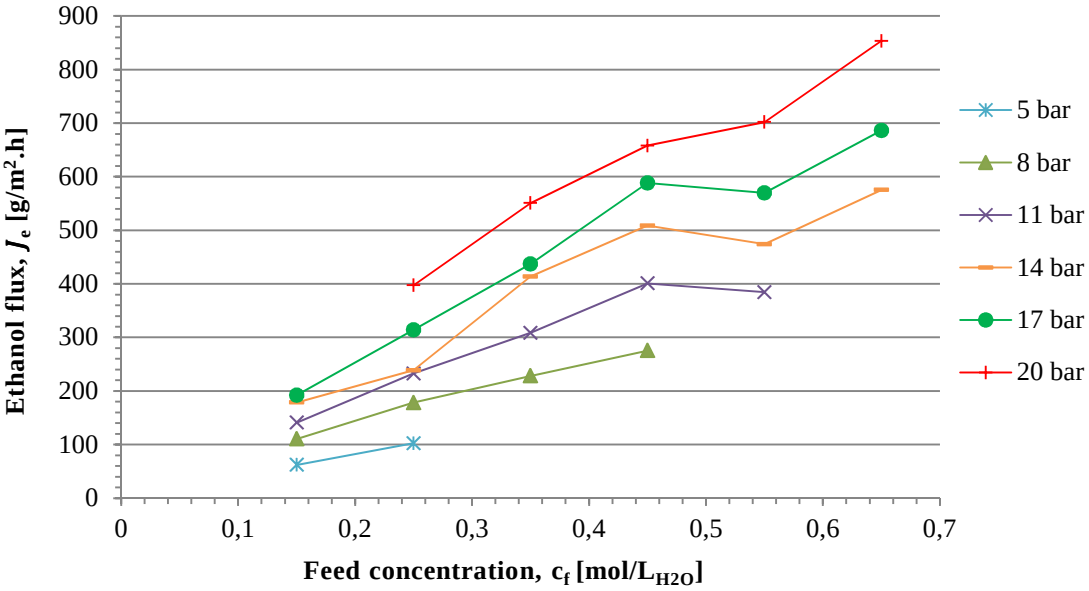

Figure 5.30. *Ethanol flux through RO98pHt®membraneat room temperature and different feed pressure, as a function of the feed concentration. Feed flow rate constant at ~107 L/h.*

Figure 5.31 and Figure 5.32 show the water flux at room temperature and different feed pressures, as a function of the feed ethanol concentrations, for TFC®-ULP and RO98pHt® membranes respectively.

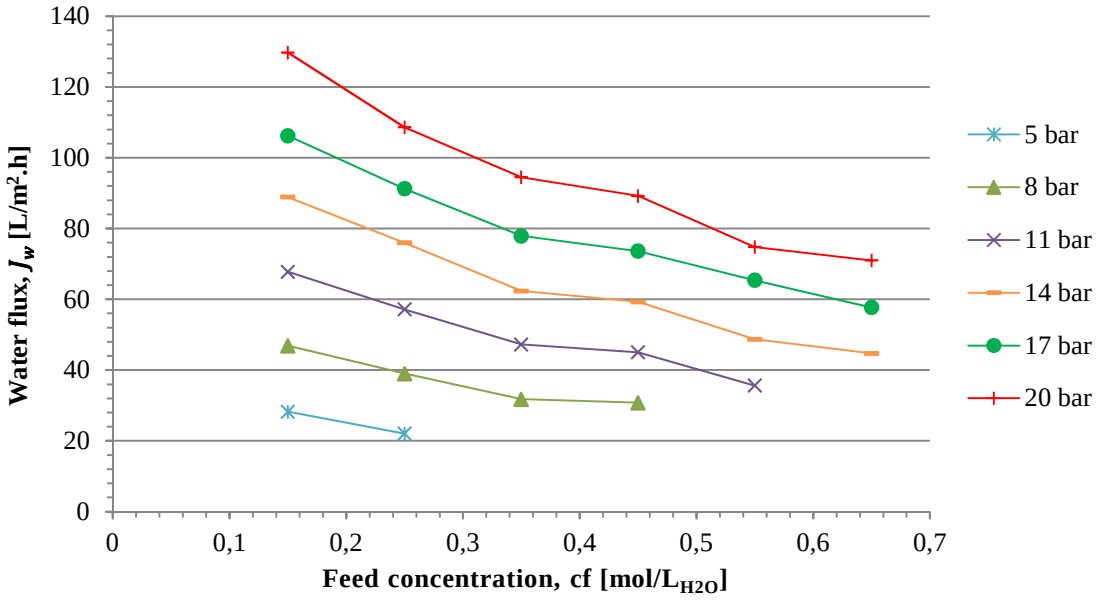

Figure 5.31. *Water flux through TFC®-ULP membrane at room temperature and different feed pressure, as a function of the feed concentration. Feed flow rate constant at ~107 L/h.*

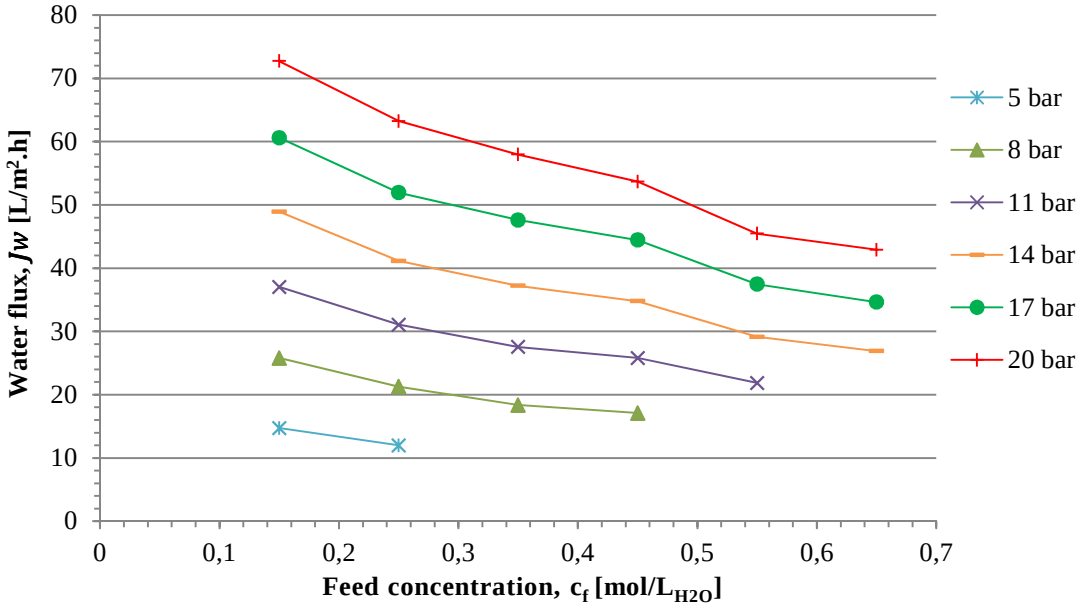

Figure 5.32. *Water flux through RO98pHt®membraneat room temperature and different feed pressure, as a function of the feed concentration. Feed flow rate constant at ~107 L/h.*

5.3.4 Mass balances

Tables 5.1 and 5.2 show the mass balances of both TFC®-ULP and RO98pHt® membranes for each water-ethanol experiment at different feed pressures and feed concentrations. In addition, the percentage error of each balance has been calculated with this equation:

$$e[\%] = \frac{(P+C)-F}{F} 100 \ . \qquad (5.11)$$

where F, P and C are the feed, the permeate and the concentrate ethanol mass flow rate [g/h], respectively. Only five mass balances out of 70 have a percentage error over 10%.

Table 5.1. *Mass balances of TFC®-ULP experiments at different feed pressures and concentrations.*

c[mol/L_{H20}]	Pressure[bar]	Fe [g/h]	P [g/h]	Co [g/h]	P+C [g/h]	e[%]
0,05	5	137,48	0,13	137,94	138,07	0,43
	8	137,60	0,15	151,17	151,32	9,97
	11	137,72	0,18	148,72	148,91	8,12
	14	137,86	0,25	142,75	142,99	3,72
	17	138,00	0,20	145,10	145,31	5,30
	20	138,12	0,30	158,33	158,62	14,84
0,15	5	590,97	0,55	581,84	582,39	-1,45
	8	591,43	0,87	584,29	585,15	-1,06
	11	591,95	1,18	587,91	589,08	-0,48
	14	592,48	1,34	589,09	590,43	-0,35
	17	592,91	1,63	579,49	581,12	-1,99
	20	593,49	1,98	605,85	607,83	2,42
0,25	5	1354,60	0,95	1328,16	1329,11	-1,88
	8	1355,57	1,67	1301,72	1303,39	-3,85
	11	1356,60	2,15	1354,52	1356,67	0,01
	14	1357,68	2,82	1367,74	1370,56	0,95
	17	1358,55	3,33	1169,75	1173,09	-13,65
	20	1359,54	3,51	1278,98	1282,49	-5,67
0,35	8	1552,19	1,70	1524,89	1526,59	-1,65
	11	1553,20	2,14	1464,93	1467,07	-5,55
	14	1554,19	2,51	1605,32	1607,83	3,45
	17	1555,20	3,08	1485,31	1488,39	-4,30
	20	1556,29	3,62	1623,34	1626,96	4,54
0,45	8	1950,98	2,03	1685,66	1687,69	-13,50
	11	1952,15	2,67	1949,67	1952,34	0,01
	14	1953,32	3,38	1916,07	1919,45	-1,73
	17	1954,50	4,58	2051,66	2056,24	5,21
	20	1955,78	4,61	1956,83	1961,44	0,29
0,55	11	2447,64	2,62	2475,18	2477,79	1,23
	14	2448,99	3,19	2478,80	2481,99	1,35
	17	2450,71	4,55	2328,81	2333,36	-4,79
	20	2451,68	4,95	2436,78	2441,72	-0,41
0,65	14	2965,46	3,00	2838,74	2841,73	-4,17
	17	2967,08	4,91	2765,55	2770,46	-6,63
	20	2968,74	5,74	2707,95	2713,69	-8,59

Table 5.2. *Mass balances of RO98pHt® experiments at different feed pressures and concentrations.*

c[mol/L_{H20}]	Pressure[bar]	F [g/h]	P [g/h]	C [g/h]	P+C [g/h]	e [%]
0,05	5	172,76	0,05	176,85	176,90	2,40
	8	172,85	0,12	176,85	176,97	2,39
	11	172,94	0,15	176,85	177,00	2,35
	14	173,04	0,17	176,85	177,03	2,31
	17	173,14	0,17	160,01	160,18	-7,48
	20	173,22	0,20	176,85	177,05	2,21
0,15	5	707,85	0,28	648,46	648,74	-8,35
	8	708,18	0,49	631,62	632,11	-10,74
	11	708,51	0,63	606,35	606,98	-14,33
	14	708,87	0,80	656,88	657,68	-7,22
	17	709,22	0,86	640,04	640,90	-9,63
0,25	5	1129,06	0,46	1136,91	1137,36	0,74
	8	1129,50	0,79	1128,49	1129,28	-0,02
	11	1129,97	1,04	1254,81	1255,85	11,14
	14	1130,44	1,07	1061,12	1062,18	-6,04
	17	1130,96	1,40	1179,02	1180,42	4,37
	20	1131,50	1,77	1187,44	1189,21	5,10
0,35	8	1731,97	1,01	1574,83	1575,84	-9,01
	11	1732,64	1,37	1625,36	1626,73	-6,11
	14	1733,34	1,84	1650,62	1652,46	-4,67
	17	1734,10	1,94	1734,84	1736,78	0,15
	20	1734,86	2,45	1650,62	1653,07	-4,71
0,45	8	2296,53	1,21	2130,65	2131,87	-7,17
	11	2297,37	1,77	2223,29	2225,06	-3,15
	14	2298,24	2,25	2366,46	2368,70	3,07
	17	2299,17	2,60	2122,23	2124,83	-7,58
	20	2300,07	2,92	2315,93	2318,84	0,82
0,55	11	2393,92	1,69	2450,67	2452,36	2,44
	14	2394,66	2,09	2526,46	2528,55	5,59
	17	2395,50	2,51	2576,99	2579,51	7,68
	20	2396,30	3,10	2585,42	2588,51	8,02
0,65	14	3199,60	2,52	2998,07	3000,59	-6,22
	17	3200,64	3,01	3099,13	3102,14	-3,08
	20	3201,76	3,75	3149,66	3153,41	-1,51

5.4 Considerations

In the following paragraphs the results are discussed in order to compare the performance of the membranes considered. Finally, suggestions for future works are reported.

5.4.1 Results comments

Pure water experiments

As regards to the pure water experiments:

- it is clear from the Figure 5.1 that the pure water permeability of the membrane is marginally affected by the hydraulic pressure difference. On the other hand the pure water permeability increases as the temperature increases and TFC®-ULP membrane exhibits higher pure water permeability values than RO98pHt® membrane;
- it can be seen from Figure 5.2 that that there is a linear relationship between the hydraulic pressure difference and the water flux across the membrane. In addition, an increase in the temperature results in an increase water flux and TFC®-ULP membrane is characterized by higher water fluxes than RO98pHt® membrane.

Salt experiments

As concerns the salt experiments, it is evident from Figures 5.3-5.8 that TFC®-ULP membrane is characterized by water flux, overall water permeability, salt permeability and salt flux all higher than RO98pHt® membrane. Furthermore, at low NAP, TFC®-ULP membrane has higher salt rejection values; however at higher NAP, both TFC®-ULP and RO98pHt® membranes display similar salt rejection value of about 91%.

Water-ethanol experiments

Concerning the water-ethanol experiments, a discussion is proposed in order to summarize and compare the operative characteristics of TFC®-ULP and RO98pHt® membranes.

Figures 5.33 and 5.34 gather the main findings:

(a) both TFC®-ULP and RO98pHt® membranes allow the passage of similar quantities of ethanol;
(b) TFC®-ULP membrane is characterized by higher ethanol and water fluxes.

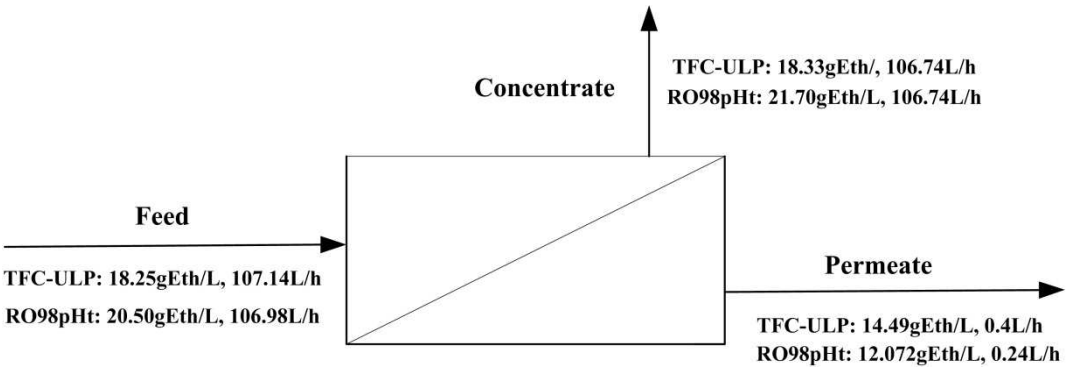

Figure 5.33. *Concentration of ethanol and flow rate in the feed, permeate and concentrate streams (2.04% m/m feed solution, 20bar) for both TFC®-ULP and RO98pHt® membranes.*

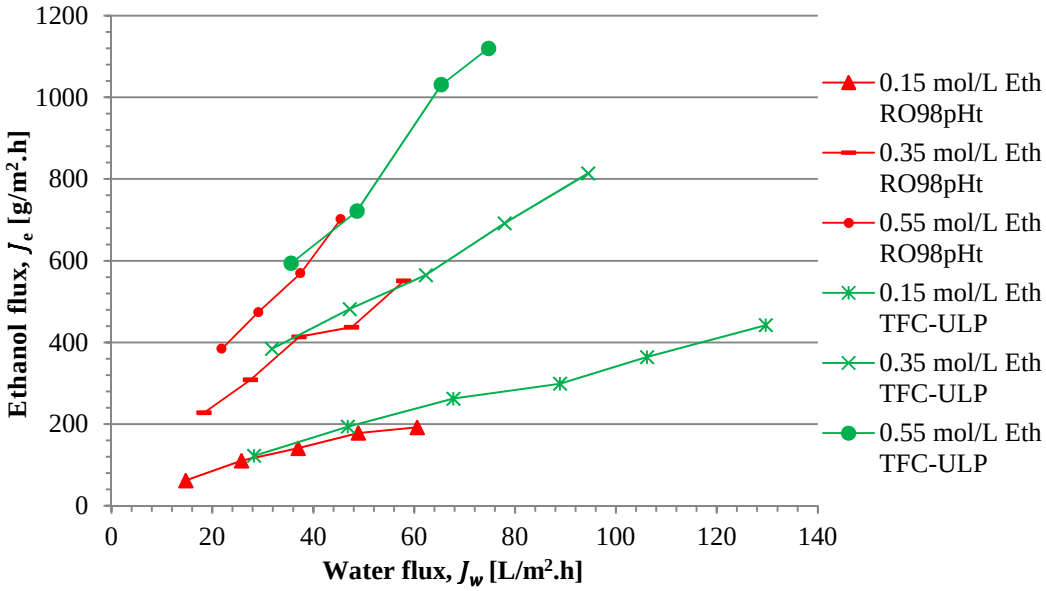

Figure 5.34. *Ethanol flux through both TFC®-ULP and RO98pHt® membrane, at room temperature, different feed pressures and ethanol concentrations, as a function of the water flux. Feed flow rate constant at ~107 L/h.*

In addition, for all the experiments carried out, it is clear that:

(a) the overall water permeability of both membranes is slightly affected by the net applied pressure and the plateau gradually decreases as the concentration of ethanol in the feed increases, as it can be seen from Figures 5.9 and 5.10.

This could be explained according to the SDPFFR model, which states that the overall water permeability is formed by the combination of a membrane material permeability and the feed solution permeability. While the membrane material permeability is a characteristic of the membrane and therefore constant at

constant temperature, the feed solution permeability tends to slightly vary with pressure and with the feed concentrations (Toffoletto *et al.*, 2010). Furthermore, the overall water permeability values of TFC®-ULP (average around 6.5L/m^2.h.bar) are always higher than RO98pHt® membrane (average about 4L/m^2.h.bar);

(b) there is a linear relationship between the water flux through the membrane and the applied pressure (NAP or ΔP), as is shown in Figures 5.11-5.14;

(c) an increase in the ethanol feed concentration results in a decrease in the water flux across the membrane due to the rise of the osmotic pressure. Moreover, the water fluxes values at different feed concentration of ethanol tend to overlap each other if they are plotted as a function of the net applied pressure (Figure 5.12 and 5.14); because the NAP consider the contribution of the osmotic pressure;

(d) the water fluxes across TFC®-ULP are always higher (about 75% higher) than RO98pHt® membrane (Figure 5.11 and 5.13);

(e) as the NAP increases, the ethanol flux and the ethanol permeability increase, as it can be seen from Figures 5.15-5.18 . Besides, it is clear that ethanol flux increases as the feed ethanol concentration increases;

(f) TFC®-ULP membrane is characterized by higher ethanol flux and ethanol permeability (about 60% and 50% respectively) than RO98pHt® membrane (Figures 5.15-5.18);

(g) the ethanol rejection increases as the NAP increases (Figures 5.19 and 5.20). Moreover it is apparent that the feed ethanol concentration slightly affects the ethanol rejection, all the data are close to each other and seems to follow the same upward trend. The ethanol feed concentration range is probably too limited to clearly understand the impact of it on the rejection;

(h) the maximum ethanol rejection is reached at the maximum operated NAP and it is about 40% for both the membranes with a peak around 50% for the 0.25mol/L ethanol solution with RO98pHt® membrane (Figures 5.19 and 5.20). Though the ethanol rejection values exhibited by both the membrane are very low, they are

consistent with other data reported by scientific papers (Duvel e*t al.,* 1975; Pozderović *et al.,* 2006; Ozaki *et al.*, 2002);

(i) the permeate ethanol concentration only marginally decreases as the NAP increases for both the membranes, as reported in Figure 5.27 and 5.28. Thus, low rejection values are justified;

(j) concerning to the specific comparison between TFC®-ULP and RO98pHt® membranes Figures 5.23 and 5.24 not only confirm that TFC®-ULP is characterized by higher overall water permeability and water flux values, but also show how the overall water permeability and the water flux are lower when the feed salt solution is used instead of the ethanol feed solution having the same osmotic pressure. The same conclusion can be made from Figure 5.25 regarding the ethanol and salt permeability as well as Figure 5.26 regarding the ethanol and salt flux. Essentially, the membranes allow the passage of more water and more solute if the feed is an ethanol solution instead of a salt solution. This behaviour could be related to the chemical nature of the solute as is described in the following paragraphs;

(k) the ethanol flux through the membrane increases as the feed ethanol concentration or the feed pressure increase, as it is shown in Figures 5.29 and 5.30. On the other hand, as illustrated in Figures 5.31 and 5.32, the water flux through the membrane decreases as the ethanol concentration and the feed pressure increase. In addition, as aforementioned, it is also clear from these diagrams that TFC®-ULP membrane allows higher ethanol and water fluxes than RO98pHt® membrane. Essentially, when the ethanol concentration increases, also the ethanol flux through the membrane increases. At the same time the water flux across the membrane shows a downward trend, because there is less water in the solution and mainly because the NAP, which forces the water to pass through the membrane, is lower due to the rising of the feed osmotic pressure.

To summarize, TFC®-ULP membrane is the most suitable option for RO water-ethanol separation in comparison to RO98pHt® membrane. In spite they reach the same ethanol rejection, TFC®-ULP membrane allows a higher water flux. Hence, in a hypothetical process, TFC®-ULP membrane is more efficient. However, the rejection values are certainly not enough to recover a high percentage of ethanol in MOD process. Thus, in the following paragraph the reasons of low rejection results are explained.

As aforementioned, the ethanol rejection is about 40% for both TFC®-ULP and RO98pHt® membranes and this data are consistent with the experimental results of several past scientific papers, which used different types of CA and aromatic polyamide TFC membranes and different feed ethanol concentrations (Duvel e*t al.,* 1975; Pozderović *et al.*, 2006; Ozaki *et al.*, 2002). The reasons of this low rejection may be attributed to the chemical properties of the water-ethanol solution and to the influence of solute, solvent and membrane interaction on membrane performance.

In 1975 Duvel and Helfgott proved that shape, size and chemical characteristic of a compound influence the rejection in a RO process. The solute rejection increases as the number of carbon atoms and the geometry complexity (cross-sectional area, structure) of an organic compound increases. Consequently, there is a trend for percentage rejection to increase in response to an increase in molecular weight. Firstly, ethanol is a primary alcohol with low molecular weight, straight chain, simple geometry and no side chains. As a result, it can easily enter the membrane (sorption or dissolution) by passing into a gap between polymer segments. Following this, once the ethanol is in the membrane, the second step of membrane permeation is the diffusion through the membrane and this could be facilitated if ethanol has chemical affinity for the membrane. In fact, according to the Solution-Diffusion Model, both the solute and solvent dissolve in the thin dense non porous surface layer of the membrane and then each diffuses across it. Furthermore, the fluxes through the membrane are strongly influenced by differences in the solubilities and diffusivities of the solvent and the solute in the membrane phase (Williams, 2003). In other words, differences in retention are caused principally by differences in diffusion rates of the solute across the membrane. Therefore, the high ethanol flux across the membranes could be explained by the interaction between ethanol and the membrane. The interaction between water, solutes and membrane are the most important factors in RO separation. The membranes used in the experiments are hydrophilic (exhibiting an affinity for water) because they carry some degree of negative surface charge. Water may diffuses through the membrane due to hydrogen bonding interaction with it and it is scientifically proved that organic hydrogen bonding interaction with the membrane polymers might reduce water flux through the membrane (Williams, 2003). Ethanol is a polar organic compound and interacts with water, the membrane and itself forming hydrogen bonding. Hence, ethanol in a RO process may interact with the membrane polymer, decrease the water content of the membrane and diffuse across the membrane leading to low rejection values. As hydrogen bonding increases, more solute enters the membrane and there is more solute available for diffusion.

To sum up, it is noteworthy to state that the ethanol passage across both TFC®-ULP and RO98pHt® membranes could be justified according to previous researches about ethanol-membrane interaction.

The simple structure of ethanol molecule, the low molecular weight, the low-cross sectional area, the chemical affinity for the membrane polymer and primarily the high tendency to form hydrogen bonding are the key factors responsible for the low ethanol rejection. The membranes are designed with hydrophilic polymers (for example cellulose esters and polyamides) in order to decrease the solute sorption and consequently increase the water sorption and the water flux. Unfortunately, the sorption of particular organic solutes with high tendency to form hydrogen bonding such ethanol could be increased instead of decreased. Hence, as is suggested in the following paragraph, the structure of the membrane should be modified in order to maximize the ethanol rejection.

Furthermore, in 1996 Kulkarni, Mukherjee and Gill used ethanol to hydrophilize RO98pHt® membrane (in the paper the old name of the membrane is used HR98PP). They stated that the increase in water flux and salt rejection may be attributed to the ethanol mild solvent characteristics with respect to polyamides. Thus, ethanol swells the membrane, removes small molecular fragments because of the partial dissolution in alcohol and removes the imperfections or defects, making the membrane a more porous structure (Kulkarni *et al.*, 1996). This confirms the aforementioned discussion about the ethanol-membrane interactions, and some non-linear trend of the results could be explained also considering that the membrane might be modified by the ethanol flux during the experiments.

5.4.2 Future work recommendations

The results of the experimental work carried out using TFC®-ULP and RO98pHt® membranes state that ethanol rejection of both membranes is not enough to recover entirely the ethanol in the MOD process. For this reason, new design process solutions and other experimental works are suggested in the following paragraphs.

Concerning the process design solutions, the results suggest considering other kind of separation processes, because a RO recovery unit, at the current state-of-the-art, is not enough to recover totally the ethanol and produce drinkable water conform to WHO (World Health Organization) standards. The feed of the reverse osmosis unit could be the product stream of another recovery unit in order to develop a hybrid water-ethanol separation system that could efficiently recover the draw solution. For instance the RO unit could be linked to a distillation column, an adsorption unit or a pervaporation unit.

However, the product water of the RO recovery unit might be suitable for specific industrial application.

As regard to the future work recommendations, first of all it is suggested to make the research focus on the membrane structures and properties, trying to understand how to possibly modify the membrane in order to be less prone to adsorb ethanol or understand which membranes are the most suitable to select. Secondly, it is recommended to repeat the experiments with other possibly suitable different types of membrane in order to have a large available database.
For instance Choundhury, Ghosh and Guha in 1985 arrived at about 90% separation of ethanol (10% v/v feed solution, 50 bar) using a modified styrene-grafted CA membrane (Choudhury et al., 1985). Furthermore, in 1976 Fang and Chan reached an ethanol rejection of 60%, 70% and 80% (40bar, 25°C) with two different types of cross-linked polyethylenmine membranes (NS-100, NS-100-T) and one type of sulfonate polymer composite membrane (NS-200) respectively (Fang *et al.,* 1976). Moreover, in 1998, Huang, Guo and Fang used a cross-linked polyacrylic acid (PAA) composite membrane to arrive at about 67% of ethanol rejection (1000ppm, 50bar, 30°C) (Huang *et al.,* 1998), and in 2003 Schutte reached 75% of ethanol rejection with a very dense cross-linked aromatic polyamide membrane (Schutte *et al.,* 2003). Therefore, reaching high ethanol rejection values with specific grafted or cross-linked membrane is possible after a considerable study of membrane structure, compound-membrane interactions, membrane charge and polarity, hydrogen bonding acceptor density and molecular complexity. In addition, there are models that can predict the rejection of a specific membrane that can be used for organic compound (For instance the Empirical (QSAR) Models Describing Organic Compound Rejection) (NWRI Project 01-EC-002, 2004).
Finally, it is suggested to use another kind of model to describe the transport mechanism inside the membrane. The Solution-Diffusion model used is a linear model very simple to use, however it is probably based on quite strong assumptions, because some parameters such as the rejection and the solute permeability do not seem to follow a linear trend. Furthermore, SD model assumes that the solute and the solvent diffusion are uncoupled inside the membrane. Although it may be true for the separation of organic system, the solute-solvent coupling should be considered (Paul *et al.,* 2004).

Conclusions

This study aimed to investigate the efficiency of the reverse osmosis recovery unit of the Manipulated Osmosis Desalination process when ethanol is used as an osmotic agent. MOD process has been developed at the University of Surrey's Centre for Osmosis Research and Applications (CORA) (Sharif & Al-Mayahi, 2005) and it is characterized by the use of a pressure-driven membrane step (Reverse Osmosis or Nanofiltration) in the recovering stage of a forward osmosis desalination process.

The experiments were carried out by using two different kinds of flat sheet commercially available thin film composite membranes (TFC®-ULP manufactured by Koch Membrane System and RO98pHt® manufactured by Alfa Laval) and a RO laboratory cell supplied by SpinTek Filtration, Inc. (USA). The membrane were tested by using different ethanol feed concentration (0.29-3.66% v/v) and different feed pressure (2-20 bar) at room temperature. The samples were analysed by a Gas Chromatographer (Agilent 6890N with flame ionisation detector) and the data was work out by using the Solution-Diffusion model.

As a general result it was evident that TFC®-ULP membrane is the most suitable option for RO water-ethanol separation in comparison to RO98pHt® membrane, because it reaches the same ethanol rejection allowing a higher water flux across the membrane. However, the ethanol rejection (about 40%) is not enough to recover completely the ethanol in the RO unit. Therefore, the obtained permeate is not drinkable according to the WHO (World Health Organization) standards, tough it might be used for industrial application. The simple structure, the low molecular weight and the low-cross sectional area of ethanol molecule in addition to the chemical affinity for the membrane polymer and primarily the high tendency to form hydrogen bonding are the key factors responsible for the low ethanol rejection.

Admittedly, the experimental works has some limitation, because more experimental data using a wider range of feed ethanol concentration and feed pressure and other kinds of membranes should be obtained. Moreover, temperature effect on the operative RO parameters has only partially been investigated and it could be the aim of future works. Nevertheless, it is suggested considering other kind of separation processes in order to develop a hybrid water-ethanol separation system (for instance the RO unit after a distillation column, an adsorption unit or a pervaporation unit) that could recover efficiently the draw solution and produce a permeate conform to the WHO standards for drinkable waters. On the other hand, the study of the ethanol-membrane interaction could lead to the development of grafted or cross-linked membrane which could arrived

at higher ethanol rejection values, as it had been done in the past (Choudhury et al.,1985; Fang *et al.*, 1976; Huang *et al.*, 1998 and Schutte *et al.*, 2003). Last but not least, the RO product water could be suitable for specific industrial application without any process modification.

Nomenclature

a	=	Activity
A	=	Solvent permeability coefficient
A_m	=	Membrane's active surface area
A_w	=	Overall water permeability
A_{wm}	=	Pure water permeability
B	=	Solute permeability coefficient
B_s	=	Solute permeability
c	=	Solute concentration
i_v	=	van't Hoff factor
J_s	=	Mass flux of solute
J_w	=	Volumetric pure water flux
K	=	Ionic strength constant
k	=	Mass transfer coefficient
MW	=	Molecular weight
n	=	Numbers of moles
P	=	Hydraulic pressure
q	=	Volumetric flow rate
R	=	Retention or Rejection
R	=	Ideal gas constant
R^2	=	Coefficient of determination
Re	=	Reynolds number
S	=	Recovery or yield
S	=	Entropy
Sc	=	Schmidt number
Sh	=	Sherwood number
T	=	Temperature
t	=	Time
U	=	Energy
V	=	Volume
v_i	=	Partial molar volume
VR	=	Volume reduction
x	=	mole fraction

Greek letters

δ_c	=	Thickness of the concentration boundary layer (feed side)
δ_m	=	Active skin layer thickness
δ_s	=	Porous layer thickness
δ_p	=	Thickness of the concentration boundary layer (permeate side)
γ	=	Activity coefficient
μ	=	Chemical potential
π	=	Osmotic pressure
ρ	=	Density
Φ	=	Osmotic coefficient

Subscripts

b	=	Bulk (feed-concentrate) side
c	=	Concentrate
e	=	Ethanol
f	=	Feed
m	=	Membrane
p	=	Permeate
s	=	Solute
w	=	Solvent

Acronyms

ASDPF	=	Analytical-Solution Diffusion-Pore Flow
BWRO	=	Brackish Water Reverse Osmosis
CA	=	Cellulose-Acetate
CAPS	=	Compact Accelerated Precipitation Softening
CORA	=	Centre for Osmosis Research and Applications
CP	=	Concentration Polarization
CTA	=	Cellulose Triacetate
DECC	=	Dynamic Equilibrium-Chemical Capacitance
DS	=	Draw Solutions
ED	=	Electrodialysis
EDR	=	Electrodialysis Reversal
ERD	=	Energy Recovery Device
ESDM	=	Extended Solution Diffusion Model

FO	=	Forward Osmosis
GC	=	Gas Chromatographer
HID	=	Hybrid RO membrane Interstage Design
HR	=	High Rejection
ICP	=	Internal Concentration Polarization
IT	=	Irreversible Thermodynamics
LCA	=	Life Cycle Assessment
LICA	=	Life Cycle Impact Assessment
LSI	=	Langelier Saturation Index
MD	=	Membrane Distillation
MED	=	Multi-Effect Distillation
MF	=	Microfiltration
MFI	=	Modified Fouling Index
MOD	=	Manipulated Osmosis Desalination
MSDS	=	Material Safety Data Sheet
MSF	=	Multi-Stage Flash
MT	=	Molecular Trap
MVC	=	Mechanical Vapour Compression
NDP	=	Net Driving Pressure
NF	=	Nanofiltration
NPA	=	Net Applied Pressure
NRC	=	National Research Council
NTU	=	Nephelometric Turbidity Units
OA	=	Osmotic Agent
PAA	=	Polyacrylic Acid
PAEW	=	Public Authority for Electricity and Water
PBI	=	Polybenzimidazole
PR	=	Performance Ratio
PRO	=	Pressure Retarded Osmosis
PV	=	Pressure Vessel
RO	=	Reverse Osmosis
S&DSI	=	Stiff and Davis Stability Index
SDI	=	Silt Density Index
SDM	=	Solution Diffusion Model
SDPFFR	=	Solution-Diffusion Pore Flow Fluid-Resistance
SEC	=	Specific Energy Consumption
SP	=	Solubility Product
SWM	=	Spiral Wound Modules

SWRO	=	Sea Water Reverse Osmosis
TDS	=	Total Dissolved Solid
TFC	=	Thin film Composite
UF	=	Ultrafiltration
ULP	=	Ultra Low Pressure
VCD	=	Vapour Compression Distillation
WDR	=	Water Desalination Report
WHO	=	World Health Organization

Appendices

APPENDIXA: Ethanol MSDS

Fisher Scientific

Part of Thermo Fisher Scientific

Material Safety Data Sheet

Creation Date 24-Apr-2009 **Revision Date** 26-Sep-2009 **Revision Number** 1

1. PRODUCT AND COMPANY IDENTIFICATION

Product Name	Ethanol, 200 Proof
Cat No.	A992-RS200; BP2818-4, BP2818-100; BP2818-500
Synonyms	Absolute Ethanol; Ethyl Alcohol; Molecular Biology Grade
Recommended Use	Laboratory chemicals

Company
Fisher Scientific
One Reagent Lane
Fair Lawn, NJ 07410
Tel: (201) 796-7100

Emergency Telephone Number
CHEMTREC®, Inside the USA: 800-424-9300
CHEMTREC®, Outside the USA: 703-527-3887

2. HAZARDS IDENTIFICATION

WARNING!

Emergency Overview

Flammable liquid and vapor. Irritating to eyes and skin. May cause irritation of respiratory tract. May cause central nervous system effects. Aspiration hazard if swallowed - can enter lungs and cause damage. This substance has caused adverse reproductive and fetal effects in humans. Substances known to cause developmental toxicity in humans.

Appearance Clear, Colorless **Physical State** Liquid **odor** sweet, Characteristic

Target Organs Eyes, Skin, Reproductive System, Central nervous system (CNS), Liver, Kidney, Blood

Potential Health Effects

Acute Effects
Principle Routes of Exposure

Eyes	Irritating to eyes.
Skin	Irritating to skin. May be harmful in contact with skin.
Inhalation	May cause irritation of respiratory tract. May be harmful if inhaled. Inhalation may cause central nervous system effects.
Ingestion	May be harmful if swallowed. Aspiration hazard if swallowed - can enter lungs and cause damage. Ingestion may cause gastrointestinal irritation, nausea, vomiting and diarrhea.

Chronic Effects This substance has caused adverse reproductive and fetal effects in humans. Substances known to cause developmental toxicity in humans. Tumorigenic effects have been reported in experimental animals.. May cause adverse liver effects. May cause adverse kidney effects.

See Section 11 for additional Toxicological information.

Aggravated Medical Conditions Central nervous system disorders. Preexisting eye disorders. Liver disorders. Skin disorders.

3. COMPOSITION/INFORMATION ON INGREDIENTS

Haz/Non-haz

Component	CAS-No	Weight %
Ethyl alcohol	64-17-5	99.5 - 100

4. FIRST AID MEASURES

Eye Contact Rinse immediately with plenty of water, also under the eyelids, for at least 15 minutes. Obtain medical attention.

Skin Contact Wash off immediately with plenty of water for at least 15 minutes. Obtain medical attention.

Inhalation Move to fresh air. If breathing is difficult, give oxygen. Do not use mouth-to-mouth resuscitation if victim ingested or inhaled the substance; induce artificial respiration with a respiratory medical device. Obtain medical attention.

Ingestion Do not induce vomiting. Obtain medical attention.

Notes to Physician Treat symptomatically.

5. FIRE-FIGHTING MEASURES

Flash Point 12°C / 53.6°F

Method No information available.

Autoignition Temperature 363°C / 685.4°F

Explosion Limits
Upper 19 vol %
Lower 3.3 vol %

Suitable Extinguishing Media Use water spray, alcohol-resistant foam, dry chemical or carbon dioxide. Use water spray to cool unopened containers.

Unsuitable Extinguishing Media Water may be ineffective

Hazardous Combustion Products No information available.

Sensitivity to mechanical impact No information available.
Sensitivity to static discharge No information available.

Specific Hazards Arising from the Chemical
Flammable. Risk of ignition. Vapors may form explosive mixtures with air. Vapors may travel to source of ignition and flash back. Containers may explode when heated.

Protective Equipment and Precautions for Firefighters
As in any fire, wear self-contained breathing apparatus pressure-demand, MSHA/NIOSH (approved or equivalent) and full protective gear. Thermal decomposition can lead to release of irritating gases and vapors.

NFPA **Health** 2 **Flammability** 3 **Instability** 0 **Physical hazards** N/A

6. ACCIDENTAL RELEASE MEASURES

Personal Precautions Remove all sources of ignition. Use personal protective equipment. Take precautionary measures against static discharges. Do not get in eyes, on skin, or on clothing.

Environmental Precautions Should not be released into the environment.

Methods for Containment and Clean Up Remove all sources of ignition. Soak up with inert absorbent material. Keep in suitable and closed containers for disposal. Take precautionary measures against static discharges.

7. HANDLING AND STORAGE

Handling Wear personal protective equipment. Ensure adequate ventilation. Use explosion-proof equipment. Keep away from open flames, hot surfaces and sources of ignition. Take precautionary measures against static discharges. Do not breathe vapors or spray mist. Do not get in eyes, on skin, or on clothing.

Storage Keep containers tightly closed in a dry, cool and well-ventilated place. Keep away from open flames, hot surfaces and sources of ignition. Flammables area.

8. EXPOSURE CONTROLS / PERSONAL PROTECTION

Engineering Measures Ensure adequate ventilation, especially in confined areas. Use explosion-proof electrical/ventilating/lighting/equipment. Ensure that eyewash stations and safety showers are close to the workstation location.

Component	ACGIH TLV	OSHA PEL	NIOSH IDLH
Ethyl alcohol	TWA: 1000 ppm	(Vacated) TWA: 1900 mg/m³ (Vacated) TWA: 1000 ppm TWA: 1900 mg/m³ TWA: 1000 ppm	IDLH: 3300 ppm TWA: 1000 ppm TWA: 1900 mg/m³

Component	Quebec	Mexico OEL (TWA)	Ontario TWAEV
Ethyl alcohol	TWA: 1000 ppm TWA: 1880 mg/m³	TWA: 1000 ppm TWA: 1900 mg/m³	TWA: 1000 ppm TWA: 1900 mg/m³

NIOSH IDLH: *Immediately Dangerous to Life or Health*

Personal Protective Equipment

Eye/face Protection Wear appropriate protective eyeglasses or chemical safety goggles as described by OSHA's eye and face protection regulations in 29 CFR 1910.133 or European Standard EN166.

Skin and body protection Wear appropriate protective gloves and clothing to prevent skin exposure.

Respiratory Protection Follow the OSHA respirator regulations found in 29 CFR 1910.134 or European Standard EN 149. Use a NIOSH/MSHA or European Standard EN 149 approved respirator if exposure limits are exceeded or if irritation or other symptoms are experienced.

9. PHYSICAL AND CHEMICAL PROPERTIES

Physical State	Liquid
Appearance	Clear, Colorless
odor	sweet, Characteristic
Odor Threshold	No information available.
pH	No information available.
Vapor Pressure	No information available.
Vapor Density	No information available.
Viscosity	No information available.
Boiling Point/Range	78°C / 172.4°F
Melting Point/Range	-114°C / -173.2°F
Decomposition temperature	No information available.
Flash Point	12°C / 53.6°F
Evaporation Rate	No information available.
Specific Gravity	No information available.
Solubility	No information available.
log Pow	No data available
Molecular Weight	46.07
Molecular Formula	C2 H6 O

10. STABILITY AND REACTIVITY

Stability	Stable under normal conditions.
Conditions to Avoid	Incompatible products. Heat, flames and sparks.
Incompatible Materials	Strong oxidizing agents, Strong acids, Acid anhydrides, Acid chlorides
Hazardous Decomposition Products	Carbon monoxide (CO), Carbon dioxide (CO_2)
Hazardous Polymerization	Hazardous polymerization does not occur.
Hazardous Reactions .	None under normal processing..

11. TOXICOLOGICAL INFORMATION

Acute Toxicity

Component Information

Component	LD50 Oral	LD50 Dermal	LC50 Inhalation
Ethyl alcohol	7060 mg/kg (Rat)	Not listed	20000 ppm/10H (Rat)

Irritation	Irritating to eyes and skin
Toxicologically Synergistic Products	No information available.

Chronic Toxicity

Carcinogenicity The table below indicates whether each agency has listed any ingredient as a carcinogen.

Component	ACGIH	IARC	NTP	OSHA	Mexico
Ethyl alcohol	Not listed	Group 1	Not listed	X	Not listed

ACGIH: (American Conference of Governmental Industrial Hygienists)
A1 - Known Human Carcinogen
A2 - Suspected Human Carcinogen
A3 - Animal Carcinogen
ACGIH: (American Conference of Governmental Industrial Hygienists)
OSHA: (Occupational Safety & Health Administration)
OSHA: (Occupational Safety & Health Administration)
X - Present
Mexico - Occupational Exposure Limits - Carcinogens
Mexico - Occupational Exposure Limits - Carcinogens
A1 - Confirmed Human Carcinogen
A2 - Suspected Human Carcinogen
A3 - Confirmed Animal Carcinogen
A4 - Not Classifiable as a Human Carcinogen
A5 - Not Suspected as a Human Carcinogen

Sensitization No information available.

Mutagenic Effects Mutagenic effects have occurred in humans.

Reproductive Effects Adverse reproductive effects have occurred in humans..

Developmental Effects Substances known to cause developmental toxicity in humans.

Teratogenicity Teratogenic effects have occurred in humans..

Other Adverse Effects Tumorigenic effects have been reported in experimental animals.. See actual entry in RTECS for complete information.

Endocrine Disruptor Information No information available

12. ECOLOGICAL INFORMATION

Ecotoxicity

Component	Freshwater Algae	Freshwater Fish	Microtox	Water Flea
Ethyl alcohol	Not listed	Leucidus idus: LC50 = 8.14 mg/L/48h	Photobacterium phosphoreum:EC50 = 34634 mg/L/30 min Photobacterium phosphoreum:EC50 = 35470 mg/L/5 min	EC50 = 9268 mg/L/48h EC50 = 10800 mg/L/24h

Persistence and Degradability Readily biodegradable.

Bioaccumulation/ Accumulation No information available

Mobility

Component	log Pow
Ethyl alcohol	-0.32

13. DISPOSAL CONSIDERATIONS

Waste Disposal Methods Chemical waste generators must determine whether a discarded chemical is classified as a hazardous waste. Chemical waste generators must also consult local, regional, and national hazardous waste regulations to ensure complete and accurate classification

14. TRANSPORT INFORMATION

DOT

UN-No	UN1170
Proper Shipping Name	ETHANOL
Hazard Class	3
Packing Group	II

TDG

UN-No	UN1170
Proper Shipping Name	ETHANOL
Hazard Class	3
Packing Group	II

IATA

UN-No	UN1170
Proper Shipping Name	ETHANOL
Hazard Class	3
Packing Group	II

IMDG/IMO

UN-No	UN1170
Proper Shipping Name	ETHANOL
Hazard Class	3
Packing Group	II

15. REGULATORY INFORMATION

International Inventories

Component	TSCA	DSL	NDSL	EINECS	ELINCS	NLP	PICCS	ENCS	AICS	CHINA	KECL
Ethyl alcohol	X	X	-	200-578-6	-		X	X	X	X	KE-13217 X

Legend:
X - Listed

E - Indicates a substance that is the subject of a Section 5(e) Consent order under TSCA.
F - Indicates a substance that is the subject of a Section 5(f) Rule under TSCA.
N - Indicates a polymeric substance containing no free-radical initiator in its inventory name but is considered to cover the designated polymer made with any free-radical initiator regardless of the amount used.
P - Indicates a commenced PMN substance
R - Indicates a substance that is the subject of a Section 6 risk management rule under TSCA.
S - Indicates a substance that is identified in a proposed or final Significant New Use Rule
T - Indicates a substance that is the subject of a Section 4 test rule under TSCA.
XU - Indicates a substance exempt from reporting under the Inventory Update Rule, i.e. Partial Updating of the TSCA Inventory Data Base Production and Site Reports (40 CFR 710(B).
Y1 - Indicates an exempt polymer that has a number-average molecular weight of 1,000 or greater.
Y2 - Indicates an exempt polymer that is a polyester and is made only from reactants included in a specified list of low concern reactants that comprises one of the eligibility criteria for the exemption rule.

U.S. Federal Regulations

TSCA 12(b) Not applicable

SARA 313
Not applicable

SARA 311/312 Hazardous Categorization

Acute Health Hazard	Yes
Chronic Health Hazard	Yes
Fire Hazard	Yes
Sudden Release of Pressure Hazard	No
Reactive Hazard	No

Clean Water Act
Not applicable

Clean Air Act
Not applicable

OSHA
Not applicable

CERCLA
Not Applicable

California Proposition 65
This product contains the following Proposition 65 chemicals: Ethyl alcohol is only a considered a Proposition 65 developmental hazard when it is ingested as an alcoholic beverage.

Component	CAS-No	California Prop. 65	Prop 65 NSRL
Ethyl alcohol	64-17-5	Developmental	-

State Right-to-Know

Component	Massachusetts	New Jersey	Pennsylvania	Illinois	Rhode Island
Ethyl alcohol	X	X	X	-	X

U.S. Department of Transportation

Reportable Quantity (RQ):	N
DOT Marine Pollutant	N
DOT Severe Marine Pollutant	N

U.S. Department of Homeland Security
This product does not contain any DHS chemicals.

Other International Regulations

Mexico - Grade Serious risk, Grade 3

Canada

This product has been classified in accordance with the hazard criteria of the Controlled Products Regulations (CPR) and the MSDS contains all the information required by the CPR.

WHMIS Hazard Class
B2 Flammable liquid
D2B Toxic materials

16. OTHER INFORMATION

Prepared By	Regulatory Affairs Thermo Fisher Scientific Tel: (412) 490-8929
Creation Date	24-Apr-2009
Print Date	26-Sep-2009
Revision Summary	*****, and red text indicates revision

Disclaimer
The information provided on this Safety Data Sheet is correct to the best of our knowledge, information and belief at the date of its publication. The information given is designed only as a guide for safe handling, use, processing, storage, transportation, disposal and release and is not to be considered as a warranty or quality specification. The information relates only to the specific material designated and may not be valid for such material used in combination with any other material or in any process, unless specified in the text.

End of MSDS

References

Al-Zuhairi, A. (2008). A Novel Manipulated Osmosis Desalination Process. *Doctoral Thesis*, Centre for Osmosis Research and Applications, Faculty of Engineering and Physical Sciences, University of Surrey.

America's Authority in Membrane Treatment (AMTA), (2007). *Water Desalination Processes*.

American Water Works Associations (AWWA) (1999). *Reverse Osmosis and Nanofiltration*. AWWA, Denver, (U.S.A.).

Aspen Technology, Inc. (1994-2012). Aspen Plus® V7.3.2

Bolto, B., Hoang, M., Xie, Z. (2012). A review of water recovery by vapour permeation through membranes. *Water research*, **46**, 259-266.

Cath, T., Y., Childress, A., E., Elimelech, M. (2006). Forward osmosis: Principles, applications, and recent developments. *Journal of Membrane Science*, **281**, 70-87.

Committee on Advancing Desalination Technology; Nation Research Council. (2008). *Desalination: A National Perspective*. National Academies Press, Washington, DC (U.S.A.).

Choudhury, J., P., Ghosh, P., Guha, B., K. (1985). Separation of Ethanol-Water Mixture by Reverse Osmosis. Biotechnology and Bioengineering, **27**, 1081-1084.

Chung, T., Zhang, S., Wang, K., Su, J., Ling, M. (2010). Forward osmosis processes: Yesterday, today and tomorrow. *Desalination*, **287**, 78-81.

Duvel, W., A., Helfgott, T. (1975). Removal of Wastewater Organics by Reverse Osmosis. *Journal of Water Pollution Control Federation*, **47**, 57-65.

Fang, H., H., P., Chain, E., S., K. (1976). Reverse Osmosis Separation of Polar Compounds in Aqueous Solution. *Environment Science & Technology*, **10**, 364-369.

Filteau, G., Moss, P. (1997). Ultra-low pressure RO membranes: an analysis of performance and cost. *Desalination*, **113**, 147-152.

Friztmann, C., Lowenberg, J., wintgens, T., & Melin, T. (2007). State-of-the-art of reverse osmosis desalination. *Desalination*, **216**, 1-76.

Greenlee, L. F., Lawler, D. F., Freeman, B. D., Marrot, B., & Moulin, P. (2009). Reverse osmosis desalination: Water sources, technology, and today's challenges. *Water Research*, **43**, 2317-2348.

Haelssig J., B., Tremblay A., Y., Thibault, J. (2012). A new hybrid membrane separation process for enhanced ethanol recovery: Process description and numerical study. *Chemical Engineering Science*, **68**, 492-505.

Haelssig, J. B., Tremblay A. Y., Thibault, J., Huang, X. (2011). Membrane Dephlegmation: A hybrid membrane separation process for efficient ethanol recovery. *Journal of Membrane Science*, **381**, 226-236.

Hamer, W., & Wu, Y. (1972). Osmotic coefficients and mean activity coefficients of univalent electrolytes in water at 25°C. *J. Phys. Chem. Ref. Data*, **1**, 1047.

Hirose, M., Ito, H., & Kamiyama, Y., (1996).Effect of skin layer surface structures on the flux behaviour of RO membranes. *J. Membr. Sci.*, **121**, 209-215.

Hoboken, N., J. (2005). Water treatment: principles and design (2nd ed.). John Wiley &Sons Inc., New Jersey, (U.S.A.).

Huang, J., Guo, Q., Ohya, H., Fang, J. (1998). The characteristic of crosslinked PAA composite membrane for separation of aqueous organic solutions by reverse osmosis. *Journal of Membrane Science*, **144**, 1-11.

Kucera, Jane (2010). *Reverse Osmosis - Design, Processes, and Applications for Engineers.*John Wiley &Sons Inc., New Jersey, (U.S.A.), and Scrivener Publishing LLC, Massachusetts, (U.S.A.).

Kulkarni, A., Mukherjee, D., Gill, W., N. (1996). Flux enhancement by hydrophilization of thin film composite reverse osmosis membranes. *Journal of Membrane Science*, **114**, 39-50.

Kumano A., Sekino M., Matsui Y., Fujiwara N., Matsuyama H. (2008).Study of mass transfer characteristic for a hollow fiber reverse osmosis module. *J. Membr. Sci.*, **324**, 136-141.

McCormick, P., Pellegrino, J., Mantovani, F., Sarti, G. (2008). Water, salt, and ethanol diffusion through membranes for water recovery by forward (direct) osmosis processes. *Journal of Membrane Science*, **325**, 467-478.

Mehdizadeh, H. (2006). Membrane desalination plants form an energy-exergy viewpoint. *Desalination*, **191**,200-209.

Menachem, E., William A. P. (2011). The future of Seawater Desalination: Energy, Technology, and the Environment. *Science*, **333**, 712-717.

Merdaw, A.A. (2009). Theoretical and Experimental Investigation of a Novel Manipulated Osmosis Desalination process. *PhD Thesis*, Centre for Osmosis Research and Applications, Faculty of Engineering and Physical Science, University of Surrey.

Merten, U. (1966). *Desalination by Reverse Osmosis*. The M.I.T. Press, Massachussetts (U.S.A.).

Norman, N., Li., Anthony, F., G., Winston, W., S., Matsuura, T. (2008). *Advanced Membrane Technology and Applications*. John Wiley & Sons, Oxford, (UK).

OLI System Inc. (2006). OLI's Stream Analyzer Software V-2.0.41. U.S.A.

Ozaki, H., Li, H. (2002). Rejection of organic compounds by ultra-low pressure reverse osmosis membrane. *Water research*, **36**, 123-130.

Paul, D., R. (2004). Reformulation of the solution-diffusion theory of reverse osmosis. *Journal of Membrane Science*, **241**, 371-386.

Penãte, B., Garcìa-Rodriguez, L. (2011). Current trends and future prospects in the design of seawater reverse osmosis desalination technology. *Desalination*, **284**, 1-8.

Pilipovik, M., V., Riverol, C. (2005). Assessing deal dealcoholisation system based on reverse osmosis. *Journal of Food Engineering*, **69**, 437-441.

Pozderović, A., Moslavac, T., Pichler, A. (2006).Concentration of aqueous solutions of organic components by reverse osmosis II. Influence of transmembrane pressure and membrane type on concentration of different alcohol solutions by reverse osmosis. *Journal of Food Engineering*, **77**, 810-817.

Pozderović, A., Moslavac, T., Pichler, A. (2008). Influence of processing parameters and membrane type on permeate flux during solution concentration of different alcohols, esters, and aldehydes by reverse osmosis. *Journal of Food Engineering*, **78**, 1092-1102.

Praunsnitz, J., Lichtethaler, R., & de Azvedo, E. (1999). *Molecular Thermodynamics of Fluid-Phase Equilibria* (3rd ed.).Prentice Hall PTR, New Jersey (U.S.A.).

Raluy, G., Serra, L., Uche, J. (2006). Life cycle assessment of MSF, MED and RO desalination technologies. *Energy*, **31**, 2361-2372.

Ren, J., Li, Z., & Woong, F. (2006).A new method for the prediction of pore size distribution and MWCO of ultrafiltration membranes. *J. Membr. Sci.*, **279**, 558-569.

Rodriguez, G., Buonora, S., Knoell, T., Phipps, D., Jr., Ridgway, H. (2004). *Rejection of Pharmaceuticals by Reverse Osmosis Membranes: Quantitative Structure Activity Relationship (QSAR) Analysis*. National Water Research Institute, NWRI Project No. 01-EC-002.

Rognoni, M. (2010).*La dissalazione dell'acqua di mare. Descrizione, analisi e valutazione delle principali tecnologie*. Flaccovio Dario Editore (Italy).

Roth T., Kreis P., Górak A. (2010). Energy efficient hybrid processes for ethanol dehydration: a comparison of benchmark and membrane assisted configurations. *Distillation Adsorption*, 199-204.

Schenkeveld, M. M., Morris, R., Budding, B., Helmer, J., & Innaen, S. (2004). *Seawater and Brackish Water Desalination in the Middle East, North Africa and Central Asia*. World Bank.

Shäfer, A., Fane, A., & Waite, T. (2000). Fouling effects on rejection in the membrane filtration of natural waters. *Desalination*, **131**, 215-224.

Shutte, F., C. (2003). The rejection of specific organic compounds by reverse osmosis membranes. *Desalination*, **158**, 285-294.

Soltanieh, M., & Gill, W. (1981). Review of reverse osmosis membranes and transport models. *Chem. Eng. Commun.*, **12**, 279-363.

Thain, J. F. (1967). *Principles of Osmotic Phenomena*. Royal Institute of Chemistry. W Heffer& Sons Ltd, Cambrige, (UK).

Thompson, N., A., Nicoll, P., G. (2011). *Forward osmosis desalination: a commercial reality*. IDA World Congress – Perth Convention and Exhibition Centre (PCEC), Perth, Western Australia. IDAWC/PER11-198.

Toffoletto, M. (2010). Reverse osmosis process: theoretical and experimental investigation. *Tesi di Laurea in Ingegneria Chimica*, DIPIC, Università di Padova.

Van der Bruggen, B. (2003). Desalination by distillation and by reverse osmosis – trends towards the future. *Membrane Technology*, 6-9.

Wilf, M., Bartels, C. (2004).Optimization of seawater RO system design. *Desalination*, **173**, 1-12.

Williams, E., M. (2003). *A Review of Reverse Osmosis Theory*. EET Corporation and Williams Engineering Services Company, Inc.

Xu, P., &Drewes, J. (2006). Viability of nanofiltration and ultra-low pressure reverse osmosis membranes for multi-beneficial use of methane produced water. *Separation and Purification Technology*, **52**, 67-76.

Xu, P., Drewes, J., Bellona, C., Amy, G., Kim, T., Adam, M., (2005). Rejection of Emerging Organic Micropollutants in Nanifiltration-Reverse Osmosis Membrane Applications. *Water Environment Research*, **77**, 40-48.

Zhao, S., Zou, L., Tang, C., Y., Mulcahy, D. (2012). Recent developments in forward osmosis: Opportunities and challenges. *Journal of Membrane Science*, **396**, 1-21.

Zhou, J., Chang, V., W.-C., Fane, A., G. (2011). Environmental life cycle assessment of reverse osmosis desalination: The influence of different life cycle impact assessment methods on the characterization results. *Desalination*, **283**, 227-236.

Web sites:

`http://www.surrey.ac.uk/cce/research/water_chemical/index.htm/` (last login: 10/08/2012)